PhD Thesis

A simplified test procedure for assessing the fatigue performance of asphalt mixes

submitted in satisfaction of the requirements for the degree
Doctor of Science in Civil Engineering
of the TU Wien, Faculty of Civil and Environmental Engineering

---

Dissertation

Vereinfachtes Prüfverfahren zur Bewertung des Ermüdungsverhaltens von Asphaltmischgut

ausgeführt zum Zwecke der Erlangung des akademischen Grads
Doktor der technischen Wissenschaften
eingereicht an der TU Wien, Fakultät für Bau- und Umweltingenieurwesen

Dipl. Ing. **Michael Steineder**, BSc

Matr.Nr.: 00728073

Betreuung:	Univ.-Prof. Dipl.-Ing. Dr.techn. **Bernhard Hofko** Institut für Verkehrswissenschaften Forschungsbereich Straßenwesen Technische Universität Wien Karlsplatz 13/E230-03, 1040 Wien, Österreich
Begutachtung:	Univ.-Prof. Dipl.-Ing. Dr.techn. **Agathe Robisson** Institut für Werkstofftechnologie, Bauphysik und Bauökologie Forschungsbereich Baustofflehre und Werkstofftechnologie Technische Universität Wien Karlsplatz 13/E207, 1040 Wien, Österreich
Begutachtung:	Dr.-Ing. habil. **Sabine Leischner** Institut für Stadtbauwesen und Straßenbau Professur für Straßenbau Technischen Universität Dresden Georg-Schumann-Straße 7/Von-Mises-Bau, 01187 Dresden, Deutschland

Wien, im September 2023

Kurzfassung

Straßen sind eine kritische Infrastruktur für die moderne Gesellschaft, und es ist wichtig, ihre Dauerhaftigkeit und Erhaltung zu gewährleisten. Österreichs Straßennetz umfasst rund 128.000 Kilometer, wobei ein Großteil des Straßennetzes nach dem Zweiten Weltkrieg wieder oder neu errichtet wurde. Die Finanzierung des Straßennetzes ist daher mit erheblichen Kosten für die Instandhaltung oder Erneuerung verbunden, und die Maximierung der Dauerhaftigkeit der Straße ist ein wesentlicher Planungsansatz moderner Fahrbahnbeläge. Die rezeptbasierten, empirischen Prüfverfahren für Asphaltmischungen zur Bewertung der Wirtschaftlichkeit und der Dauerhaftigkeit von Asphaltfahrbahnen waren lange Zeit der Standardansatz für die Optimierung der Mischrezeptur. Mit der Einführung leistungsbezogener Prüfverfahren Mitte der 1990er Jahre, bei denen die Auswirkungen des Verkehrs und des Klimas auf das Ermüdungs-, Steifigkeits- und Verformungsverhalten von Asphaltmischgut unter realistischen Prüfbedingungen simuliert werden, stehen neue Verfahren zur Beurteilung von Asphaltmischgut zur Verfügung.

Mit dem nationalen Umsetzungsdokument ÖNORM B 3580-2 wurde in Österreich im Jahr 2007 die leistungsbezogene Asphaltmischgutbeschreibung eingeführt. Derzeit sind in den europäischen Prüfnormen EN 12697-xx die leistungsbezogenen Prüfverfahren für Asphaltmischgut enthalten. Diese Methoden umfassen unter anderem die Bewertungen des Tieftemperaturverhaltens, der Steifigkeit, der Ermüdungsfestigkeit und des Widerstands gegen bleibende Verformung bei hohen Temperaturen. Experten sind der Ansicht, dass leistungsbasierte Tests besser geeignet sind, da sie unter realitätsnahen Laborbedingungen durchgeführt werden, dadurch erfordern sie aber auch deutlich mehr Zeit und Material als empirische Tests. Aus diesem Grund wird der leistungsbezogene Ansatz für die Optimierung von Asphaltmischgut in Österreich nur selten verwendet.

Das Ziel dieser Arbeit ist es, die leistungsbezogenen Ermüdungsprüfungen von Asphaltmischgutebene auf ein vereinfachtes Prüfkonzept auf Asphaltmastixebene zu übertragen. Die Asphaltmastixebene wurde als Beurteilungsebene gewählt, da sie die wesentliche bindende Komponente in einem Asphaltmischgut ist. Ziel ist es, Korrelationen zwischen Ermüdungsprüfungen auf Asphaltmischgutebene und Asphaltmastixebene zu identifizieren und daraus ein vereinfachtes Prüfverfahren zur Bewertung des Ermüdungsverhaltens von Asphaltmischgut auf Asphaltmastixebene ableiten zu können, um die Materialauswahl für das Asphaltmischgut schnell bewerten und kontrollieren zu können. Dadurch sollen zusätzliche Ermüdungsprüfungen auf Asphaltmischgutebene weitgehend überflüssig werden.

Die Dissertation gliedert sich in drei wesentliche Teile: die Untersuchung möglicher Ermüdungsprüfungen auf Asphaltmastixebene, die Korrelation der Ermüdungsperformance beider Ebenen und die Untersuchung der möglichen Einflüsse von Füllereigenschaften auf die Ermüdungsleistung der Asphaltmastix. Es wurden verschiedene Mischgüter auf Asphalt- und Mastixebene untersucht, und die Analysen der Ergebnisse zeigten, dass die dissipierte Energie pro Lastzyklus (DELC) in Kombination mit einem gängigem Ermüdungskriterium ein effizientes Prüfverfahren auf Asphaltmastixebene ist, um den Ermüdungswiderstand eines Asphaltmischguts zu bewerten. Ein Einfluss des Füllers auf die Ermüdungsperformance konnte beobachtet werden, jedoch Bedarf es eine größere Datenmenge, um diesen Einfluss bestätigen zu können.

Abstract

Roads are a critical infrastructure for modern civilisation; hence, ensuring their durability and maintenance is essential. Austria's road network comprises approximately 128,000 km, with its road system mainly constructed following World War II. Therefore, the road network funding is linked to substantial maintenance or renewal costs and maximising the road durability is a critical component of modern pavements. In terms of evaluating the economic effectiveness and durability of flexible pavements, recipe-based empirical test methods for asphalt mixtures have long been the standard approach for mix design optimisation and quality control.

New techniques for assessing asphalt mixtures have been made available with the introduction of performance-based test methods in the middle of the 1990s. These methods simulate the effects of field traffic and climate according to the fatigue, stiffness and deformation behaviour of asphalt mixtures under realistic test settings.

The national implementation document, called ÖNORM B 3580-2, introduced the performance-based asphalt mix design method in Austria in 2007. The European testing standards, EN 12697-xx, have incorporated performance-based test techniques for asphalt mixtures. These methods comprise evaluations of the low-temperature performance, stiffness, fatigue resistance and resistance to permanent deformation at high temperatures. Past research has shown that performance-based tests are appropriate because they are conducted in realistic laboratory settings, but require significantly longer testing times and more materials than empirical tests. Therefore, the performance-based approach for asphalt mix design has been rarely used in Austria.

This thesis aims to transfer the performance-based fatigue tests of asphalt mixes to a simplified test concept on the asphalt mastic level. The asphalt mastic level is chosen as the assessment level because it is the main binding component in an asphalt mixture. The objective of this work is to identify the correlations between fatigue testing at the asphalt mix and asphalt mastic levels and apply a practical testing procedure at the asphalt mastic level to quickly assess and control the material selection for the asphalt mix, consequently making additional fatigue tests on the asphalt mix level largely unnecessary.

The thesis is divided into three essential parts to examine the possible fatigue tests on the asphalt mastic level, correlate the fatigue performance of both levels and investigate the potential influences of filler properties on the fatigue performance of asphalt mastic. Various asphalt- and mastic-level mixtures are investigated. The analysis results show that the dissipated energy per load cycle (DELC) in combination with an applicable fatigue failure criterion is a practical asphalt mastic-level testing procedure that assesses the fatigue performance of an asphalt mix. The influence of the filler on the fatigue performance is observed, but a more extensive set of data is needed to confirm this influence.

Contents

List of abbreviations

Abbreviation	Definition
γ	Strain for asphalt mastic;
γ_5	Strain required to achieve 10^6 load cycles for asphalt mastic;
γ_i	Strain level in cycle i for asphalt mastic;
δ	Phase angle for asphalt mastic;
δ_i	Phase angle in cycle i for asphalt mastic;
ϵ_6	Strain required to achieve 10^6 load cycles for asphalt mix;
σ_i	Stress level in cycle i for asphalt mastic;
τ	Shear stress for asphalt mastic;
τ_5	Shear stress required to achieve 10^5 load cycles for asphalt mastic;
τ_6	Shear stress required to achieve 10^6 load cycles for asphalt mastic;
ω	Angular frequency;
4PB	Four-point bending;
$\mathbf{A_0}$	Estimation of the level of loading, Q;
$\mathbf{A_1}$	Slope of the fatigue curve;
AC	Asphalt concrete;
CD	Strain-controlled;
CS	Stress-controlled;
$\mathbf{D_f}$	Damage accumulation at the time of failure
DELC	Dissipated energy per load cycle;
$\mathbf{DELC_6}$	DELC required to achieve 10^6 load cycles;
DENT	Double edge notched tension;
DER	Dissipated energy ratio;
DMA	Dynamic mechanical analyser
DSR	Dynamic shear rheometer;
$\lvert E^* \rvert$	Mean value of initial complex modulus for asphalt mix;
FAM	Fine aggregate matrix;
G'	Storage modulus;
G''	Loss modulus;
$\lvert G^* \rvert$	Complex shear modulus for asphalt mastic, is the quotient of the maximum stress τ and the maximum deformation, γ;
$\lvert G^* \rvert_{initial}$	Initial complex shear modulus for asphalt mastic;
LAS	Linear amplitude sweep;
$\mathbf{N_f}$	Number of load applications at failure;

Abbreviation	Definition
$\mathbf{N_{f/50}}$	Number of load applications at conventional failure when the modulus of the complex modulus S_{mix} has decreased to half its initial value;
$\mathbf{N_{p20}}$	Number of load cycles until the DER deviates by 20 % from the undamaged linear line;
PA	Peak of phase angle;
PAV	Pressure aging vessel;
PG	Performance grading;
Q	Level of the loading mode test condition corresponding to 10^6 cycles for the fatigue life according to the chosen failure criteria;
RDEC	Ratio of dissipated energy change;
RS	Reduction of stiffness;
RTFOT	Rolling thin film oven test;
$\mathbf{S_{mix}}$	Magnitude of the calculated complex modulus for asphalt mix;
$\mathbf{S_{mix,0}}$	Initial magnitude of the complex modulus after 100 load cycles for asphalt mix;
SBS	Styrene–butadiene–styrene;
SHRP	Strategic highway research program;
TS	Time-sweep;
VECD	Viscoelastic continuum damage;
$\mathbf{W_i}$	Dissipated energy in cycle i

Chapter 1

Introduction and overview

Undoubtedly, an efficient road network is significant in modern civilisation. Without roads, we cannot conduct businesses, produce goods or perform other daily tasks (Schönfelder, 2015). Therefore, roads must be durable and their conditions must be maintained. Approximately 128,300 km (i.e. 2250 km of motorways and expressways, 33,820 km of state highways B+L and 92,240 km of federal roads) compose the length of the Austrian road network (Bundesministerium für Klimaschutz, Umwelt, Energie, Mobilität, Innovation und Technologie, 2023). Ensuring safe travels on all roads is essential when considering a road's economic function. Most road systems have been constructed in the decades following World War II and have since been maintained or renewed (Schönfelder, 2015). As a result, the road network funding is linked to some substantial maintenance or renewal costs. Therefore, maximising the road durability is a crucial component of modern road building.

The economic effectiveness and durability of flexible pavements cannot be adequately evaluated by the conventional empirical test method of the binder and asphalt mix because of the continual increase in heavy traffic on Austrian and European road networks. The classification for designing an asphalt mix using the empirical method is based on the binder, binder content, void content and particle size distribution (ÖNORM EN 13108-1, 2016). Therefore, expanded testing methods are required to guarantee that the quality requirements are satisfied in accordance with the current performance requirements.

Performance-based test procedures were first standardised in the middle of the 1990s with the release of the EN 12697-xx family of standards. This move allowed the evaluation of the fatigue, stiffness and deformation behaviour of asphalt mixtures under realistic test settings. By implementing the harmonised European standards EN 13108-xx, performance-based test methods have been established for the initial asphalt concrete testing (i.e. type testing) with a performance-based mix design. The national implementation document, called ÖNORM B 3580-2 (ÖNORM B 3580-2, 2018), introduced the performance-based asphalt mix design method in Austria in 2007. Thus, the asphalt mixture conception can be done using either an empirical test or performance-based test approach. Considering the coexistence of equality and standards, a client can select the method used for the initial and acceptance tests related to designing and controlling the asphalt mix.

The initial performance-based asphalt concrete tests include the testing of the low-temperature (ÖNORM EN 12697-46, 2020), stiffness (ÖNORM EN 12697-26, 2018), fatigue (ÖNORM EN 12697-24, 2018) and deformation (ÖNORM EN 12697-25, 2016) behaviours. Past research depicted that, although performance-based tests are appropriate because they are conducted in realistic laboratory settings, they still require a longer testing time than empirical tests (e.g. grading curve, void content, etc.) (Wistuba and Büchner, 2019).

Table 1.1 outlines the typical time frame and the material quantity required for a performance-based test of an asphalt mixture, whereby the stiffness and fatigue tests are performed on the same specimen. Accordingly, the type tests require an average of 12 working days and 240 kg of

Tab. 1.1: Timeframe and quantity requirements for an initial performance-based test of an asphalt mixture

Time	**4PB test**	**Triax test**	**Low-temperature test**
Specimen Preparation	2 days	2 days	2 days
Test preparation	1 day	-	1 day
Testing	9 days	2 days	2-7 days
Total	**12 days**	**4 days**	**5-10 days**

Material	**4PB test**	**Triax test**	**Low-temperature test**
Aggregates	140 kg	40 kg	45 kg
Asphalt binder	10 kg	2 kg	3 kg
Total		**Approx. 240 kg**	

material. Therefore, the performance-based approach for the asphalt mix design is rarely used in Austria. Stiffness and fatigue tests especially require more time and materials.

The mortar is a crucial component of asphalt mixtures. It comprises fine aggregates, fillers and an asphalt binder, but excludes coarse aggregates. Mortars can be defined based on the maximum aggregate size that varies from 0.5 to 2.36 mm and the compaction method (i.e. self-compacting or assisted). Self-compacting mortar samples have the advantages of a small sample size and the ability to be cast into complex shapes. They, however, require a certain viscosity and are limited to a smaller maximum aggregate size. In contrast, compacted samples, which are also referred to as the fine aggregate matrix (FAM), are drilled from compressed cylindrical tablets or compacted into metal molds. These differences influence the testing methods and devices. Self-compacting samples are typically tested with dynamic shear rheometers (DSRs), while FAM samples are tested with dynamic mechanical analysers (DMAs). DMAs can apply higher torques compared to DSRs (Margaritis et al., 2021; Caro, Sánchez, et al., 2015). As with asphalt binders, the tests can be performed using the strain–sweep test and the viscoelastic continuum damage (VECD) theory or time-sweep tests. Numerous studies have indicated that the fatigue behaviour of asphalt mixtures is closely linked to the FAM because fatigue cracking typically originates from the FAM before propagating (Z. Zhang et al., 2021).

Li et al. (2018) showed that the stiffness and the fatigue resistance of the FAM are highly correlated with those of asphalt mastic, indicating that the filler has an important influence. Asphalt mastic is the critical material scale for evaluating the stiffness and the fatigue performance of asphalt mixes at mean temperatures.

This thesis aims to transfer the performance-based fatigue tests of asphalt mixes to a simplified test concept on the asphalt mastic level. Asphalt mastic combines asphalt binder and fine aggregate fractions and forms the main binder in asphalt mixes. Consequently, it significantly influences the material properties of asphalt mixes. Therefore, this thesis aims to identify the correlations between fatigue testing at asphalt mix and asphalt mastic levels to apply a practical quick and easy testing procedure at the asphalt mastic level. As a result, the quick assessment and control of the material selection for the asphalt mix becomes possible, making additional fatigue tests on the asphalt mix level largely unnecessary. Simple asphalt mastic-level fatigue tests could be used to predict the fatigue performance of asphalt mixes.

The fatigue behaviour of asphalt, mortar or mastic can be improved by various means. A common approach is the usage of modified binders, such as styrene–butadiene–styrene (SBS) polymer-modified asphalt binders, which offers advantages in terms of high- and low-temperature performances and fatigue resistance (Tauste-Martínez et al., 2022; Y. Zhang and Leng, 2017). Another method is the addition of fibres or other additives (e.g. graphene oxide) to improve the material's rheological properties (Adnan et al., 2021).

This thesis presents a detailed study of the current asphalt mastic-level fatigue tests and their relationship with asphalt mix-level fatigue tests. It is based on three publications produced as a part of the author's research activities. Chapter 3 to 5 summarize the main contents of these publications. The Appendix presents the original publications referred to in this work.

Chapter 2 explains the standardised fatigue test procedure at the asphalt mix level and the various fatigue test procedures at the asphalt mastic level. This chapter intends to provide an overview of the state of the art and acts as a starting point for all tests in this thesis.

Chapter 3 focuses on the contents of the publication titled 'Comparing different fatigue test methods at asphalt mastic level (Steineder, Peyer, et al., 2022)'. This chapter compares the various asphalt mastic-level fatigue testing methods based on laboratory tests. The research question is as follows: Which of the various fatigue tests can be used for all further tests in this thesis without influencing the applicability of the test results by loading method or fatigue criterion?

Chapter 4 and 5 focus on the two publications titled 'Correlation between stiffness and fatigue behaviour at asphalt mastic and asphalt mixture level (Steineder, Donev, et al., 2022)' and 'Assessing the impact of filler properties, moisture and ageing regarding fatigue resistance of asphalt mastic (Steineder and Hofko, 2023)' building on the findings of Chapter 3. These chapters compare the fatigue tests at the asphalt mix level with those at the asphalt mastic level. The two main research questions in this chapters are as follows: Can a correlation be established between the two fatigue tests? If so, will the filler influence the fatigue performance?

Chapter 6 presents a new approach that describes an alternative perspective for comparing the asphalt mix- and asphalt mastic-level fatigue tests based on the dissipated energy per load cycle, thereby introducing a novel method that goes beyond the content of the publications. This thesis provides more than a simple summary of the abovementioned publications and comprehensively presents the entire research work. The detailed analyses of the publications in Chapter 3–5 and unpublished results in Chapter 6 allow us to set the developed approaches, methods and findings into a broader context and present a global view of the research field.

Chapter 2

Test methods

This chapter explains one of the standardised fatigue test procedures at the asphalt mix level in Europe and provides a comprehensive overview of the various fatigue test procedures at the asphalt mastic level. These test methods are considered state of the art in the field and serve as a crucial starting point for all subsequent tests conducted within the scope of this thesis.

In addition to discussing the test procedures themselves, this chapter focuses on the test setup, result evaluation and fatigue criteria employed for assessing the asphalt mix and mastic performance. These aspects play a significant role in ensuring the accuracy and the reliability of the test outcomes.

2.1 Fatigue test method at the asphalt mix level in Austria

In Austria, the performance-based approach for the asphalt mix design is regulated by ÖNORM B 3580-2 (ÖNORM B 3580-2, 2018). Accordingly, the asphalt concrete (AC) is tested for fatigue resistance in accordance with ÖNORM EN 13108-20 (ÖNORM EN 13108-1, 2016) (Table D.4, reference number D.4.4). Hence, the performance-based test method according to ÖNORM EN 12697-24 (ÖNORM EN 12697-24, 2018), Method D — Four-point bending test on prismatic specimens is applied.

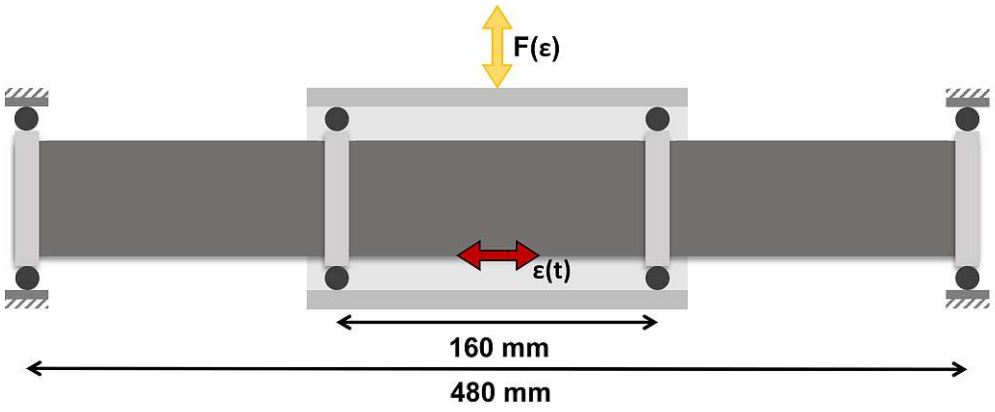

Fig. 2.1: Schematic figure of the performance-based test method according to ÖNORM EN 12697-24, Method D — Four-point bending test on prismatic specimen

ÖNORM EN 12697-24, Method D describes the test method for determining the fatigue performance of asphalt mixtures through strain-controlled four-point bending (4PB) testing. In this test method, a prismatic specimen is subjected to an oscillating load until a fatigue stage is reached. The following method is used to

- evaluate the fatigue performance of asphalt,

- evaluate the capability of asphalt,
- obtain data for the structural behaviour estimation, and
- evaluate the asphalt properties in relation to existing specifications.

For this test method, the prismatic specimen must be clamped in the testing machine using four symmetrically arranged clamps (Figure 2.1). The specimen dimension is 60 × 60 × 500 mm (width/height/length). The distance between the outer clamps is 480 mm while that between the inner clamps is 160 mm. The maximum grain size D should not exceed one-third of the width and height. All clamps must allow torsion and horizontal displacements. The outer clamps are fixed in position. The two inner clamps apply the periodic load in a vertical direction perpendicular to the longitudinal axis. The required load depends on the deformation amplitude at the bottom of the specimen. The load is symmetrically applied to the specimen axis and sinusoidal. The load applied, deformation and phase shift between these two parameters must be measured and recorded over the test duration. These measurement data can be used to determine the fatigue performance of the asphalt mix (ÖNORM EN 12697-24, 2018).

The fatigue test result comprises the number of load cycles $N_{f/50}$ until the fatigue failure criterion is reached at a defined load. The conventional failure criterion defines the fatigue stage according to EN 12697-24. The conventional criterion of fatigue defines the fatigue state of the specimen when the complex modulus S_{mix} decreases to half its initial value $S_{mix,0}$ (see Figure 2.2). The initial value $S_{mix,0}$ is defined as the magnitude of the complex modulus S_{mix} after 100 load cycles.

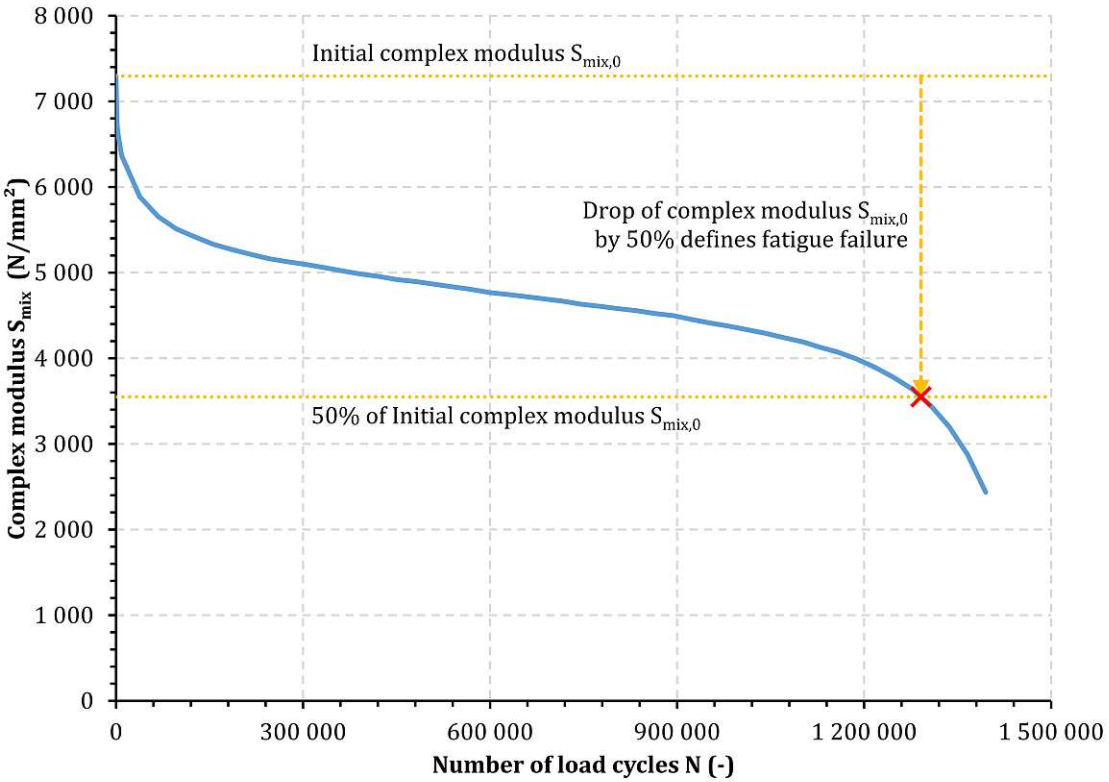

Fig. 2.2: Exemplaric complex modulus S_{mix} evolution with number of load cycles during a 4PB test

The test is performed in a thermostatically controlled test chamber, with a temperature of +20°C. The sinusoidally applied load frequency is 30 Hz. Figure 2.2 shows an example plot of the complex modulus S_{mix} over the load cycles. The red cross in Figure 2.2 depicts the load cycles $N_{f/50}$, the number of load cycles to failure according to the stated failure criterion. According to EN 12697-24, the fatigue criterion should occur within 10,000 to 2,000,000 load cycles.

For a complete asphalt mixture test, six specimens are tested at three different strain amplitudes. The strain amplitude ϵ corresponds to the maximum horizontal strain at the bottom of the specimen (see Figure 2.1). The 18 tests yielded a fatigue curve, namely the Wöhler curve. The fatigue curve function is determined as follows by regression analysis:

$$log\,(N) = A_0 + A_1 \cdot log\,(\epsilon) \tag{2.1}$$

The fatigue curve is used to determine the fatigue parameters ϵ_6 required by EN 12697-24. The strain ϵ_6 corresponds to the strain required to achieve 1,000,000 load cycles according to the fatigue curve for the selected failure criteria and test conditions. The parameter A_0 corresponds to the level of loading Q and the parameter A_1 corresponds to the slope of the fatigue curve. The parameters of the fatigue curve are ascertained through regression analysis. Figure 2.3 shows an exemplary fatigue curve and the derived characteristic values.

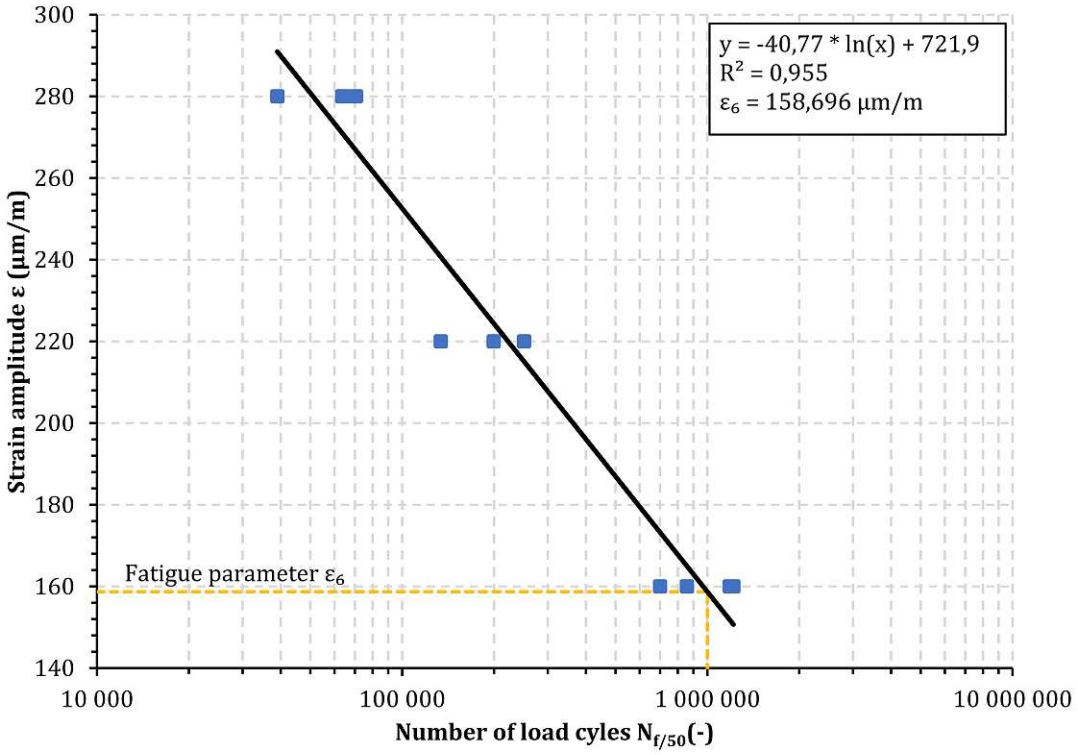

Fig. 2.3: Exemplary fatigue curve and derived characteristic value ϵ_6

The fatigue process can be characterized by the energy dissipation observed in a material during a load cycle. Energy is dissipated in a material subjected to repeated loading due to factors such as microcracking, heat generation, friction, and plastic deformation. These effects can collectively contribute to material failure. The greater the dissipated energy, the greater the potential for material damage and the greater the chance of a fatigue failure. The dissipated

energy of the load cycles in asphalt mixes is divided into the three following parts according to EN 12697-24:

- viscous energy dissipation in the beam due to bending;
- fatigue damage (e.g. occurrence of microdefects, etc.); and
- system losses (damping).

The influence of system losses can generally be neglected because the test frequency is far below the primary resonance frequency of the test equipment. These losses can usually be set equal to zero. The energy dissipated due to fatigue damage is usually much smaller than viscous energy dissipation. An exact magnitude assignment is impossible.

2.2 Fatigue test methods at the asphalt mastic level

The asphalt binder and mastic levels still require a standardised test method for evaluating the fatigue performance worldwide. For many years, attempts to determine the fatigue performance of asphalt mixtures have been made through simple tests on the asphalt binder or mastic level. The major problem is that, although many different fatigue testing methods at the asphalt binder and mastic levels are available, no test has yet been established internationally or nationally.

The subsequent section explains the developments and specifics of the major test methods used in this domain to provide a better overview of the various fatigue tests at the asphalt mastic level. This compact explanation allows us to clearly understand how the field has evolved over time and what techniques and procedures are used today. Chapters 2.2.1 and 2.2.1 present more detailed descriptions of the test methods relevant to this thesis.

Asphalt binder and the materials made from it are viscoelastic materials. In a purely viscous material, when stress is applied, it deforms and flows. The rate of deformation is proportional to the applied stress. Viscous materials resist shear flow and strain linearly with time when a stress is applied. In a purely elastic material, when stress is applied, it deforms and returns to its original shape once the stress is removed. Elastic materials store energy during deformation and release it during recovery. Asphalt binder's behaviour is a combination of these two. At higher temperatures or under slow loading, bitumen behaves more like a viscous liquid. At lower temperatures or under rapid loading, it behaves more like an elastic solid. The dynamic shear rheometer (DSR) is employed to assess the viscoelastic properties of asphalt binder, asphalt mastic or asphalt mortar. The DSR applies a sinusoidal shear strain to a sample and measures the resulting shear stress for strain-controlled tests. Conversely, in stress-controlled tests, the DSR applies a sinusoidal shear stress and measures the resulting shear strain. By analyzing the phase angle difference between the stress and strain, the instrument can determine the material's degree of viscoelasticity. The behaviour of viscoelastic materials is characterized by the complex modulus G^*. The complex modulus G^* encompasses two components: the storage modulus G', reflecting the material's elastic part, and the loss modulus G'', indicating its viscous part. These relationships can be visualized through a vector diagram (Figure 2.4).

In Figure 2.4, the component G' (storage modulus) represents the elastic portion of the material's behaviour. It indicates how much energy is stored and recovered during loading. The component G'' (loss modulus) represents the viscous portion of the material's behaviour. It indicates how much energy is dissipated. The phase angle (δ) represents the lag between the applied strain and the resulting stress or vice versa. It provides insight into the balance between the material's elastic and viscous behaviour.

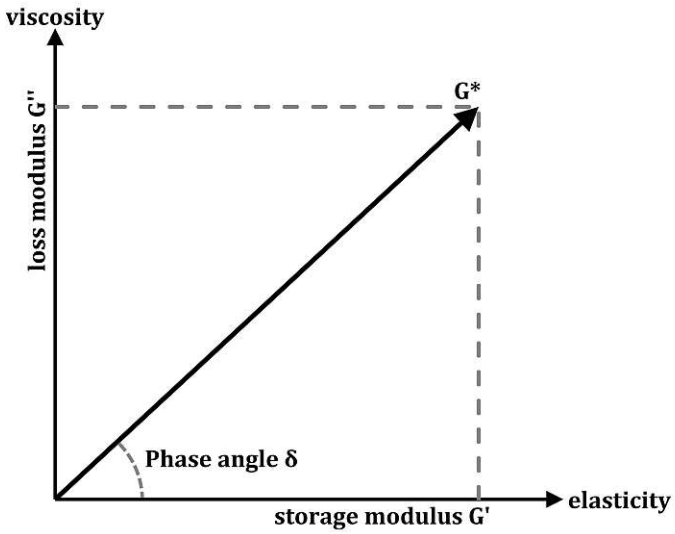

Fig. 2.4: Visualisation of the relationship between complex modulus G^*, storage modulus G', and the loss modulus G''

The Performance Grading (PG) specification of the asphalt binder in accordance with AASHTO M 320-17 (AASHTO M 320-17, 2017) has been developed within the Strategic Highway Research Program (SHRP) framework. The viscoelastic properties of the asphalt binder are determined and evaluated in relation to the fatigue behaviour of the asphalt mixture using a DSR (Anderson and Kennedy, 1993). However, studies have shown that the SHRP parameter ($|G^*| \cdot sin\,(\delta)$) that describes the fatigue performance of asphalt binders is not correlated with the fatigue behaviour of the asphalt mixtures, especially when modified asphalt binders are used (Zhou et al., 2013).

The time-sweep (TS) test has been further developed to describe the fatigue performance of asphalt binders. This test method is based on the conventional theory of material fatigue in asphalt pavements. The experiment simulates the pulsating load on an asphalt pavement caused by the stresses and strains generated by the passing tires (Hospodka et al., 2018). In the TS tests, the material is subjected to sinusoidal stress until material failure occurs. The test temperature, stress or strain amplitude and frequency can be selected individually. However, a standard that regulates this test method is still necessary. Different fatigue criteria have also been described in the literature, defining a material's fatigue state.

A significant advantage of the TS test compared to the PG test is the realistic load simulation on the material. In addition, the test can be adapted to different conditions by adjusting the frequency, temperature and loading type (stress or strain controlled). Tests outside the linear viscoelastic range are also possible. A clear disadvantage of the TS test is its long duration. A test can take several hours at low loads. The high stiffness of the mastic compared to the asphalt binder can push the DSR device to its performance limits.

For example, motor cooling can influence the results through the high system load (Y. S. Kim et al., 2021). To test the mastic, nevertheless, the system load on the DSR must be minimised. One possibility is using a hyperbolic specimen instead of a cylindrical one (Figure 2.5).

The use of axisymmetric notched specimens dates back to the early days of material science and mechanical engineering. Their simplicity in design, combined with the wealth of data they provide, has made them a staple in laboratories worldwide. Over the years, as our understanding of materials has evolved, so has the design and application of these specimens. However, their fundamental role in material characterization and fatigue testing remains unchanged (Hancock and Brown, 1983; Robisson, 2000; Olufsen et al., 2020).

Due to the necking in the specimen centre, the DSR requires less torque to apply the required load. In other words, the DSR does not reach its system limits. A disadvantage is that the measured rheological data cannot be used because no calculation model is available for converting data to this specific specimen geometry. However, the ratio of the number of load cycles until fatigue criteria between the two specimen geometries remains the same. Thus, the TS test with a hyperbolic specimen shape can be used to characterise the fatigue performance of asphalt mastic.

Fig. 2.5: Cylindrical (left) and hyperbolic (right) specimens

A further test evolution is the linear amplitude sweep (LAS) test. Cylindrical specimens made of asphalt binder or mastic with 8 mm diameter and 2 mm specimen height are tested according to AASHTO TP 101 (AASHTO TP 101, 2012). A significant advantage compared to the TS test is the short test duration of approximately 15 minutes per test. However, the test does not correspond to a realistic load simulation. The results of the LAS tests also show only slight correlations with results from comparative VECD-modeled fatigue tests (Zhou et al., 2013).

Numerous other specimen shapes have been observed aside from the cylindrical and hyperbolic specimens. These include different column specimen shapes with or without necking/notch (Van den bergh and Van de Ven, 2012; Shine et al., 2023).

In addition to these fatigue tests on the asphalt binder level using the DSR device, other test methods can be used to characterise the fatigue performance of binders using other devices, such as the double-edge notched tension test method (Ministry of Transportation Canada, 2012). However, a DSR is already part of the standard equipment of a road engineering laboratory; thus, only tests with the DSR are considered and performed in this thesis.

2.2.1 Time-sweep test

The TS test is a simple customisable fatigue test on the DSR for binders. In the TS test, a cylindrical specimen with 8 mm diameter and 2 mm height is usually mounted in the DSR. The binder specimen is prepared in a silicone mold, then mounted in the DSR and trimmed to a cylindrical shape. The specimen is then subjected to a predefined oscillating load (stress- or strain-controlled test) at the chosen temperature and frequency until fatigue is reached.

The fatigue failure determination has various definitions. You can either test until the material breaks or select a fatigue failure criterion. The basic parameters in this study were selected based on the following aspects considering the various TS test conditions and the lack of a standardised test procedure for the TS test:

- A test frequency of 30 Hz was selected for the TS test. A 10 Hz frequency is widely used in the literature (Y.-R. Kim, D. N. Little, et al., 2003; Martono et al., 2007; Mo et al., 2012). However, this thesis focuses on establishing a link between the fatigue performances between the 4PB and DSR tests; hence, the same test frequency of 30 Hz was selected for

the 4PB test on the asphalt mix level. This ensures that the tests can be quickly performed. However, the sufficient cooling capacity of the DSR must be ensured because the rapid oscillating load leads to a higher internal friction in the asphalt mastic and to higher heat generation in the specimen, which can negatively influence the test results.

- A +10°C test temperature was selected for the TS tests. In the literature (Smith and Hesp, 2000; Y.-R. Kim, D. N. Little, et al., 2003; Martono et al., 2007; Shen et al., 2006; Mo et al., 2012), temperatures between 0°C and +25°C have typically been used for the fatigue tests. While the test temperature for the 4PB test was at +20°C, a lower temperature was selected due to the mastic's low initial complex shear modulus $|G^*|_{initial}$ at +20°C. At low levels of $|G^*|_{initial}$ <15 MPa, the test result may be affected by the edge cracking formation (Anderson, Le Hir, et al., 2001). A high $|G^*|_{initial}$ is required to mainly obtain the material fatigue damage. In addition, +10°C approximately corresponds to the average annual temperature in Austria.

Numerous different fatigue failure criteria for evaluating fatigue performance tests exist in the literature. The following section summarises the most influential fatigue criteria for the evaluation of the TS tests of asphalt mastic. The fatigue failure criteria are separated into two categories: phenomenological criteria and that based on dissipated energy. The criteria can be applied to both stress- and strain-controlled tests.

The plot of the complex shear modulus $|G^*|$ and the phase angle δ is the most relevant when applying a fatigue failure criteria. Figure 2.6 shows a plot of the complex shear modulus $|G^*|$ and the phase angle δ of a strain-controlled (CD) TS test. Figure 2.7 presents the plot of the complex shear modulus $|G^*|$ and the phase angle δ of a stress-controlled (CS) TS test.

Figure 2.6 and 2.7 illustrate an initial transient phase for both loading methods. $|G^*|$ decreases in the short transient phase, while δ significantly increases. This phase is dominated by thixotropy (Shan, Tan, S. Underwood, et al., 2010; Shan, Tan, B. S. Underwood, et al., 2011; Hospodka et al., 2018). In rheology, thixotropy describes the time dependence of the binder's flow properties. In other words, the viscosity decreases due to the continuous mechanical loading and again increases after the loading stops. This phenomenon is, therefore, reversible.

After the transient phase, a phase dominated by material fatigue follows. Repeated loading causes microcracks in the specimen, which results in a $|G^*|$ decrease. These two phases can be observed in both plots (Figure 2.6 and 2.7), regardless of the loading type. The differences become apparent at the end of both fatigue plots.

In the stress-controlled tests, the phase angle increases as the stiffness decreases until fatigue failure occurs due to a test specimen fracture. This is recognised by the sharp drop in the phase angle after it reaches a maximum. The complex shear modulus also abruptly drops.

In the strain-controlled tests, the load decreases as the complex shear modulus decreases. Due to reduced $|G^*|$, less load is required to reach the defined strain. The fracture failure state in the specimen cannot be determined because the stiffness and the phase angle steadily decrease. Still, no abrupt drop happens in these parameters, which would correspond to a fracture failure. Therefore, using a fatigue failure criteria is necessary to define the fatigue failure state.

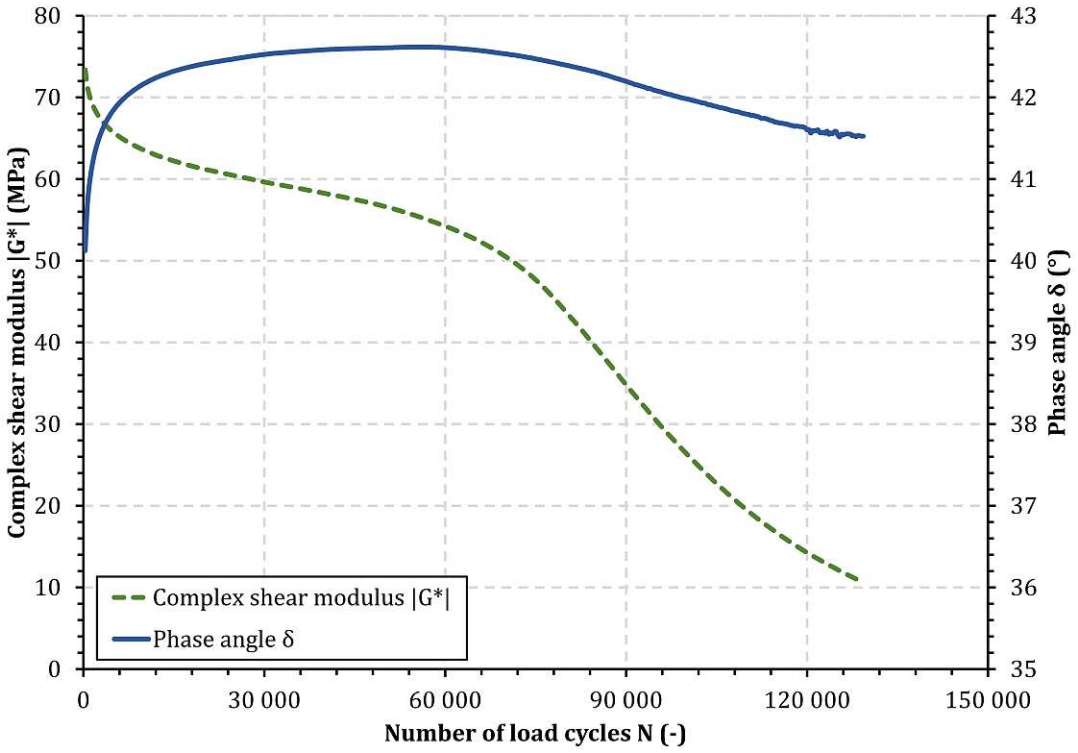

Fig. 2.6: Plot of a strain-controlled TS test

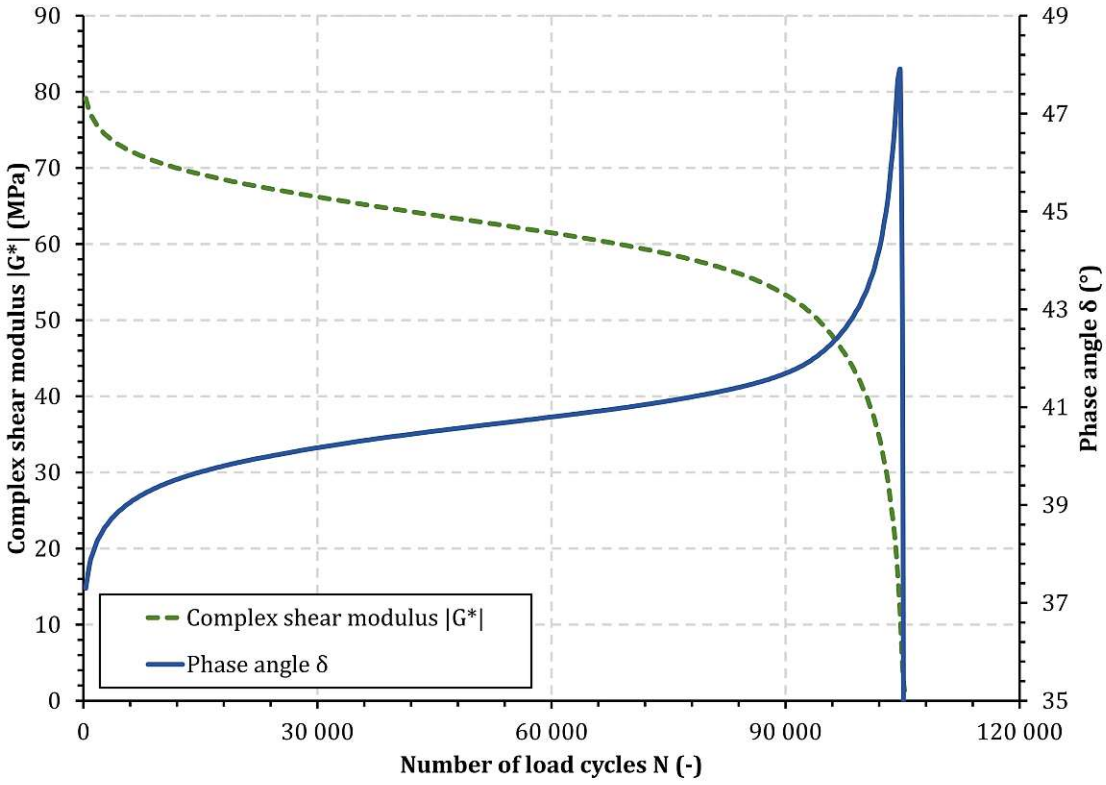

Fig. 2.7: Plot of a stress-controlled TS test

Phenomenological fatigue failure criteria:

- Reduction of stiffness (RS)
  At the asphalt mix level, the criterion of stiffness reduction to 50 % of the initial stiffness is applied as the definition of fatigue failure in Austria. It is defined in ÖNORM EN 12967-24 (ÖNORM EN 12697-24, 2018), AASHTO T 321-17 (AASHTO T 321-17, 2017), and SHRP A-404 (SHRP A-404, 1994). It can also be applied at the asphalt mastic level. The fatigue failure criterion RS defines the specimen failure when the complex shear modulus $|G^*|$ reaches 50 % of the initial complex shear modulus $|G^*|_{initial}$.

- Peak of phase angle (PA)
  The maximum phase angle can be used as a fatigue failure criterion. A maximum in the phase angle plot defines the fatigue state (Reese, 1997; Y.-R. Kim, D. Little, et al., 2003; Hospodka et al., 2018). However, a difference is observed between CS-TS and CD-TS tests. While the CS-TS tests show an apparent increase in the phase angle with a peak near the end of the test (Figure 2.7), the CD-TS tests illustrate a smooth increase. Multiple peaks that can bias the fatigue point determination can also often be found (Figure 2.6).

The dissipated energy is another option for use in defining a fatigue failure criterion at the mastic level. The following concepts are based on dissipated energy. The energy approach for asphalt mix and binders was developed in 1972 by van Dijk, Moreaud, Quedeville and Uge (van Dijk, W. and Moreaud, H. and Quedeville, A. and Uge, P., 1972). Their approach was based on the relationship between the fatigue life (N_f) and the cumulative dissipated energy at the fatigue state (van Dijk, W. and Moreaud, H. and Quedeville, A. and Uge, P., 1972; van Dijk, W. and Visser, W., 1977). For a viscoelastic material, the energy is dissipated during a loading cycle in the form of mechanical work, heat generation or fatigue damage (Rowe, 1993; Rowe, G., 1996).

- Dissipated energy ratio (DER)
  One of the best-known concepts based on dissipated energy is the DER fatigue criterion accepted by researchers worldwide as an applicable criterion. This approach calculates the dissipated energy for each load cycle (W_i) using Eq. (2.2). Although the application of Eq. (2.2) is limited to the linear viscoelastic region, it has nonetheless established itself as a method for comparative assessment of the fatigue performance of asphalt binder and asphalt mix even outside the linear viscoelastic region. Due to a comprehensive assessment of fatigue performance, an examination outside the linear viscoelastic region is necessary and common.

$$W_i = \pi \cdot \sigma_i \cdot \gamma_i \cdot sin\,(\delta_i) \tag{2.2}$$

  In Eq. (2.2), W_i is the dissipated energy in cycle i; σ_i is the stress level in cycle i; γ_i is the strain level in cycle i; and δ_i is the phase angle in cycle i. By summation, the cumulative dissipated energy up to load cycle n is calculated from the dissipated energy of all load cycles. The relationship between the cumulative dissipated energy up to load cycle n and the dissipated energy in load cycle n (W_n) is described by the DER in Eq. (2.3):

$$DER = \frac{\sum_{i=1}^{n} W_i}{W_n} \tag{2.3}$$

  The DER evaluation initially plots a linear increase for both load types (i.e. CS and CD). However, with the increasing test duration, the DER deviates from the linear gradient,

indicating a fatigue state. The parameter N_{p20} was defined by Bonnetti et al. (2022) and describes the number of load cycles until the DER deviates by 20 % from the undamaged linear line. Therefore, N_{p20} defines the fatigue failure point.

- Ratio of dissipated energy change (RDEC)
  A further development of the fatigue characterisation based on dissipated energy is depicted by the RDEC approach (Carpenter and Shen, 2006; Shen et al., 2006). RDEC defines the change in the dissipated energy between cycles n and n + 1 divided by the total dissipated energy up to load cycle n. In this approach, fatigue failure is defined by an abrupt increase in the RDEC because, by initiating material failure, a larger fraction of the energy dissipates when compared in the previous cycle (Ghuzlan, 2006). This behaviour cannot be observed in an undamaged sample. The RDEC is calculated in Eq. (2.4) as follows:

$$RDEC = \frac{W_{(n+1)} - W_n}{W_n \cdot \left(N_{(n+1)} - N_n\right)} \tag{2.4}$$

  In Eq. (2.4), W_n is the dissipated energy of the load cycle n, $W_{(n+1)}$ is the dissipated energy of load cycle (n + 1), $N_{(n+1)}$ are the total number of load cycles up to cycle n+1 and N_n are the total number of load cycles up to cycle n.

  The RDEC plot over the test duration is divided into three phases: an initial phase with a decreasing tendency, a plateau phase and a phase with a rapid increase. No common criterion for fatigue has yet been defined in the literature.

2.2.2 Linear amplitude sweep test

The LAS test is a fatigue test for asphalt binders based on the viscoelastic continuum damage (VECD) model performed with the DSR. Compared to the TS test, the LAS test is a standardised test method according to AASHTO TP 101 (AASHTO TP 101, 2012). For this test, a cylindrical specimen with 8 mm diameter and 2 mm height is used. The binder sample is prepared in a silicone mold, then mounted in the DSR and trimmed to the cylindrical shape. The test is performed in two phases according to AASHTO TP 101:

1. The rheological properties of the undamaged specimen are determined in the first phase. The material behaviour is determined using a strain-controlled frequency sweep test. The specimen is loaded at a constant temperature by an oscillating strain amplitude of 0.1 % (strain-controlled). The rheological behaviour is determined according to AASHTO TP 101 for 12 defined frequencies ranging from 0.2 to 30 Hz (frequency sweep). The measurements determine the complex shear modulus $|G^*|$ and the phase angle δ for the 12 frequency steps (Figure 2.8).

   The specimen retains in the linear viscoelastic material behaviour due to the low stress of 0.1 % strain. Consequently, no damage occurs in the specimen during this test phase. The parameter α can be determined with Eq. (2.5), (2.6) and (2.7) based on the plotted quantities $|G^*|$ and δ. Parameter α is needed to determine the number of load cycles N_f. The storage modulus G' required to calculate α is calculated from $|G^*|$, δ and the angular frequency ω (depending on the frequency) according to Eq. (2.5).

$$G'(\omega) = |G^*|(\omega) \cdot cos(\delta(\omega)) \tag{2.5}$$

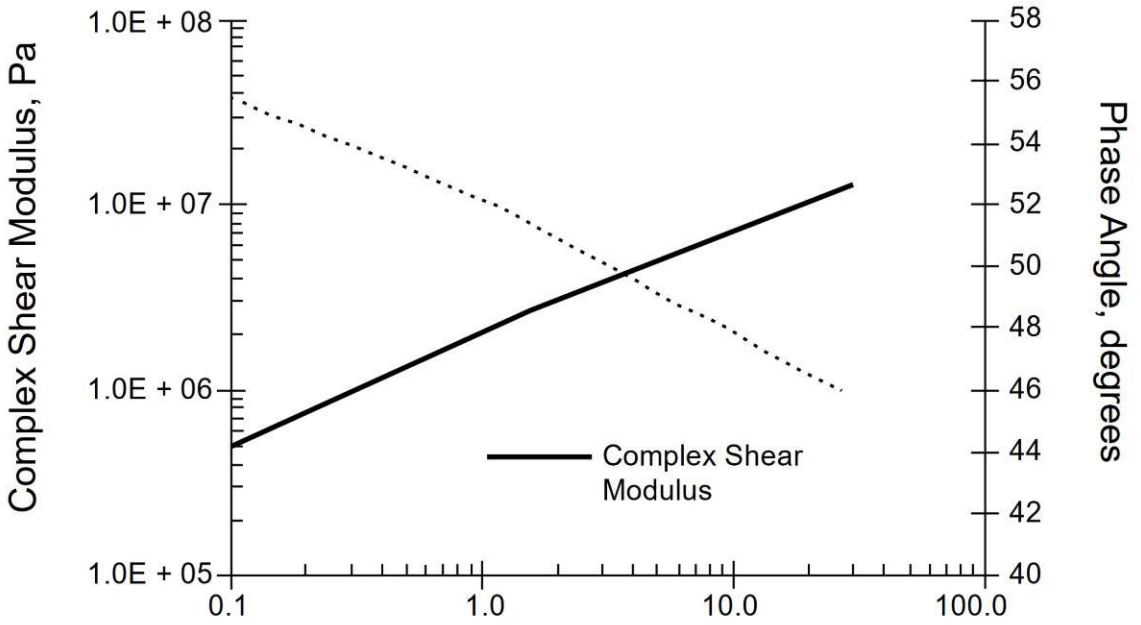

Fig. 2.8: Plot of $|G^*|$ and δ of a strain-controlled frequency sweep test (AASHTO TP 101, 2012)

By fitting a logarithmic linear graph to the storage modulus G'-plot, the slope parameter m is approximately determined by Eq. (2.6).

$$log\left(G'\left(\omega\right)\right) = m \cdot log\left(\omega\right) + b \tag{2.6}$$

According to AASHTO TP 101, parameter α corresponds to the reciprocal of the slope parameter m from Eq. (2.6) and is required to determine the number of load cycles N_f.

$$\alpha = \frac{1}{m} \tag{2.7}$$

2. In the second test phase, a strain-controlled amplitude sweep test is performed on the same mounted specimen at a 10 Hz constant frequency and temperature. The test lasts 310 s, during which the applied strain amplitude is linearly increased from 0 % to 30 %. The shear strain, shear stress, complex shear modulus and phase angle are plotted every second. Using the viscoelastic continuum damage model (VECD) according to AASHTO TP 101, the damage accumulation at the time of failure D_f and two model parameters A and B can be determined with parameter α from the first test phase and the results from the second test phase (Eqs. (2.8), (2.9) and (2.10)).

$$A = \frac{f \cdot (D_f)^k}{k \cdot (\pi \cdot C_1 \cdot C_2)^\alpha} \tag{2.8}$$

$$B = 2 \cdot \alpha \tag{2.9}$$

$$k = 1 + (1 - C_2) \cdot \alpha \tag{2.10}$$

In Eqs. (2.8), (2.9) and (2.10), f is the applied frequency in the second test phase (f = 10 Hz); D_f is the damage accumulation at the time of failure; and C_1 and C_2 are the fatigue coefficients according to AASTHO TP 101. Parameters A and B, which can be determined using Eq. (2.8) and (2.9), are applied for the fatigue law in Eq. (2.11):

$$N_f = A \cdot (\gamma_{max})^{-B} \tag{2.11}$$

In Eq. (2.11), N_f is a characteristic parameter for fatigue performance; A and B are the model parameters according to the viscoelastic continuum damage model; and γ_{max} is the maximum shear strain expected in the asphalt binder of a given asphalt structure. Using Eq. (2.11), a linear correlation can be established between the parameter N_f and the expected strain γ_{max}. Value A corresponds to the initial y displacement while value B corresponds to the slope (Figure 2.9).

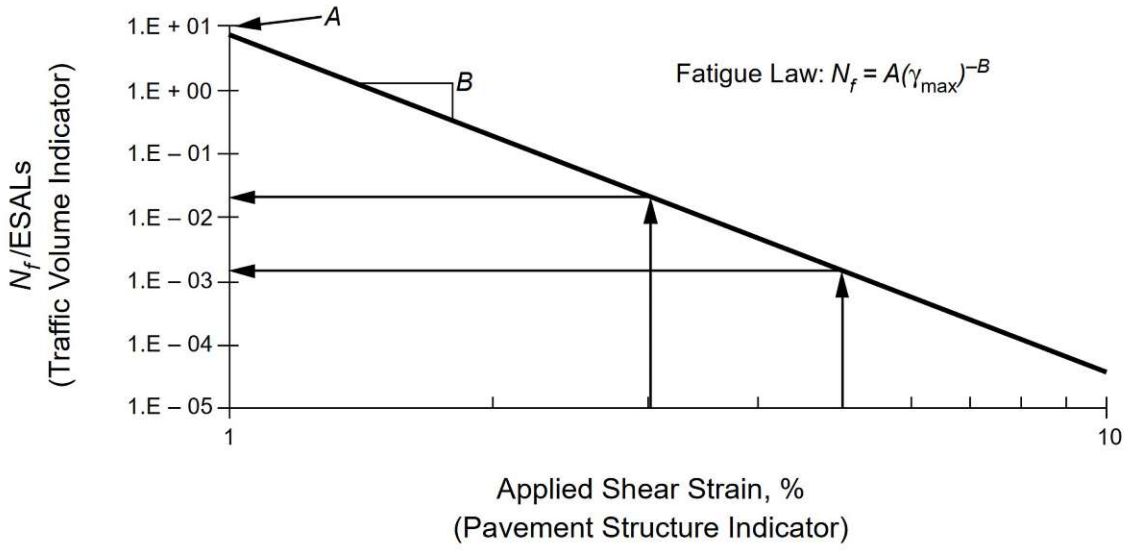

Fig. 2.9: Fatigue performance as a function of γ_{max} (AASHTO TP 101, 2012)

Chapter 3

Comparison of the fatigue performance tests and their fatigue failure criteria at the asphalt mastic level

A practical fatigue performance test for asphalt mastic is necessary when applying a practical testing procedure at the asphalt mastic level, which can quickly and accurately be correlated to the fatigue performance of an asphalt mix. Based on the test methods presented in Chapter 2, this chapter sets the baseline for all further fatigue testing procedures of the asphalt mastic conducted in this thesis. The decision on which test method to use has a significant impact; therefore, this chapter will be addressed in more detail to determine the best possible approach. The intention is to investigate the comparability of the fatigue tests with varying loading modes, geometries and fatigue failure criteria to find a fatigue test with a high accuracy, a simple application and a good comparability with other fatigue performance tests. The main parts of this chapter are presented in the publication title 'Comparing different fatigue test methods at asphalt mastic level (Steineder, Peyer, et al., 2022)' (Appendix 1).

Four different mastic mixes are tested for the fatigue performance on the DSR using the described test methods and criteria in Chapters 2.2.1 and 2.2.1 to select a fatigue performance test method and a suitable fatigue failure criterion for this thesis. Two different fatigue performance tests with the DSR are used for this comparison, namely TS and LAS tests. Both tests are performed with cylindrical and hyperbolic specimen shapes. The fatigue failure criteria PA, RS, DER and RDEC for the fatigue evaluation are applied for the TS tests. For the LAS tests, the VECD method is used for the fatigue evaluation. Figure 3.1 shows the range of fatigue performance tests performed.

The fatigue performance of four different asphalt mastic mixes is examined to study the different test methods and fatigue criteria. Four fillers are used for the asphalt mastic mixes, including limestone and quartz from Europe and stone dust and glass powder from India. The fillers were mixed with asphalt binder to create mastics with a filler–binder ratio of 1.5 by weight. The various filler densities result in different filler–volume ratios of the asphalt mastic mixes (Table 3.1).

Tab. 3.1: Mixed mastic for comparing the fatigue performance tests

Mixture	Binder	Filler	Filler–Binder Ratio (-)	Filler–volume Ratio (%)
Mastic 1 (M1)	70/100	Lime stone	1.5	24.2
Mastic 2 (M2)	70/100	Quartz	1.5	25.7
Mastic 3 (M3)	70/100	Stone dust	1.5	25.2
Mastic 4 (M4)	70/100	Glass powder	1.5	28.7

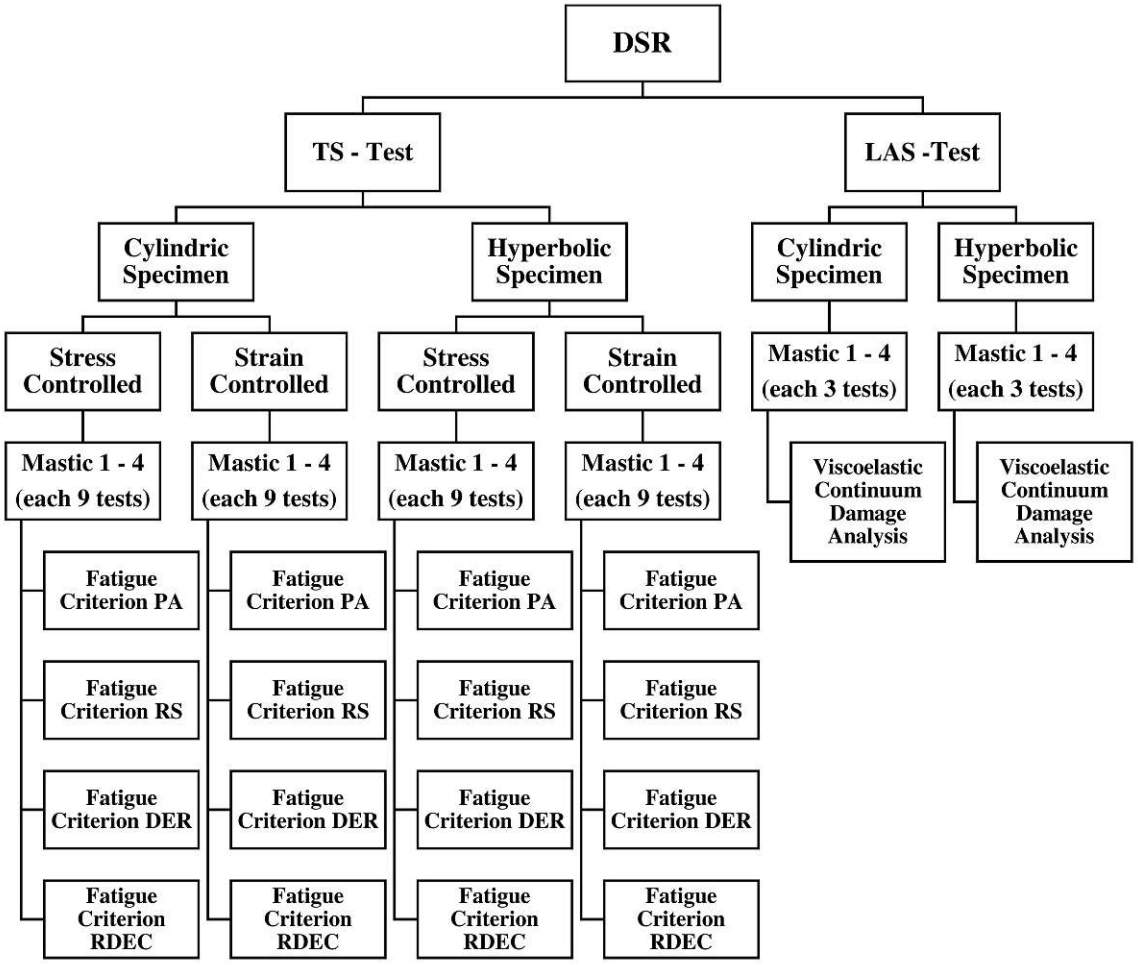

Fig. 3.1: Test range for the different test methods and fatigue criteria

While the LAS test is standardised, the test parameters must be selected for the TS test. Nine individual TS tests were performed at three different loading levels for a fatigue curve resulting from the TS tests. Based on the chosen fatigue failure criterion, a fatigue curve, namely the Wöhler curve, can be constructed similar to the fatigue curve at the asphalt mix level (Figure 2.3). The fatigue curve can then be used to analyse and compare the fatigue performance tests for the asphalt mastics.

All TS tests are performed at a 30 Hz frequency and a +10°C temperature. The stress-controlled tests are conducted at 300, 400 and 500 kPa for the hyperbolic specimens and 700, 1000 and 1200 kPa for the cylindrical specimens. The strain-controlled tests are conducted at 0.5 %, 0.75 % and 1.00 % for both the specimen geometries. Meanwhile, the PA, RS and DER fatigue failure criteria are clearly defined. The RDEC lacks a clear definition of the fatigue point. For this study, the fatigue point is defined as follows: failure occurs if the RDEC is twice as large as that in the plateau phase. The plateau value corresponds to the average value of all the RDEC values between decreasing and increasing. The LAS tests are performed at a +10°C temperature. For the LAS test, three replicates per mastic are performed.

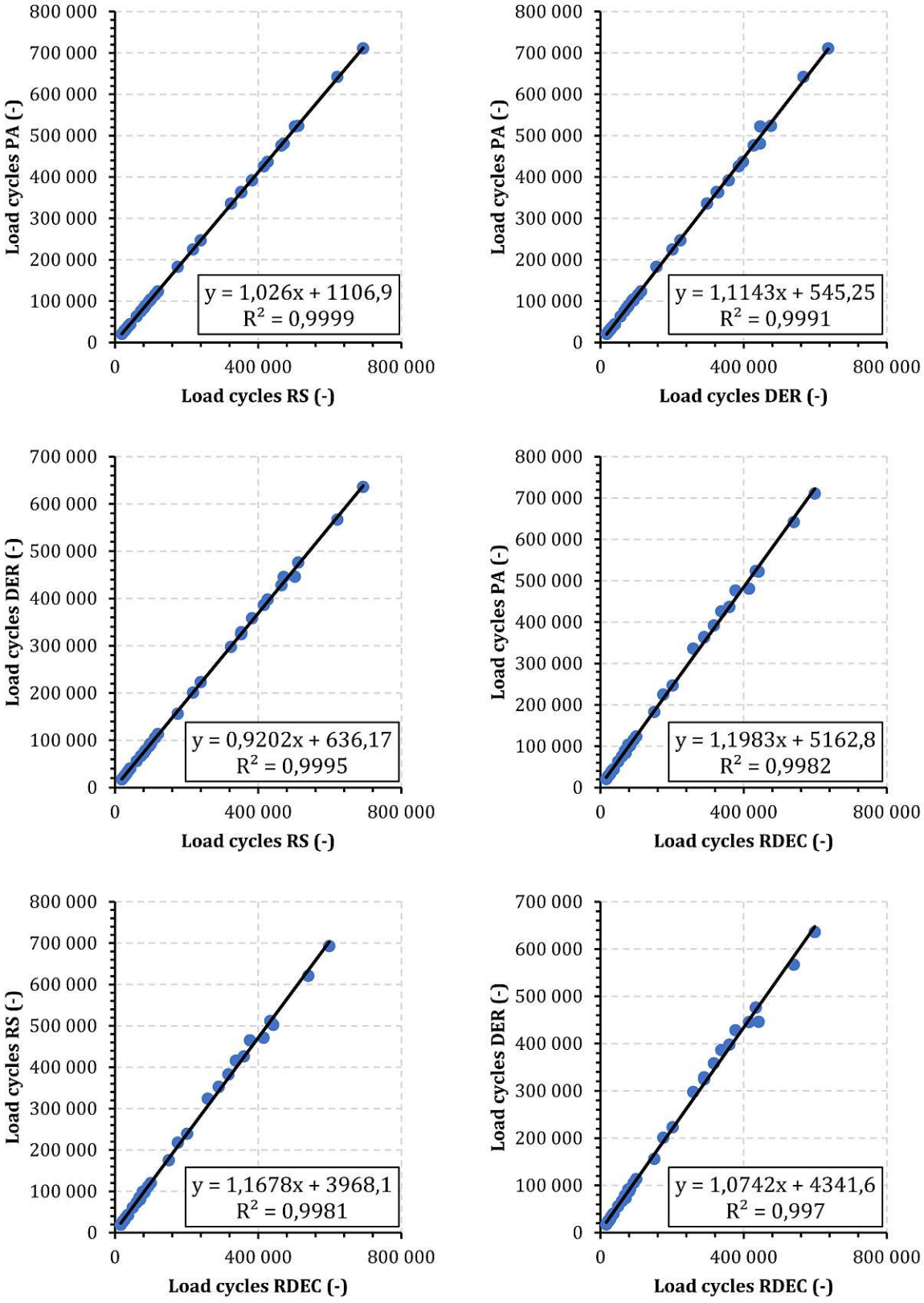

Fig. 3.2: Comparability of the fatigue failure criteria in the CS-TS tests with hyperbolic specimen shape (36 data points used for linear regression analysis).

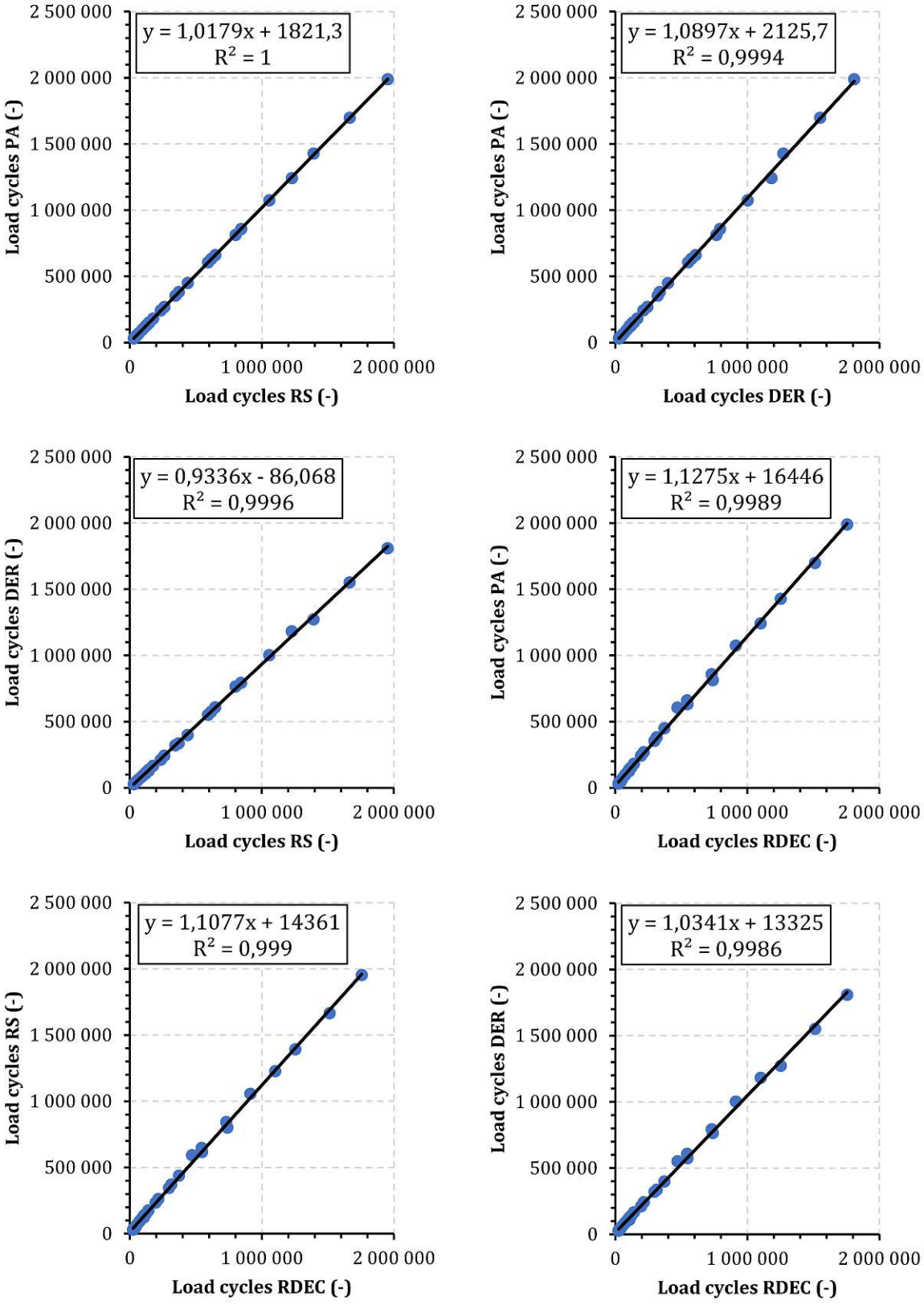

Fig. 3.3: Comparability of the fatigue failure criteria in the CS-TS tests with cylindrical specimen shape (36 data points used for linear regression analysis).

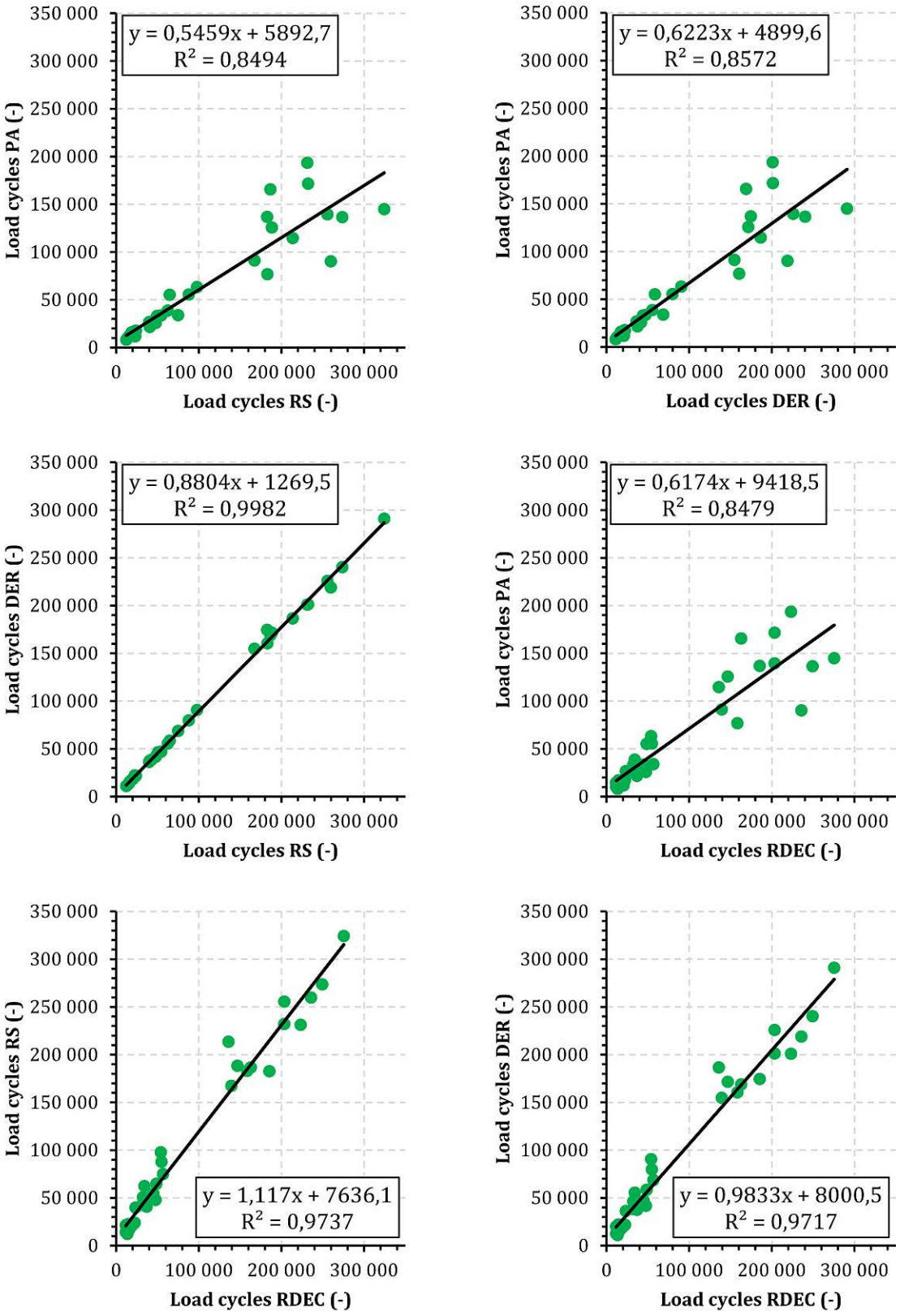

Fig. 3.4: Comparability of the fatigue failure criteria in the CD-TS tests with hyperbolic specimen shape (36 data points used for linear regression analysis).

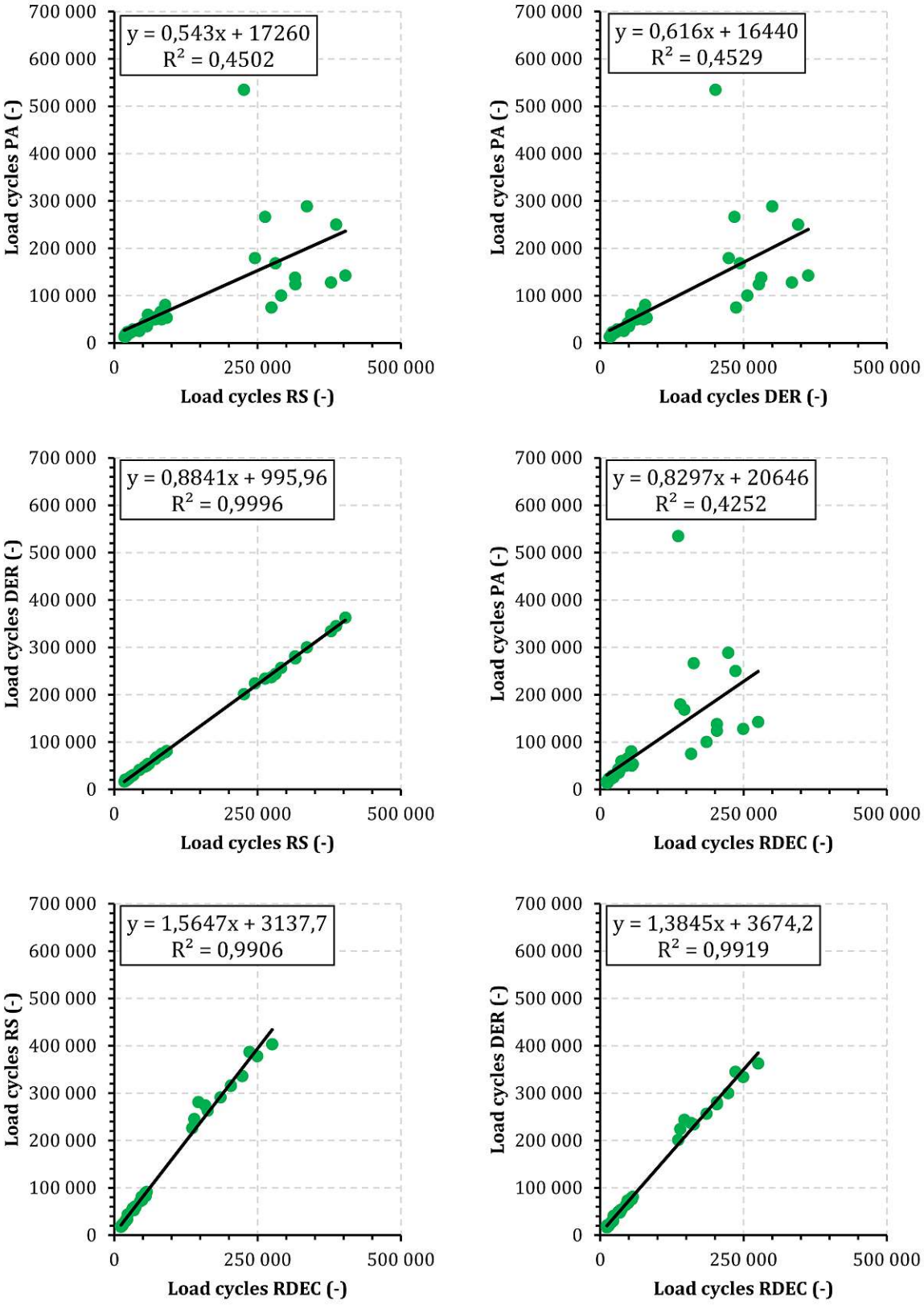

Fig. 3.5: Comparability of the fatigue failure criteria in the CD-TS tests with cylindrical specimen shape (36 data points used for linear regression analysis).

The comparability of the different fatigue performance tests was studied based on the obtained data. The different fatigue failure criteria applied to the TS tests were compared in the first step. The determined number of load cycles according to the different fatigue failure criteria were compared using a simple linear regression analysis. In Figures 3.2 and 3.3, all four fatigue failure criteria (i.e. PA, RS, DER and RDEC) show an excellent comparability in all the CS-TS tests. For the CD-TS tests, the fatigue failure criteria RS and DER demonstrate an excellent comparability (Figures 3.4 and 3.5).

The PA criterion leading to a large scatter in the number of load cycles for the CD-TS may be attributed to the phase angle evolution over the test duration. While a clear maximum in the phase angle can be seen in the stress-controlled tests, the phase angle in the strain-controlled tests formed a horizontal plateau (Figure 2.6), which precisely determined the fatigue point to be more difficult. The RDEC criterion leading to a large scatter in the number of load cycles for the CD-TS tests may be attributed to the shear stress evolution over the test duration. In the stress-controlled tests, the shear stress remained constant, whereby increasing the fatigue caused the specimen deformation to become larger to apply the necessary shear stress. As fatigue proceeded and the loading cycles increased, a significant increase in the deformation occurred toward the end of the test, leading to an actual specimen fracture. Consequently, the dissipated energy also significantly increased (Figure 3.6). By contrast, the deformation remained constant in the strain-controlled tests. As fatigue proceeds and the loading cycles increased, less shear stress was required to maintain the required deformation. Consequently, the dissipated energy fell flat toward the end of the test (Figure 3.7) and an actual fracture did not necessarily occur. Consequently, the abrupt increase in the RDEC was not as clear-cut as in the CS-TS tests, which can result in some scatter.

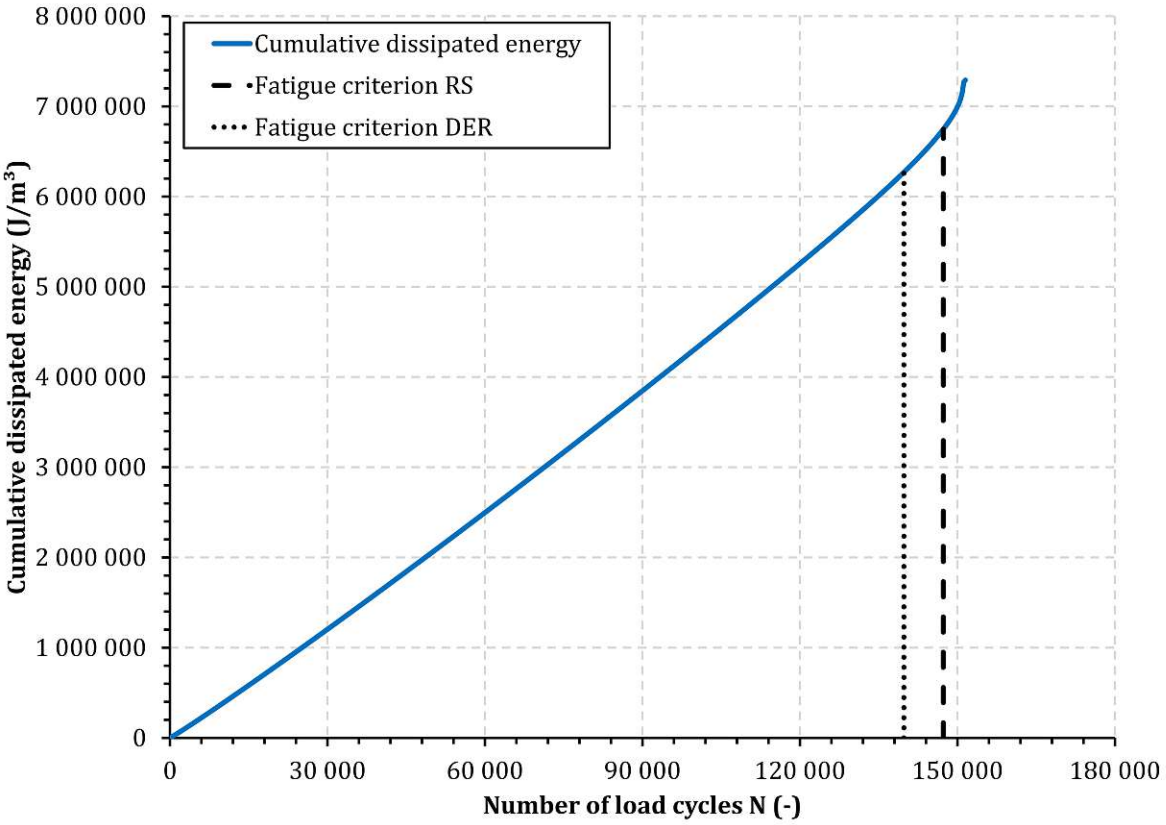

Fig. 3.6: Exemplary plot of the cumulative dissipated energy for CS-TS

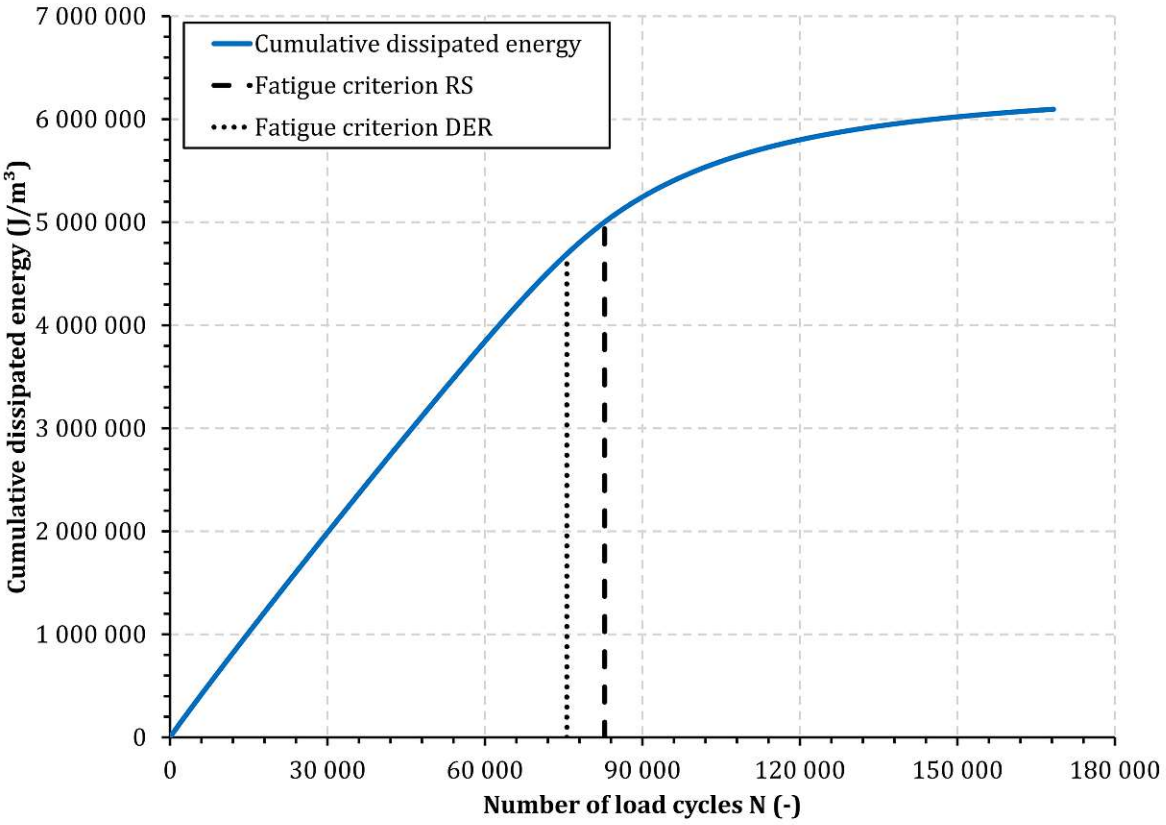

Fig. 3.7: Exemplary plot of the cumulative dissipated energy for CD-TS

The different test methods were compared in the second step. For this purpose, a characteristic value of the fatigue curve was used. The characteristic value corresponded to the load (stress or deformation) required to achieve 100,000 load cycles according to the derived fatigue curve, abbreviated as τ_5 for CS tests and γ_5 for CD tests. All tests listed in Figure 3.1 were compared, whereby only the fatigue failure criteria RS and DER were used for the TS tests. Statistical evaluations were not performed due to the low number of mastics. Only the fatigue performance ranking was compared. Table 3.2 and 3.3 summarizes the rankings of the different tests. One represents the highest stress τ_5 or deformation γ_5 required to achieve 100,000 load cycles. Four is the lowest stress τ_5 or deformation γ_5 required to achieve 100,000 load cycles.

Table 3.2 and 3.3 shows that the TS tests with different loading modes and the LAS tests lead to different fatigue performance rankings. However, the hyperbolic specimen shape does not influence the ranking in the TS tests. The results of mastics 2 and 3 in the CS-TS tests are very close to each other; hence, the ranking does not make a significant difference here. The hyperbolic specimen shape might influence the fatigue performance ranking in the LAS tests. In conclusion, the loading type in the fatigue tests affects the fatigue performance ranking. Moreover, using hyperbolic specimens in the LAS tests can only be applied with further analysis model adjustments.

Tab. 3.2: Ranking of the fatigue performance parameter τ_5 from tests performed at the asphalt mastic level

Shape	**Hyperbolic**		**Cylindric**	
Test	CS-TS			
Value	τ_5			
Crit.	RS	DER	RS	DER
Mastic 1	4	4	4	4
Mastic 2	3	3	2	2
Mastic 3	2	2	3	3
Mastic 4	1	1	1	1

Tab. 3.3: Ranking of the fatigue performance parameter γ_5 from tests performed at the asphalt mastic level

Shape	**Hyperbolic**			**Cylindric**		
Test	CD-TS		LAS	CD-TS		LAS
Value	γ_5					
Crit.	RS	DER	VECD	RS	DER	VECD
Mastic 1	3	3	3	3	3	4
Mastic 2	1	1	2	1	1	3
Mastic 3	2	2	1	2	2	2
Mastic 4	4	4	4	4	4	1

The results show a need for an assessment method for the fatigue performance that is independent of the loading mode (CS or CD). Therefore, a new assessment method was developed herein to evaluate the fatigue performance independent of the loading mode (CS or CD).

Assessing the cumulative dissipated energy, the CS-TS and CD-TS plots reveal that the cumulative dissipated energy almost linearly increases up to the fatigue points according to the RS and the DER criteria (Figure 3.6 and Figure 3.7). Dividing this by the number of load cycles achieved reveals the dissipated energy per load cycle (DELC) (Eqs. (3.1) and (3.2)).

$$DELC_{RS} = \frac{\sum_{i=1}^{N_{RS}} W_i}{N_{RS}} \tag{3.1}$$

$$DELC_{DER} = \frac{\sum_{i=1}^{N_{DER}} W_i}{N_{DER}} \tag{3.2}$$

In Eqs. (3.1) and (3.2), W_i is the cumulative dissipated energy until load cycle i and N denotes the number of load cycles to failure as defined by the criteria RS or DER. With the DELC method, the accepted fatigue failure criteria RS and DER can continuously be used, but with the advantage that the test results with different loading types can be combined into a common fatigue curve (Figure 3.8).

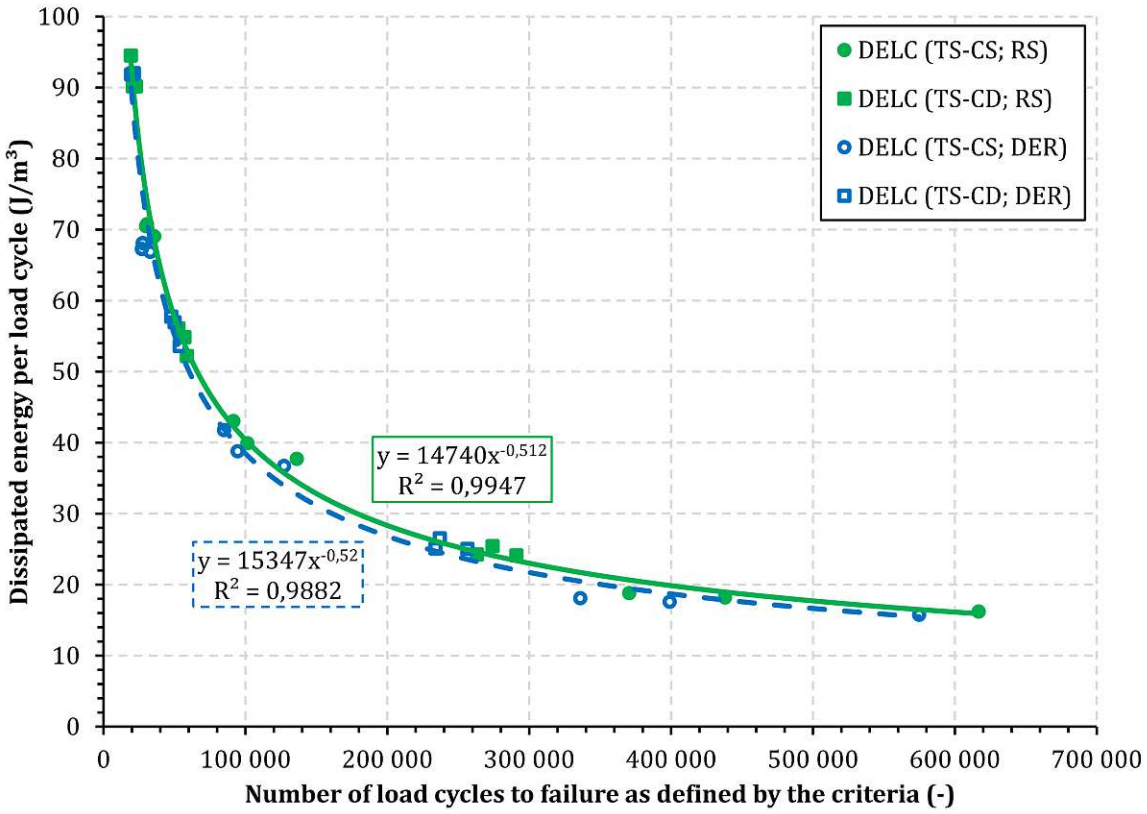

Fig. 3.8: Exemplary fatigue curve evaluated with the DELC method

According to the DELC method, a high dissipated energy per load cycle caused by the load in the DSR leads to a low number of load cycles until fatigue. By contrast, a low dissipated energy per load cycle leads to a high number of load cycles until fatigue. This also corresponds to the observation that high loads lead to a shorter lifetime compared to small loads. However, the energy dissipates due to internal friction, viscous deformation and fatigue. This thesis does not include distinguishing between these impact factors. Different fatigue criteria and specimen shapes lead to the same rankings in the CS-TS tests and applying the DELC criterion is reasonable. Hence, the CS-TS tests with a hyperbolic specimen shape were conducted in this work.

Chapter 4

Statistical correlation between fatigue performance testing at the asphalt mix and asphalt mastic levels

The previous chapter outlined the challenges encountered by different loading modes (CS or CD) and fatigue failure criteria in the context of assessing the fatigue performance. After a careful consideration, the CS-TS method was chosen because of the good comparability of all the fatigue criteria investigated in CS-TS. The PA criterion was selected as the fatigue failure criterion because it accurately describes the actual fatigue failure in the specimens and a good comparability is observed with the other fatigue failure criteria studied in the CS-TS tests. The main parts of this chapter are presented in the publication titled 'Correlation between stiffness and fatigue behaviour at asphalt mastic and asphalt mixture level (Steineder, Donev, et al., 2022)' (Appendix 2).

In this publication, a comprehensive investigation was conducted to identify statistical correlations that link material behavior both at the asphalt mix level and the asphalt mastic level. It is important to emphasize that this study did not delve into detailed micromechanics. This means that certain factors, such as the volume proportion of aggregate, the properties of coarse aggregate, and the air void content in the asphalt mix, were not taken into account. However, such factors can have a significant impact on the overall behavior of the material and should be considered in future studies.

Recipe-based empirical tests have traditionally been used for asphalt mix design optimisation and quality control. Accordingly, performance-based tests have also been introduced to simulate the effects of traffic and climate load on asphalt mixtures because they can better predict the mechanical behaviour and performance. These tests require a high amount of materials and time; thus, all parties seek a more efficient method of assessing the fatigue performance of the asphalt mixtures. One option is to shift the performance-based fatigue test from the asphalt mix level to the asphalt mastic level.

Fatigue is an important failure mechanism in asphalt pavements, with microcracks in the asphalt binder assumed to initiate the crack formation. Previous studies (Liao et al., 2011; Chen et al., 2020) have shown that adding mineral filler to the asphalt binder, which is defined as mastic, can improve its fatigue life. Therefore, asphalt mastic affects the fatigue performance of asphalt mixes, providing a reasonable basis for assessing the fatigue performance at the asphalt mix level.

The publication titled 'Correlation between stiffness and fatigue behaviour at asphalt mastic and asphalt mixture level (Steineder, Donev, et al., 2022)' discusses different regression models for linking the fatigue performance between the asphalt mix and asphalt mastic levels. The objective here is to simplify performance-based fatigue tests at the asphalt mix level with simpler fatigue performance tests at the asphalt mastic level. The 4PB test is used in Austria; thus, the focus is on fatigue tests for asphalt mixes using this test method.

The data for the regression models were collected from extensive fatigue tests at the asphalt mix and asphalt mastic levels. Accordingly, 14 asphalt mixes and the corresponding asphalt mastic were tested for the fatigue performance. The results were used to generate regression models linking the two levels. Table 4.1 summarizes the compositions of the tested asphalt mixes and mastic mixtures.

Tab. 4.1: Summary of the studied mixes on the asphalt mix and asphalt mastic levels

Asphalt mix (asphalt mastic + aggregates (>0.125 mm)				
	Asphalt mastic			
No.	Asphalt binder	Filler (<0.125 mm)	Aggregates (<0.125 mm)	Aggregates (>0.125 mm)
1	Manufacturer 1 — 50/70	Limestone	Gabbro	Gabbro
2	Manufacturer 1 — PmB 25/55-55	Limestone	Gabbro	Gabbro
3	Manufacturer 2 — 50/70	Limestone	Gabbro	Gabbro
4	Manufacturer 2 — PmB 25/55-55	Limestone	Gabbro	Gabbro
5	Manufacturer 3 — 50/70	Limestone	Gabbro	Gabbro
6	Manufacturer 3 — PmB 25/55-55	Limestone	Gabbro	Gabbro
7	Manufacturer 4 — 50/70	Limestone	Gabbro	Gabbro
8	Manufacturer 4 — PmB 25/55-55	Limestone	Gabbro	Gabbro
9	Manufacturer 4 — 70/100	Limestone	Gabbro	Gabbro
10	Manufacturer 4 — PmB 45/80-65	Limestone	Gabbro	Gabbro
11	Manufacturer 4 — 70/100	Limestone	Porphyry	Porphyry
12	Manufacturer 4 — PmB 45/80-65	Limestone	Porphyry	Porphyry
13	Manufacturer 4 — 70/100	Limestone	Silicate	Silicate
14	Manufacturer 4 — PmB 45/80-65	Limestone	Silicate	Silicate

The selected asphalt mix design was AC with 11 mm maximum grain size and a binder content of 5.9 % per mass. All mix designs were optimised to achieve comparable grading curves and void contents despite the different aggregates used. A 3.5 % void content by volume was aimed for all mixes, presenting an acceptable range of 2.5 % to 4.5 % by volume. The mixing temperature was set to 160°C according to EN 12697-35 (ÖNORM EN 12697-35, 2016). The filler's proportion and composition (mineral fractions <0.125 mm) in the asphalt mastic were equal with asphalt mix formulations. The filler comprised its own filler from the different aggregate fractions (gabbro, porphyry or silicate) and the added limestone filler. Combined with the binder content of 5.9 % per mass, this resulted in various asphalt mastic mixes (Table 4.1).

The test programme used different aggregates, fillers and asphalt binders from Central and Western Europe to produce asphalt mastics and mixtures. Ten asphalt binders were selected, including unmodified and polymer-modified ones. The particle size distribution was determined for the aggregates. Various tests were then conducted on the asphalt binders, including softening point, needle penetration depth, and performance grade. Appendix 2 (publication 2) presents the results for all 10 asphalt binders.

The stiffness for the asphalt mixes was tested according to EN 12697-26 (ÖNORM EN 12697-26, 2018). The fatigue performance was assessed according to EN 12697-24 (ÖNORM EN 12697-24, 2018). The fatigue performance of the asphalt mastic was tested by the DSR using a stress-controlled TS test on hyperbolic specimens. The PA was selected as the fatigue failure criterion because it defines the exact point of material failure with the CS-TS tests and correlates well with the other criteria.

This publication presented a statistical correlation between both experimental levels. A direct correlation existed between the dynamic modulus $|E^*|$ of the asphalt mix (mean value of initial complex modulus at 30 Hz from all single tests of one asphalt mix) and the initial complex shear modulus of the asphalt mastic (mean value of the complex shear modulus $|G^*|$ after 300 load cycles from nine single tests of one asphalt mastic mix). Figure 4.1 shows the correlation in graphical form. According to general assumptions, a softer asphalt binder in terms of penetration grade has a lower stiffness than a harder asphalt binder. The needle penetration test for asphalt binder is a standard laboratory method according to ÖNORM EN 1426 (ÖNORM EN 1426, 2015), used to determine the consistency of bituminous materials. In this test, a standard needle is vertically penetrated into a sample of the asphalt binder at a specified temperature, usually +25°C. The depth to which the needle penetrates the binder within a given time period, typically 5 seconds, is measured in tenths of a millimeter and indicates the binder's consistency or softness. A higher penetration value suggests a softer binder, while a lower value indicates a harder binder.

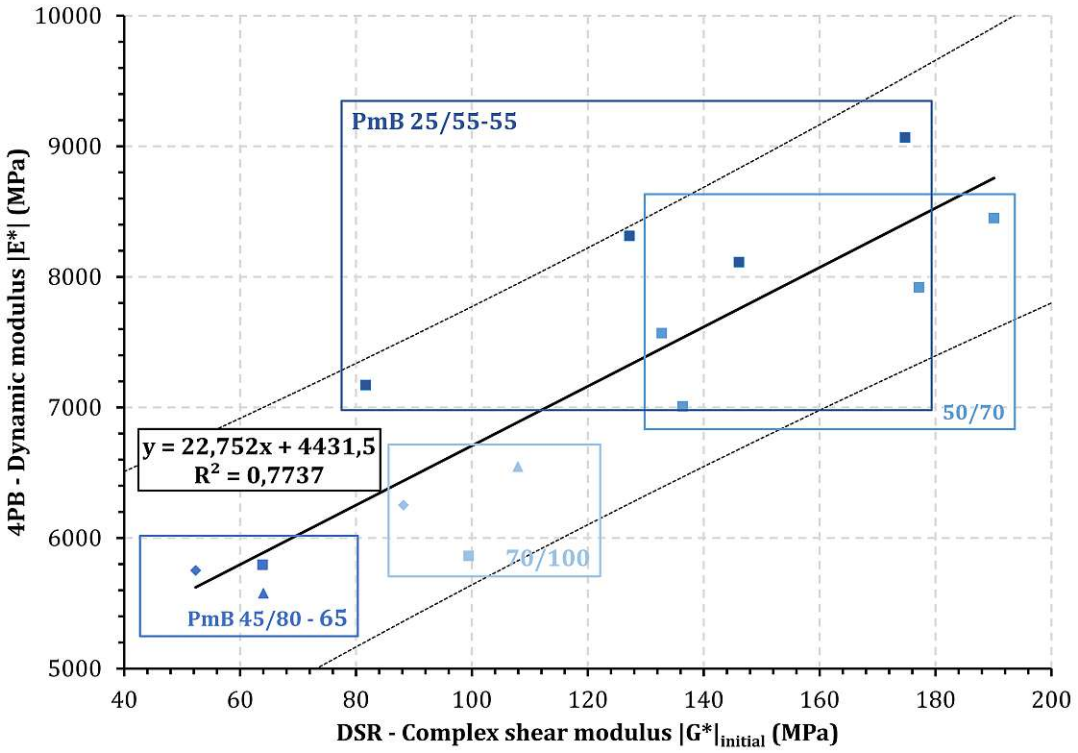

Fig. 4.1: Stiffness correlation between the asphalt mix and the asphalt mastic level

Furthermore, a correlation can be found between the characteristic fatigue parameter ϵ_6 at the asphalt mix level according to EN 12697-24 (ÖNORM EN 12697-24, 2018) and the characteristic fatigue parameter τ_6 in combination with the initial complex shear modulus $|G^*_{initial}|$ at the asphalt mastic level (Figure 4.2). The shear stress, represented as τ_6, is a characteristic parameter

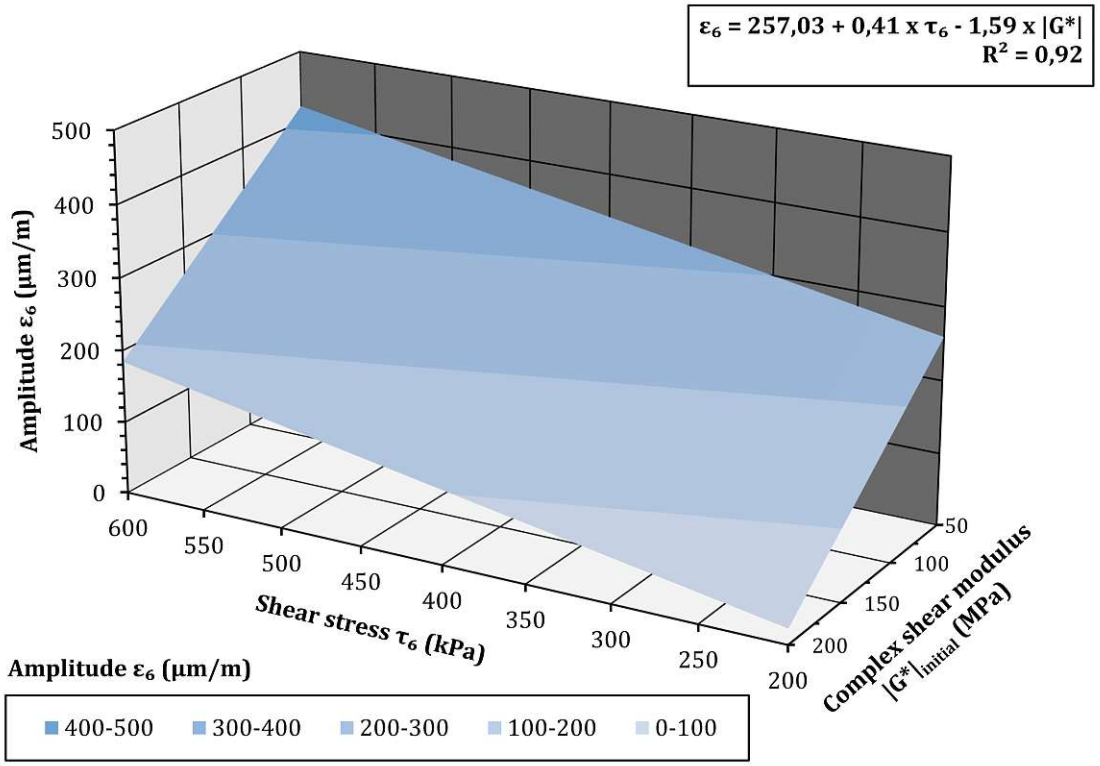

Fig. 4.2: Correlation of the fatigue performances between the asphalt mix and asphalt mastic levels

of a fatigue curve. Specifically, τ_6 denotes the shear stress level at which the material is expected to fail after being subjected to 1,000,000 load cycles. The fatigue curve can be obtained similarly to the fatigue curve at the asphalt mix level (see Figure 2.3).

Chapter 5

Effect of fillers, moisture and ageing on the fatigue performance of asphalt mastic

The previous chapter illustrated that a prediction of the fatigue performance of asphalt mixtures could be made using the fatigue tests at the asphalt mastic level. In other words, the choice of filler material significantly influences the fatigue behaviour of asphalt mixtures. However, moisture and ageing can also accelerate damage in asphalt pavements. Premature pavement failure is becoming increasingly common on some parts of the nation's road network. The poor durability of the asphalt mastic is suspected to be responsible for this damage. It can be postulated that microcracks form within the asphalt mastic and subsequently combine into macrocracks. This chapter examines the influences of the fillers, moisture and ageing on the fatigue performance of asphalt mastic. The main parts of this chapter are presented in the publication titled 'Assessing the impact of filler properties, moisture and ageing regarding fatigue resistance of asphalt mastic (Steineder and Hofko, 2023)' (Appendix 3).

For this purpose, AC with a binder content of 5.2 % per mass and 11 mm maximum grain size was selected as the asphalt mix design to study the fatigue performance of the asphalt mastic. The asphalt mastic comprised an asphalt binder, its own filler from coarse aggregates and an added filler from different sources. Two different asphalt binder grades and six different added fillers were used to produce 12 different mastic types. The filler–asphalt binder ratio by mass was 2.02 for all mastic mixes. The resulting filler–volume ratio varied between 40 % and 45 %. The asphalt binder grades used herein were an unmodified asphalt binder 70/100 and a polymer-modified asphalt binder PmB 45/80-65.

The production of polymer-modified asphalt binder typically involves the blending of the base asphalt binder with Styrene-Butadiene-Styrene (SBS). Styrene-Butadiene-Styrene (SBS) is a block copolymer consisting of alternating blocks of styrene and butadiene. SBS is characterized by its long polymeric chains, which provide the material with its characteristic elastomeric (rubber-like) properties. Thus, SBS enhances the elasticity and temperature susceptibility of the asphalt binder. The production of polymer-modified asphalt binder typically involves the physical blending of the base asphalt binder with SBS, using high shear mixing to ensure a homogeneous distribution of the polymer within the binder. Over time and under specific conditions, polymer chains can migrate within the binder matrix. This migration can lead to phase separation, where the polymer and the asphalt binder form distinct phases. Such separation can affect the long-term performance of the modified asphalt.

Table 5.1 summarizes the asphalt mastic mixes used and their source materials. In addition to the selected mastic mixes for this publication (Table 5.1), asphalt mixes with an unmodified asphalt binder 70/100 were prepared to extend the correlation model depicted in Section 4.

Tab. 5.1: Used asphalt mix and asphalt mastic mixes and their source materials

Asphalt mix (asphalt mastic + aggregates (>0.125 mm)				
Asphalt mastic				
No.	Asphalt binder	Filler (<0.125 mm)	Aggregates (<0.125 mm)	Aggregates (>0.125 mm)
15	Manufacturer 4 — 70/100	Porphyry	Porphyry	Porphyry
16	Manufacturer 4 — PmB 45/80-65	Porphyry	Porphyry	
17	Manufacturer 4 — 70/100	Granite	Porphyry	Porphyry
18	Manufacturer 4 — PmB 45/80-65	Granite	Porphyry	
19	Manufacturer 4 — 70/100	Basalt	Porphyry	Porphyry
20	Manufacturer 4 — PmB 45/80-65	Basalt	Porphyry	
21	Manufacturer 4 — 70/100	Lime	Porphyry	Porphyry
22	Manufacturer 4 — PmB 45/80-65	Lime	Porphyry	
23	Manufacturer 4 — 70/100	Hydrated lime	Porphyry	Porphyry
24	Manufacturer 4 — PmB 45/80-65	Hydrated lime	Porphyry	
25	Manufacturer 4 — 70/100	Quartz	Porphyry	Porphyry
26	Manufacturer 4 — PmB 45/80-65	Quartz	Porphyry	

The physical properties below were determined for the fillers to investigate the influences of the different fillers.

True density

The true filler density was determined using a helium pycnometer according to DIN 66137-2 (DIN 66137-2, 2019). The system comprised two chambers with the same volume. The sample was weighed and placed in one of the chambers while the other remained empty. Helium was then added to the chamber with the sample. The resulting pressure difference between the two chambers was measured, allowing the calculation of the displaced gas volume. The true density was then calculated by dividing the substance mass by its volume without pores. Each sample passed 10 measurement cycles. The mean value was used to determine the true density of each filler. The fillers showed true densities between 2.57 and 3.0 g/m^3. The hydrated lime exhibited the smallest value, while basalt showed the highest true density.

Particle size of fillers up to 0.002 mm

A Laser Particle Sizer (FRITSCH Analysette 22 MicroTec Plus) is used to determine the particle size of fillers up to 0.002 mm. This method offers several advantages over traditional sieving techniques, including high accuracy, short analysis times and good reproducibility. The Laser Particle Sizer uses laser diffraction to determine the particle size distribution based on the electromagnetic wave scattering by the particles. The scattered light is focused onto a sensor by a lens system. The particle size distribution is calculated using the intensity distribution of the scattered light and complex mathematics. The particle diameters obtained from laser diffraction correspond to the sphere diameter with identical light-scattering properties. The Analysette 22 MicroTec Plus has a measurement range of 0.0008 to 2 mm and is used to determine the size distribution of suspensions, emulsions and powders.

The data can be used to derive sieve-related parameters characterising different grading curves. They can be used for the later analysis, as well. The key parameters include the percentage of filler mixture passing through the 0.002, 0.016 and 0.063 mm sieves expressed in mass percentage (% per mass) calculated by dividing the weight of the material passing through the sieve by the total sample weight. In addition, the grading curve characteristics (d_{10}, d_{30} and d_{60}) were derived, representing the maximum mesh size in millimetres of a sieve by 10 %, 30 % and 60 % of the sample passes, respectively. The curvature (C_C) and nonuniformity (C_U) indices also describe the grading curve. C_C represents the grading line curvature and C_U represents the degree of uniformity of the grading curve calculated as the ratio of the grading curve characteristics d_{60} and d_{10}.

Specific surface

The Brunauer, Emmett and Teller (BET) method measures the specific internal and external surface areas of dispersed and/or porous solids by determining the physically adsorbed gas quantity according to ISO 9277 (ISO 9277, 2014). This method is based on determining the required amount of adsorbates or adsorptive gases to cover the outer and inner accessible surfaces of the solid sample with a complete adsorbate monolayer. Inaccessible pores cannot be detected. The BET equation calculates the monolayer substance amount from the adsorption isotherm. Any gas adsorbed to the sample surface through weak physical bonding (van der Waals forces) and desorbed by pure pressure reduction at a constant temperature can be used for the measurement. The BET method cannot be used for materials absorbing the measuring gas.

Dynamic image analysis

Dynamic image analysis was used to study the filler particle shape. The fillers were dispersed in a solution and imaged using a high-resolution camera and a high-speed flash unit. Various particle properties (e.g. diameter, length, width, Feret aspect ratio, circularity, ellipticity and rectangularity) were calculated from the obtained images. A detailed description of each parameter can be found in the publication stated here (Steineder and Hofko, 2023).

Fractional void (aka Rigden void)

According to ÖNORM EN 1097-4 (ÖNORM EN 1097-4, 2008), the filler was compacted using a standardised device for this test method. The compacted filler–volume was determined by measuring the layer height, from which the void percentage was calculated. The filler was placed in the hole of the drop block for the test and covered with filter paper. The drop piston was then carefully inserted into the hole. The drop block and the piston were raised to stop, and then dropped 100 times at approximately one-second intervals. The layer height of the compacted filler was then measured to 0.01 mm accuracy. The void content was calculated from the measured height, compacted filler's mass, filler's density, and drop hole diameter in the drop block.

Regression analyses were performed based on various filler properties to analyse the effect of the filler properties on the fatigue performance of the asphalt mastic to identify the influencing filler property. The results were compared with the literature findings to evaluate the observations. Due to the asphalt binder variation, the mastic mixes with different asphalt binders was considered separately in the analyses because a joint evaluation was not feasible. The fatigue tests were performed as the CS-TS tests at 30 Hz frequency and +10°C temperature.

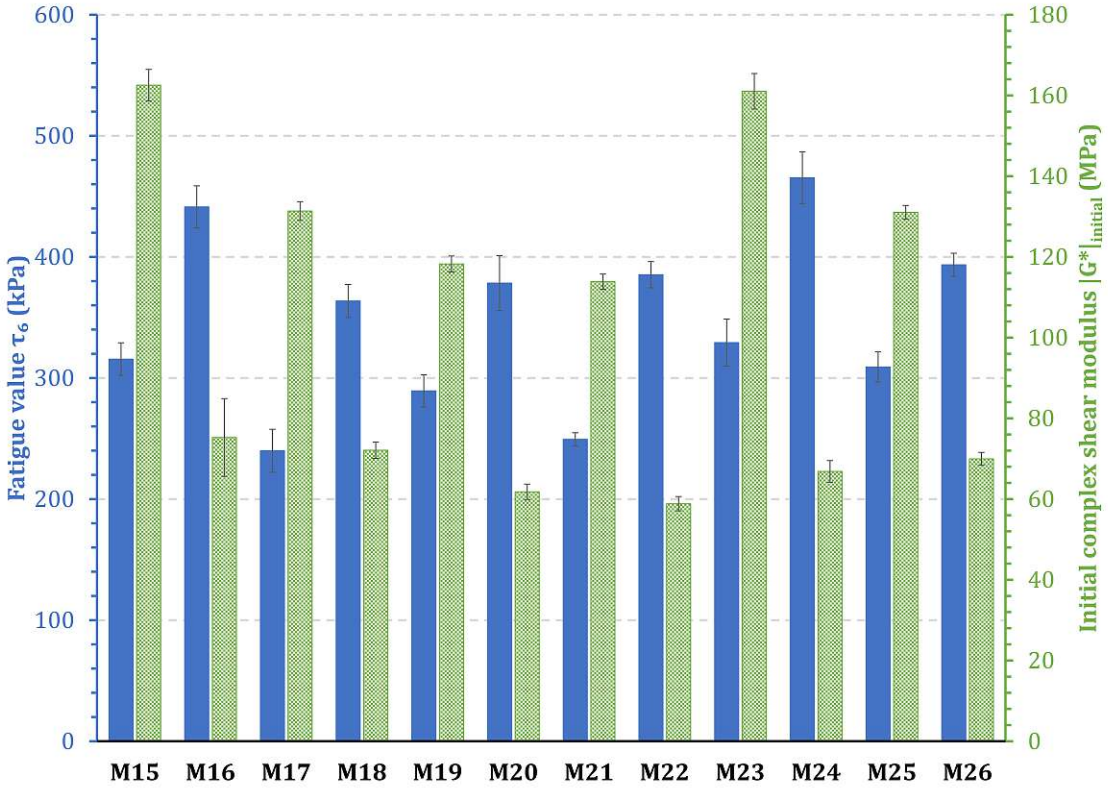

Fig. 5.1: Results of τ_6 and $|G^*_{initial}|$ of all 12 asphalt mastics

The results in Figure 5.1 show that the polymer-modified binders improved the fatigue performance, but the filler properties (e.g. true density, grading curve and grain shape) had no direct effect.

In Table 5.2, the fatigue performance ratio of asphalt mastic with polymer-modified asphalt binder and asphalt mastic with unmodified asphalt binder is presented. The data indicates that the fatigue performance of asphalt mastic produced with polymer-modified asphalt binder is 1.4 times higher than that of asphalt mastic with unmodified asphalt binder.

Tab. 5.2: Fatigue performance ratio of asphalt mastic with polymer-modified asphalt binder and asphalt mastic with unmodified asphalt binder

Polymer-modified asphalt binder		**Unmodified asphalt binder**		τ_6 **(Polymer-modified asphalt binder) /** τ_6 **(Unmodified asphalt binder)**
No.	τ_6 (kPa)	No.	τ_6 (kPa)	(-)
15	315,55	16	441,27	1,40
17	239,87	18	363,60	1,52
19	289,36	20	378,38	1,31
21	249,30	22	385,31	1,55
23	329,20	24	465,40	1,41
25	309,09	26	393,45	1,27

Moreover, a correlation was found between the fatigue performance and the fractional void (Figure 5.2), along with a limited relationship with the specific surface area. Other studies have already identified that a higher specific surface area value is associated with a better mastic performance in terms of stiffness, ageing, fatigue and rutting (Rochlani et al., 2019).

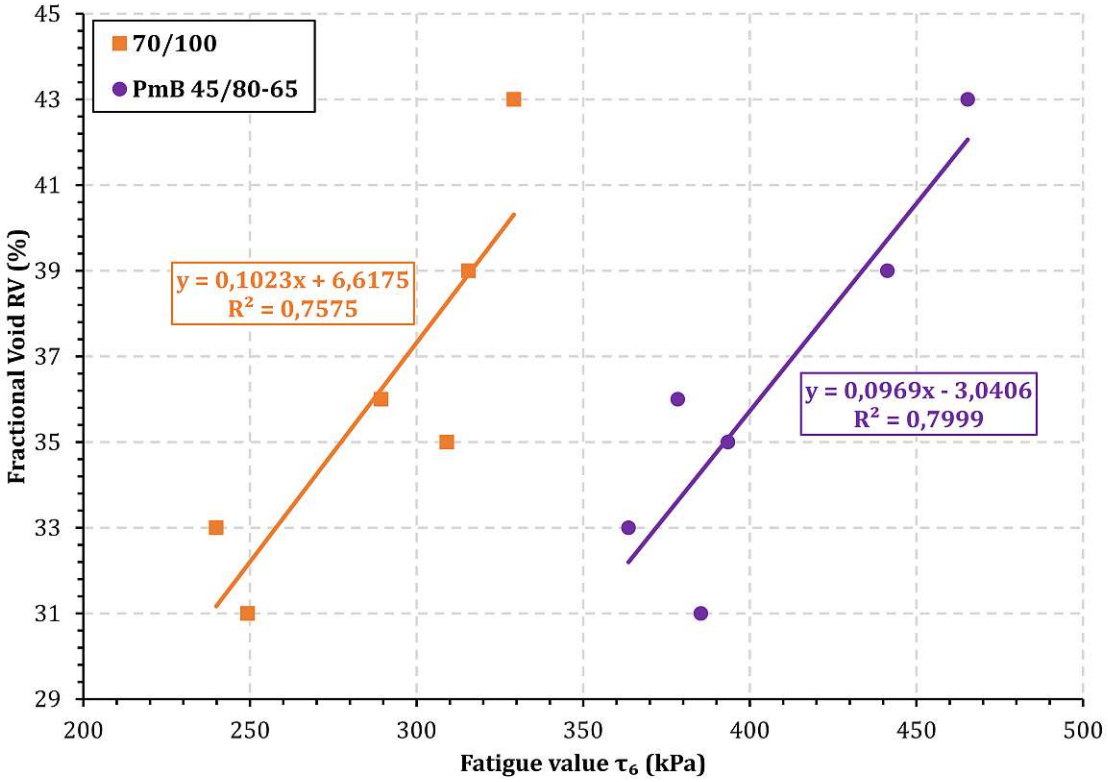

Fig. 5.2: Correlation of the fatigue performance and the fractional void

In addition to the filler properties, the effects of moisture or ageing on the fatigue performance were also investigated. Two preparation methods were used to examine the effect of moisture:

- mastic was prepared with a moist filler
- mastic was stored in a water bath at elevated pressure and temperature for 24 h

The results showed that the moist filler negatively affected the fatigue performance of the asphalt mastic. The negative effects of moisture on the fatigue performance were already observed in the FAM specimens (Caro, Beltrán, et al., 2012).

Two preparation methods were used to investigate the effects of ageing:

- mastic was aged with RTFOT + PAV
- mastic was prepared with an aged asphalt binder (RTFOT + PAV)

The results showed that ageing increased the complex shear modulus. The fatigue value τ_6 also increased. The observed increase in fatigue performance defies initial expectations and is primarily attributed to the stress-controlled test. This can be explained by the general assumption of CS-TS tests: a specimen with high initial stiffness in a CS-TS test requires lower strain to

achieve the specified stress. Consequently, small strains result in slower micro and macro crack development, increasing the number of load cycles to fatigue failure. Based on this general assumption, it can be concluded that CS-TS tests may not be a suitable method for assessing the impact of ageing behavior of asphalt mixtures on their fatigue resistance.

Chapter 6

Application of the DELC criterion as a simplified test method for evaluating the fatigue performance of asphalt mixes

Chapter 3 showed that the loading mode (strain- or stress-controlled) choice influenced the fatigue performance ranking of asphalt mastic. The loading mode choice can affect the assessment. Chapter 4 depicted the relationship between the fatigue performances of the asphalt mixtures and mastic. However, it was not optimal to combine the strain-controlled (asphalt mix level) and stress-controlled (asphalt mastic level) fatigue tests for this relationship. To eliminate this influence, the DELC method described in Chapter 3 was developed to provide a comparable evaluation of the fatigue tests on the asphalt mastic, regardless of the loading mode. This method can also be used for the asphalt mix-level fatigue testing. As with asphalt mastic, the cumulative dissipated energy up to the fatigue criteria was divided by the number of cycles achieved.

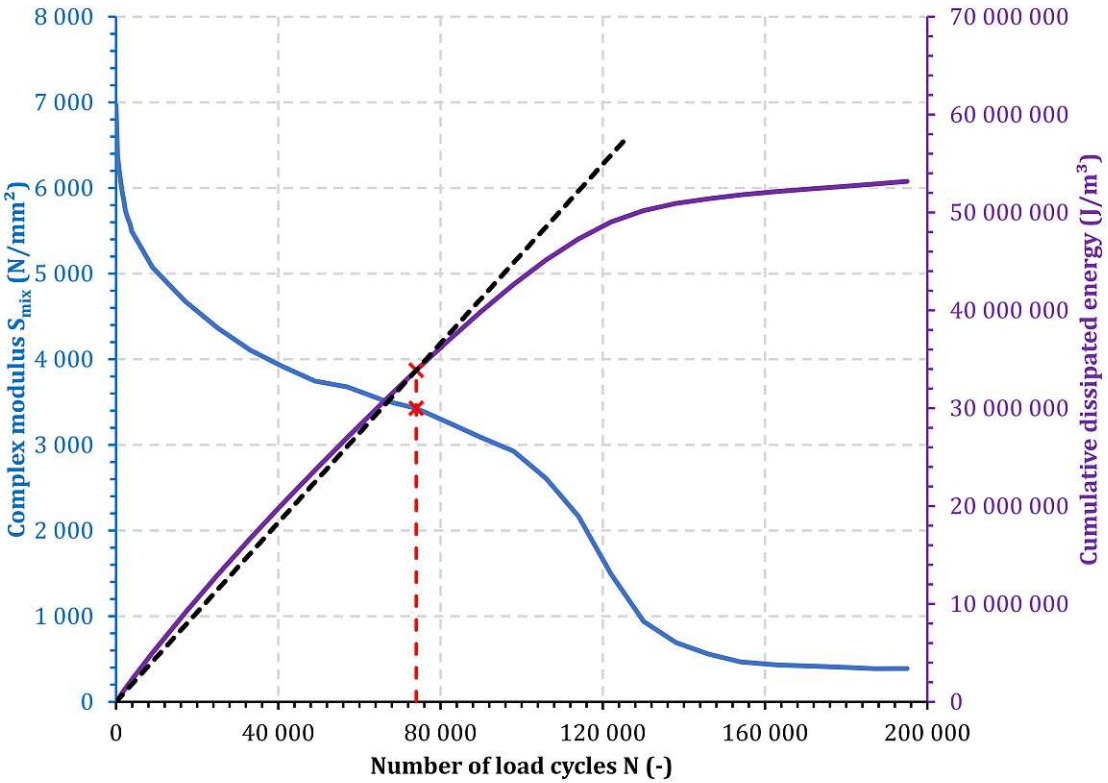

Fig. 6.1: Exemplary plot of the cumulative dissipated energy of asphalt mix with a 4PB test and number of load cycles to failure as defined by RS

Figure 6.1 shows an exemplary trend of the dissipated energy of the 4PB test at the asphalt mix level. The dissipated energy trend was approximately linear up to the conventional failure criterion according to EN 12697-24 (black dotted line). The linear trend was a requirement for the application of the DELC method; otherwise, Eqs. (3.1) and (3.2) cannot be applied. The purple plot in Figure 6.1 corresponded to the plot of the cumulative dissipated energy in a CD-TS test (Figure 3.7). This almost linear cumulative dissipated energy trend until fatigue criteria was observed in all the 4PB tests.

Chapter 4 identified a correlation between the fatigue performances at the asphalt mix and mastic levels. For this multiple regression model, the strain-controlled tests at the asphalt mix level and the stress-controlled ones at the asphalt mastic level were mixed as the input data. The DELC method was not yet developed at that time; hence, it was of particular interest to see if the correlation between the two levels also holds for the DELC results. The correlation between the two levels using the DELC method was based on the hypothesis that the asphalt mastic significantly contributes to the cumulative dissipated energy at the asphalt mix level. A possible correlation was established by performing all the fatigue tests at both the asphalt mix and asphalt mastic levels using the same source materials from Chapters 4 and 5 evaluated using the DELC method. Table 6.1 summarizes the fatigue test results.

Tab. 6.1: Fatigue parameters ϵ_6 and $DELC_6$ for asphalt mix and mastic from test in Chapters 4 and 5 using the fatigue failure criteria RS.

No.	Asphalt mix		Asphalt mastic
	ϵ_6 (μm/m)	$DELC_6$ (kPa)	$DELC_6$ (kPa)
1	193.6	258.2	180.1
2	233.1	328.3	416.0
3	88.2	180.1	118.9
4	237.8	416.0	634.8
5	129.9	148.0	104.5
6	176.4	251.4	231.2
7	163.8	174.9	175.7
8	298.0	414.6	480.3
9	196.4	222.6	172.6
10	296.7	436.1	427.2
11	184.6	232.7	168.8
12	357.9	*	516.2
13	188.8	245.8	171.9
14	336.1	471.4	653.7
15	103.7	115.9	134.1
17	140.3	122.6	115.5
19	114.7	120.9	166.9
21	158.7	168.4	134.8
23	142.4	172.0	162.8
25	150.7	156.9	171.2

*No evaluation of the dissipated energy was possible due to missing data.

The regression model in Figure 6.2 shows a very good correlation between the dissipated energies per load cycle ($DELC_6$) at the asphalt mix and mastic levels. Considering the different asphalt binder types used for the mixes, the polymer-modified asphalt binder types dissipated more energy per load cycle than the plain asphalt binder types. The dissipated energy was composed of internal friction, viscous deformation and fatigue; thus, the measurement results ($DELC_6$) were not informative about the fatigue performance of the asphalt mastic. These energy dissipations and their proportions were influenced by the physicochemical properties between the asphalt binder and the aggregate/filler and the mechanical properties of the aggregate/filler.

In Figure 6.3, the $DELC_6$ values of the asphalt mastic tests were correlated with the benchmark values ϵ_6 of the asphalt mix test according to EN 12697-24 (ÖNORM EN 12697-24, 2018). A very good correlation was found between the two values. A simplified test procedure can be derived from the available data to evaluate the fatigue performance of the asphalt mixtures. This will allow an estimation of the fatigue performance of the asphalt mix through simple tests of the asphalt mastic using the DSR. The available data suggest that a mastic with a high $DELC_6$ value will exhibit a good fatigue performance at the asphalt mix level. The influence of the analysed filler properties on the $DELC_6$ value could not be found. In addition, the impact of the asphalt binder is stronger than that of the filler properties.

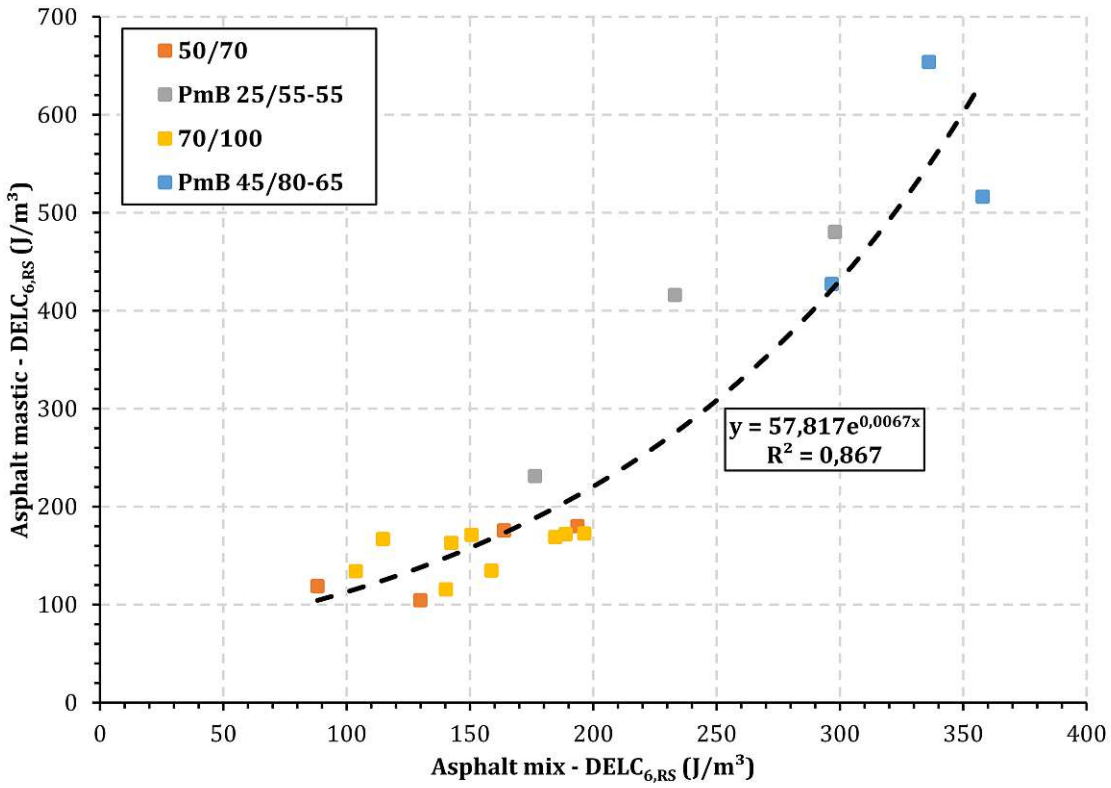

Fig. 6.2: Correlation of the $DELC_6$ values for asphalt mix and asphalt mastic using the fatigue failure criteria RS

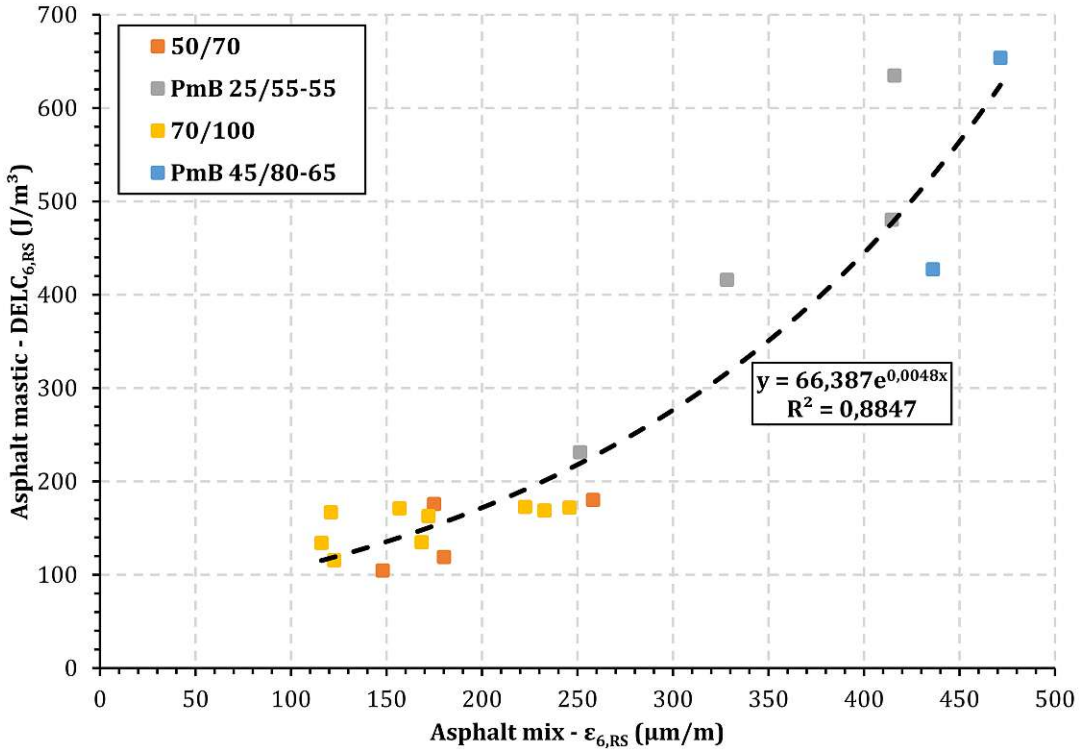

Fig. 6.3: Correlation of the fatigue parameter ϵ_6 for asphalt mix and $DELC_6$ values for asphalt mastic using fatigue the failure criteria RS

Chapter 7

Conclusions

This thesis aimed to find a simplified test method for assessing the fatigue performance of asphalt mixtures to avoid the fatigue performance estimation using complex tests on the asphalt mixture. The asphalt mastic level was chosen as the assessment level because this is the main binding component in an asphalt mixture. This work was divided into three essential parts. The first part examined the possible fatigue tests on the asphalt mastic level. The second part dealt with the correlation between the fatigue performances of both levels. The third part investigated the possible influences of the filler properties on the fatigue performance of asphalt mastic. Different mixtures at the asphalt and mastic levels were investigated. The following conclusions are summarised based on the obtained analysis results:

- No correlation exists among the CS-TS, CD-TS and LAS tests. However, by combining the stress-controlled and strain-controlled TS tests using the dissipated energy approach, uniform fatigue curves can be derived from the CS-TS and CD-TS tests. The TS tests are found independent of the loading mode by using the DELC and the applicable fatigue criteria. The RS and DER fatigue failure criteria showed a good applicability in all the TS tests.
- Overall, the hyperbolic specimen shape is a possible alternative for determining the fatigue performance of asphalt mastic.
- A good positive correlation exists between the dynamic modulus of the asphalt mix determined according to EN 12697-25 and the complex shear modulus of the respective asphalt mastic determined with the CS-TS tests. A multiple linear regression model with the independent variables of the complex shear modulus and the fatigue performance allowed for a reliable prediction of the fatigue performance of asphalt mixtures. The fatigue performance of mixtures with the polymer-modified asphalt binder is higher on both asphalt mixture and asphalt mastic mixture levels.
- The true density, grading curve's properties and filler's grain shape do not significantly affect the fatigue performance determined with the CS-TS tests. A correlation is found between the fatigue performance determined with the CS-TS tests and the fractional void of the filler. The specific surface area of the filler has a limited relationship with the fatigue performance of the asphalt mastic. The moist filler negatively affects the fatigue performance. However, the thesis notes that the CS-TS tests are not suitable for investigating the influences of ageing on the fatigue performance.
- A strong correlation is found between the $DELC_6$ values of the asphalt mastic tests and the benchmark values ϵ_6 of the asphalt mix test according to EN 12697-24. This correlation allows the development of a simplified test procedure for evaluating the fatigue performance of asphalt mixtures using the DSR. The data suggest that a mastic with a high $DELC_6$ value will show a good fatigue performance at the asphalt mix level.

- No influence of the filler properties on the $DELC_6$ value is detected.

Overall, the correlation of the fatigue performance between the asphalt mastic and asphalt mix levels offers a great potential for assessing the fatigue performance of asphalt mixes. Applying the DELC method helps improve the assessment reliability and increases the safety and durability of pavements. Therefore, further research has much scope of enhancing the DELC method and facilitating its application in practice.

Chapter 8

Outlook

Assessing the fatigue performance of asphalt mixtures by TS tests on asphalt mastic is possible using conventional fatigue failure criteria, including RS and DER, combined with the DELC method. In this thesis, the method was tested on only a single asphalt mix (AC 11 D S) with different mineral aggregate types and binders. Therefore, applying this method on other mix types will be particularly interesting. Void content and maximum aggregate size significantly influence this simple prediction tool. Given the comprehensive expertise established in fatigue testing at the asphalt mortar level, a comparative study examining the fatigue performance of both asphalt mastic and asphalt mortar holds considerable scholarly interest.

Based on the available data, no negative influence on the fatigue performance of the asphalt mastic due to ageing was determined. A precise cause for this phenomenon could not be found in this thesis, as well. Therefore, comparative tests between aged samples at the asphalt mix and mastic levels should be considered. This is the only way to analyse the different test methods for the influence of ageing, whereby the main difficulty lies in the equivalent ageing of the two mix levels.

Hence, there is a demand for research on the effects of different dissipated energy components on the fatigue performance. The dissipated energy in a fatigue test of viscous materials is mainly composed of internal friction, viscous deformation and fatigue. There are currently no practical approaches for measuring or calculating the proportions of various parts. This kind of calculation model will significantly improve the fatigue performance estimation of asphalt mixtures through tests on asphalt mastic because only the fatigue components can be examined.

One disadvantage of the hyperbolic specimen shape can be observed when the rheological properties of the asphalt mastic are needed. That is, all measurement results are miscalculated by the DSR due to the necking in the specimen centre. A correction factor will solve this issue, and it will be easier to use a measurement geometry with a 6 mm diameter. However, this can lead to a potentially more significant scatter of the measurement data due to trimming. A plate—plate measuring geometry with a 6 mm diameter is a special equipment, which is not available in every road engineering laboratory. Therefore, the test procedure can only be performed with significant adaptations in the measuring equipment.

Investigating the abovementioned issues will require a large data quantity to confirm the applicability of the simplified test method at the asphalt mastic level and improve the method further.

Bibliography

AASHTO M 320-17 (2017). *Standard Specification for Performance-Graded Asphalt Binder*. Washington, D.C.: American Association of State and Highway Transportation Officials.

AASHTO T 321-17 (2017). *Standard Method of Test for Determining the Fatigue Life of Compacted Asphalt Mixtures Subjected to Repeated Flexural Bending*. Washington, D.C.: American Association of State and Highway Transportation Officials.

AASHTO TP 101 (2012). *Standard Method of Test for Estimating Fatigue Resistance of Asphalt Binders Using the Linear Amplitude Sweep*. Washington, D.C.: American Association of State and Highway Transportation Officials.

Adnan, A. M., C. Lü, X. Luo, and J. Wang (2021). "Impact of Graphene Oxide on Zero Shear Viscosity, Fatigue Life and Low-Temperature Properties of Asphalt Binder". In: *Materials* 14, pp. 1–15. DOI: 10.3390/ma14113073.

Anderson, D. A. and T. W. Kennedy (1993). "Development of SHRP binder specification". In: *Journal of the Association of Asphalt Paving Technologists*, pp. 481–507.

Anderson, D. A., Y. M. Le Hir, M. O. Marasteanu, J.-P. Planche, D. Martin, and G. Gauthier (2001). "Evaluation of Fatigue Criteria for Asphalt Binders". In: *Journal of the Transportation Research Board* 1766 (1), pp. 48–56. DOI: 10.3141/1766-07.

Bonnetti, K. S., K. Nam, and H. U. Bahia (2022). "Measuring and Defining Fatigue Behavior of Asphalt Binders". In: *Journal of the Transportation Research Board* 1810 (1), pp. 33–43. DOI: 10.3141/1810-05.

Bundesministerium für Klimaschutz, Umwelt, Energie, Mobilität, Innovation und Technologie (2023). *Statistik Straße und Verkehr*. Wien: Abteilung IV/IVVS1.

Caro, S., D. P. Beltrán, A. E. Alvarez, and C. Estakhri (2012). "Analysis of moisture damage susceptibility of warm mix asphalt (WMA) mixtures based on Dynamic Mechanical Analyzer (DMA) testing and a fracture mechanics model". In: *Construction and Building Materials* 35, pp. 460–467. DOI: 10.1016/j.conbuildmat.2012.04.035.

Caro, S., D. B. Sánchez, and B. Caicedo (2015). "Methodology to characterise non-standard asphalt materials using DMA testing: application to natural asphalt mixtures". In: *International Journal of Pavement Engineering* 16 (1), pp. 1–10. DOI: 10.1080/10298436.2014.893328.

Carpenter, S. and S. Shen (2006). "Dissipated Energy Approach to Study Hot-Mix Asphalt Healing in Fatigue". In: *Journal of the Transportation Research Board* 1970 (1), pp. 178–185. DOI: 10.3141/1970-21.

Chen, Y., S. Xu, G. Tebaldi, and E. Romeo (2020). "Role of mineral filler in asphalt mixture". In: *Road Materials and Pavement Design* 23 (2), pp. 247–286. DOI: 10.1080/14680629.2020.1826351.

DIN 66137-2 (2019). *Determination of solid state density - Part 2: Gaspycnometry*. Berlin: DIN Deutsches Institut für Normung e. V.

Ghuzlan Khalid A.; Carpenter, S. H. (2006). "Energy-Derived, Damage-Based Failure Criterion for Fatigue Testing". In: *Journal of the Transportation Research Board* 1723 (1), pp. 141–149. DOI: 10.3141/1723-18.

Hancock, J. and D. Brown (1983). "On the role of strain and stress state in ductile failure". In: *Journal of the Mechanics and Physics of Solids* 31 (1), pp. 1–24. DOI: 10.1016/0022-5096(83)90017-0.

Hospodka, M., B. Hofko, and R. Blab (2018). "Introducing a new specimen shape to assess the fatigue performance of asphalt mastic by dynamic shear rheometer testing". In: *Materials and Structures* 51 (46). DOI: 10.1617/s11527-018-1171-6.

ISO 9277 (2014). *Determination of the specific surface area of solids by gas adsorption - BET method*. Genf: International Organization for Standardization.

Kim, Y.-R., D. Little, and R. L. Lytton (2003). "Fatigue and Healing Characterization of Asphalt Mixtures". In: *Journal of Materials in Civil Engineering* 15 (1), pp. 75–83. DOI: 10.1061/(ASCE)0899-1561(2003)15:1(75).

Kim, Y.-R., D. N. Little, and I. Song (2003). "Effect of Mineral Fillers on Fatigue Resistance and Fundamental Material Characteristics: Mechanistic Evaluation". In: *Journal of the Transportation Research Board* 1832 (1), pp. 1–8. DOI: 10.3141/1832-01.

Kim, Y. S., T. Sigwarth, J. Büchner, and M. P. Wistuba (2021). "Accelerated Dynamic Shear Rheometer Fatigue Test for investigating asphalt mastic". In: *Road Materials and Pavement Design* 22, pp. 383–396. DOI: 10.1080/14680629.2021.1911832.

Li, Q., X. Chen, G. Li, and S. Zhang (2018). "Fatigue resistance investigation of warm-mix recycled asphalt binder, mastic, and fine aggregate matrix". In: *Fatigue & Fracture of Engineering Materials & Structures* 41, pp. 400–411. DOI: 10.1111/ffe.12692.

Liao, M.-C., J.-S. Chen, and K.-W. Tsou (2011). "Fatigue Characteristics of Bitumen-Filler Mastics and Asphalt Mixtures". In: *Journal of Materials in Civil Engineering* 24 (7), pp. 916–923. DOI: 10.1061/(ASCE)MT.1943-5533.0000450.

Margaritis, A., G. Pipintakos, A. Varveri, G. Jacobs, N. Hasheminejad, J. Blom, and W. Van den bergh (2021). "Towards an enhanced fatigue evaluation of bituminous mortars". In: *Construction and Building Materials* 275. DOI: 10.1016/j.conbuildmat.2020.121578.

Martono, W., H. U. Bahia, and J. D'Angelo (2007). "Effect of Testing Geometry on Measuring Fatigue of Asphalt Binders and Mastics". In: *Journal of Materials in Civil Engineering* 19 (9), pp. 746–752. DOI: 10.1061/(ASCE)0899-1561(2007)19:9(746).

Ministry of Transportation Canada (2012). *Method of test for the determination of asphalt cement resistance to ductile failure using double edge notched tension test (DENT)*. Ontario, Canada: Ministry of Transportation.

Mo, L. T., M. Huurman, S. P. Wu, and A. A. A. Mo (2012). "Research of Bituminous MortarFatigue Test Method Based on Dynamic Shear Rheometer". In: *Journal of Testing and Evaluation* 1728 (1), pp. 75–81. DOI: 10.1520/JTE103738.

Olufsen, S. N., A. H. Clausen, D. W. Breibyb, and O. S. Hopperstada (2020). "X-ray computed tomography invastigation of dilation of mineral-filled PVC under monotonic loading". In: *Mechanics of Materials* 142. DOI: 10.1016/j.mechmat.2019.103296.

ÖNORM B 3580-2 (2018). *Bituminous mixtures - Material specifications - Asphalt Concrete - Part 2: Performance based requirements - Rules for the implementation of ÖNORM EN 13108-1*. Wien: Austrian Standards.

ÖNORM EN 1097-4 (2008). *Tests for mechanical and physical properties of aggregates - Part 4: Determination of the voids of dry compacted filler (German version)*. Wien: Austrian Standards.

ÖNORM EN 12697-24 (2018). *Bituminous mixtures - Test methods - Part 24: Resistance to fatigue*. Wien: Austrian Standards.

ÖNORM EN 12697-25 (2016). *Bituminous mixtures - Test methods - Part 25: Cyclic compression test*. Wien: Austrian Standards.

ÖNORM EN 12697-26 (2018). *Bituminous mixtures - Test methods - Part 26: Stiffness*. Wien: Austrian Standards.

ÖNORM EN 12697-35 (2016). *Bituminous mixtures - Test methods - Part 35: Laboratory mixing*. Wien: Austrian Standards.

ÖNORM EN 12697-46 (2020). *Bituminous mixtures - Test methods - Part 46: Low temperature cracking and properties by uniaxial tension tests*. Wien: Austrian Standards.

ÖNORM EN 13108-1 (2016). *Bituminous mixtures - Material specifications - Part 1: Asphalt Concrete*. Wien: Austrian Standards.

ÖNORM EN 1426 (2015). *Bitumen and bituminous binders - Determination of needle penetration*. Wien: Austrian Standards.

Reese, R. A. (1997). "Properties of aged asphalt binder related to asphalt concrete fatigue life". In: *Journal of the Association of Asphalt Paving Technologists*, pp. 604–632. DOI: 10.1061/(ASCE)0899-1561(2003)15:1(75).

Robisson, A. (2000). *Comportement visco-hyperélastique endommageable d'élastomères SBR et PU : prévision de la durée de vie en fatigue*. France, Ecole des Mines de Paris: PhD thesis.

Rochlani, M., S. Leischner, G. C. Falla, D. Wang, S. Caro, and F. Wellner (2019). "Influence of filler properties on the rheological, cryogenic, fatigue and rutting performance of mastics". In: *Construction and Building Materials* 227, pp. 1–11. DOI: 10.1016/j.conbuildmat.2019.116974.

Rowe, G. (1993). "Performance of asphalt mixtures in the trapezoidal fatigue test". In: *Journal of the Association of Asphalt Paving Technologists*, pp. 344–384.

Rowe, G. (1996). *Application of the dissipated energy concept to fatigue cracking in asphalt pavements*. United Kingdom, University of Nottingham: PhD thesis.

Schönfelder, S. (2015). *Volks- und regionalwirtschaftliche Bedeutung von Verkehrsinfrastruktur. Schwerpunkt niederrangiges Straßennetz (Economic and Regional Economic Impact of Transport Infrastructure. Focus on Secondary and Local Roads)*. Wien: Österreichisches Institut für Wirtschaftsforschung.

Shan, L., Y. Tan, B. S. Underwood, and Y. R. Kim (2011). "Separation of Thixotropy from Fatigue Process of Asphalt Binder". In: *Journal of the Transportation Research Board* 2207 (1), pp. 89–98. DOI: 10.3141/2207-12.

Shan, L., Y. Tan, S. Underwood, and Y. R. Kim (2010). "Application of Thixotropy to Analyze Fatigue and Healing Characteristics of Asphalt Binder". In: *Journal of the Transportation Research Board* 2179 (1), pp. 85–92. DOI: 10.3141/2179-10.

Shen, S., G. D. Airey, S. H. Carpenter, and H. Huang (2006). "A Dissipated Energy Approach to Fatigue Evaluation". In: *Road Materials and Pavement Design*, pp. 47–69. DOI: 10.1080/14680629.2006.9690026.

Shine, A. M., G. C. Falla, E. Kamratowsky, F. Wellner, S. Caro, A. Zeißler, and S. Leischner (2023). "Fatigue testing on bitumen binder using different column specimen shapes". In: *Road Materials and Pavement Design* 24 (sup1), pp. 654–671. DOI: 10.1080/14680629.2023.2181067.

SHRP A-404 (1994). *Fatigue response of asphalt-aggregate mixes*. Washington, D.C.: Strategic Highway Research Program, National Research Council.

Smith, B. J. and S. A. M. Hesp (2000). "Crack Pinning in Asphalt Mastic and Concrete: Regular Fatigue Studies". In: *Journal of the Transportation Research Board* 40 (1), pp. 1–6. DOI: 10.3141/1728-11.

Steineder, M., V. Donev, B. Hofko, and L. Eberhardsteiner (2022). "Correlation between Stiffness and Fatigue Behavior at Asphalt Mastic and Asphalt Mixture Level". In: *Journal of Testing and Evaluation* 50 (2), pp. 803–817. DOI: 10.1520/JTE20210204.

Steineder, M. and B. Hofko (2023). "Assessing the impact of filler properties, moisture, and aging regarding fatigue resistance of asphalt mastic". In: *Road Materials and Pavement Design*, pp. 1–16. DOI: 10.1080/14680629.2023.2172066.

Steineder, M., M. J. Peyer, B. Hofko, M. Chaudhary, N. Saboo, and A. Gupta (2022). "Comparing different fatigue test methods at asphalt mastic". In: *Materials and Structures* 55 (132), pp. 1–16. DOI: 10.1617/s11527-022-01970-4.

Tauste-Martínez, R., A. E. Hidalgo, G. García-Travé, F. Moreno-Navarro, and M. d. C. Rubio-Gámez (2022). "Influence of Type of Filler and Bitumen on the Mechanical Performance of Asphalt Mortars". In: *Materials* 15. DOI: 10.3390/ma15093307.

Van den bergh, W. and M. Van de Ven (2012). "The Influence of Ageing on the Fatigue and Healing Properties of Bituminous Mortars". In: *Procedia - Social and Behavioral Sciences* 53, pp. 256–265. DOI: 10.1016/j.sbspro.2012.09.878.

van Dijk, W. and Moreaud, H. and Quedeville, A. and Uge, P. (1972). *The fatigue of bitumen and bituminous mixes*. Grosvenor House, Park Lane, London, England: Third International Conference on the Structural Design of Asphalt Pavements.

van Dijk, W. and Visser, W. (1977). *Energy Approach to Fatigue for Pavement Design*. Texas, United States: Association of Asphalt Paving Technologists - Proceedings of the Technical Sessions.

Wistuba, M. P. and J. Büchner (2019). "Abschätzung der Performance von Asphalt anhand von Bitumenprüfungen". In: *Straße und Autobahn* 70 (6), pp. 479–489.

Zhang, Y. and Z. Leng (2017). "Quantification of bituminous mortar ageing and its application in ravelling evaluation of porous asphalt wearing courses". In: *Materials and Design* 119, pp. 1–11. DOI: 10.1016/j.matdes.2017.01.052.

Zhang, Z., S. Han, H. Guo, X. Han, and C. Wu (2021). "Fatigue performance evaluation of recycled asphalt fine aggregate matrix based on dynamic shear rheometer test". In: *Construction and Building Materials* 300. DOI: 10.1016/j.conbuildmat.2021.124025.

Zhou, F., W. Mogawer, H. Li, A. Andriescu, and A. Copeland (2013). "Evaluation of Fatigue Tests for Characterizing Asphalt Binders". In: *Journal of Materials in Civil Engineering* 25, pp. 610–617. DOI: 10.1061/(ASCE)MT.1943-5533.0000625.

Appendix 1 (Publication 1)

Materials and Structures (2022) 55:132
https://doi.org/10.1617/s11527-022-01970-4

ORIGINAL ARTICLE

Comparing different fatigue test methods at asphalt mastic level

Michael Steineder · Martin Johannes Peyer · Bernhard Hofko · Mohit Chaudhary · Nikhil Saboo · Ankit Gupta

Received: 13 September 2021 / Accepted: 22 April 2022 / Published online: 16 May 2022

Abstract Latest research is focused on predicting the fatigue behavior of asphalt mixtures through cost-effective and simple test methods on asphalt mastic level (asphalt binder + mineral fines). There are numerous fatigue test methods for asphalt binders and mastic using the dynamic shear rheometer (DSR). However, up to now, the results of the different fatigue tests on DSR have not been directly compared. Therefore, four different asphalt mastic mixes were prepared, and each was tested with the two most popular fatigue tests [linear amplitude sweep (LAS) test and time sweep (TS) test] and then compared to each other. The TS tests were performed as stress-controlled and as strain-controlled tests. All LAS and TS tests were performed with cylindrical and hyperbolic specimen shapes to identify impact of specimen shape. Different fatigue criteria were applied for evaluation to investigate the comparability of the results. Stress-controlled TS tests, strain-controlled TS tests, and LAS tests reveal different rankings of fatigue performance. However, a dissipated energy approach can combine stress-controlled and strain-controlled TS tests into one fatigue curve. The hyperbolic specimen shape can be used for TS tests and results in the same rankings. The hyperbolic specimen shape is not applicable for LAS tests. A calculation model could be derived to establish a relationship between the measured and actual stresses and strains in the necking of a hyperbolic specimen. TS tests using the dissipated energy approach appear to be the most promising mastic fatigue tests.

Keywords DSR · Fatigue · Aspahlt mastic · Time sweep · LAS

M. Steineder (✉) · M. J. Peyer · B. Hofko
Institute of Transportation, Vienna University of Technology, Karlsplatz 13/E230-3, 1040 Vienna, Austria
e-mail: michael.steineder@tuwien.ac.at

M. Chaudhary · N. Saboo · A. Gupta
Department of Civil Engineering, Indian Institute of Technology (BHU), Varanasi, Uttar Pradesh 221005, India

1 Introduction

The occurrence of cracks due to material fatigue, mainly caused by repeated traffic loads, is one of the most frequently encountered patterns of damage in asphalt pavements. The traffic-induced loads led to stresses and strains with each load cycle, which accumulated damage in the form of growing micro-cracks on the underside of the asphalt pavement which increased with duration. After these micro-cracks have combined to form macro-cracks, they would move up to the road pavement's surface. Therefore, the prevention of fatigue-related cracks plays a key role in sustainable asphalt pavement engineering [1, 2]. Numerous laboratory test methods for asphalt mixtures are reported in the literature to classify their

fatigue performance. Thus, the test equipment, specimen geometry, and loading configurations change for each test [1, 3]. Widely used test setups are the tension-compression test, the 2-point-bending beam test, the 3-point-bending beam test, the 4-point-bending beam test, and the indirect tensile test according to EN 12697-24 [4].

All of the above-mentioned tests have the same disadvantages: Specimen preparation and the testing are time-consuming and need high amounts of material and personpower. Besides, for each test setup, special test equipment is necessary. Therefore, there is a strong incentive to move the characterization of the fatigue performance from asphalt mixture level to the asphalt binder or mastic level.

A number of studies have already shown a connection between the fatigue behavior of asphalt mixtures and that of asphalt binder or asphalt mastic [5–8]. The test methods for asphalt binder or asphalt mastic for this purpose are primarily performed with DSR. However, different test setups are used. Therefore, the objective of this paper is to compare the most commonly used fatigue tests on DSR and examine the comparability, since no direct comparison has been made in any studies until now. This study forms part of a larger project to provide a reliable prediction of the fatigue performance of asphalt mixtures based on DSR fatigue tests on asphalt mastic. As a result of this study, those test setups and evaluation methods should be found to be comparable. Consequently, these fatigue tests can serve as a basis for a correlation with the fatigue performance on the asphalt mixture level.

1.1 Background

As a result of the Strategic Highway Research Program (SHRP), the Performance Grading (PG) specification according to AASHTO M 320-17 [9] was developed. Using a Dynamic Shear Rheometer (DSR), the viscoelastic properties of asphalt binders are evaluated in terms of the fatigue potential of asphalt mixes [10].

However, studies on this PG specification showed that the linear viscoelastic SHRP parameter used to evaluate fatigue performance ($|G^*|sin(\delta)$) did not correlate with the fatigue behavior of the respective asphalt mix, especially when modified asphalt binders are used [11].

As a further development, the Time-Sweep (TS) test was used to describe the fatigue behavior of asphalt binder. The basis for this test is the deterioration of material integrity under repeated loading. This loading model corresponds with the classical theory of pavement fatigue. The rolling wheel causes compressive and tensile stresses on the underside of an asphalt concrete layer due to the weight of the over rolling vehicle [12]. Due to a large number of vehicles, this creates a pulsating load, as applied in a TS test. In the TS test, sinusoidal loading at a defined frequency and stress or strain amplitude is used to test until material failure. However, there is no standardized criterion that defines fatigue failure for TS tests [13]. There are many different fatigue criteria in the literature. The most widely used criterion in the context of asphalt fatigue is the decrease in stiffness. It states that the specimen fails when the stiffness reaches 50% of the initial stiffness. It is defined in the AASHTO T 321 [14], EN12967-24 [4], and SHRP-A-404 [15].

A further definition of fatigue failure is the use of phenomenological parameters. For example, notable changes in damage progression such as the peak of the phase angle would define the failure of asphalt and mastic [16–18]. Dissipated energy approaches are also applicable as a definition of fatigue failure. These fatigue criteria comprise the dissipated energy ratio (DER) [6, 19–21] and the ratio of dissipated energy change (RDEC) [22–26]. Based on the dissipated energy approach, another simple phenomenological indicator was derived. The peak of the product value ($S \times N$), according to the multiplication of the stiffness ratio (S) and the load cycles (N), is used as a fatigue criterion [27]. The maximum SxN is also applied in ASTM D7460-10 for asphalt mixture [28].

The main advantage of TS tests is the simulation of a realistic loading. In addition, the parameters can be adjusted by controlling the temperature, frequency, and type of loading (stress- or strain-controlled). Furthermore, there is no restriction to the linear viscoelastic range. A significant disadvantage of this method is the long duration of the experiment (often several hours per experiment). In addition, the high stiffness of the mastics can bring the DSR to its performance limits. Motor cooling can also influence the results [29]. One way to minimize the system loading of the DSR is to use a hyperbolic specimen

shape. The hyperbolic specimen shape has a necking in the middle of the specimen [16]. This specimen shape reduces the necessary torque, which relieves the DSR. The disadvantage of the hyperbolic specimen shape is that the measured rheological data cannot be used without converting them. However, such a calculation model is currently not available. Nevertheless, the load cycles up to the fatigue criterion can be used to characterize the durability.

A quicker fatigue test on the DSR is the linear amplitude sweep (LAS) test. According to AASHTO TP101-14 [30], cylindrical asphalt binder samples with a diameter of 8 mm and a height of 2 mm are used as test specimens. The test procedure according to AASHTO TP101-14 [30] is divided into two sections. The first test section determines the material behavior and the rheological characteristics of the undamaged specimen through a strain-controlled frequency sweep test in the DSR. During the second test section, the specimen is subjected to a strain-controlled amplitude sweep test, performed at a constant frequency of 10 Hz and a constant test temperature. The amplitude of the applied shear strain is increased linearly from 0% to 30% throughout 3100 load cycles. By applying the viscoelastic continuum damage model (VECD) in the form of the associated formulas from AASTHO TP101 [30], a linear correlation can be found between the parameter load cycles and the expected shear strain in terms of a linear equation.

The main advantage of the LAS test is the very fast test procedure (approx. 20 min/test). In addition, by regulating the temperature, tests can be carried out at different temperature ranges. But, the results of LAS tests show only a low correlation with the results of other fatigue tests [11].

In addition to the tests mentioned above with the DSR, there are other test methods for determining the fatigue resistance of asphalt binder, such as the DENT [31] test method. However, as the DSR is a widely used laboratory instrument and is already part of the standard equipment of a road construction laboratory, only tests on the DSR were considered in this study.

1.2 Research approach

As part of a large study to accurately predict the fatigue behavior of asphalt mixtures based on fatigue testing of asphalt mastic, this work focuses on the applicability and comparability of the most popular fatigue tests on DSR. Since asphalt mastic (asphalt binder + mineral fines) is the main binder component in asphalt mixes [32], fatigue tests are carried out at the mastic level in this study. On the one hand, mastic fills the spaces between the contact points of large aggregates, and on the other hand, mastic binds the aggregates together [33, 34]. The properties of asphalt mastic are primarily influenced by the relative amount of filler in relation to the asphalt binder content of the mix. Generally, the ratio of filler and asphalt binder used to produce the asphalt mastic is called filler - binder (F-B) ratio [35]. Studies by Liao et al. [2] using DSR on samples of asphalt mastic and asphalt binder have revealed changes in fatigue properties as a result of the addition of filler to asphalt binder. It was found that the stiffness of asphalt mastic, especially with increasing filler content, is significantly higher than that of pure asphalt binder. Furthermore, several studies [36–42] show that the physicochemical interaction between asphalt binder and fillers and the geometrical characteristics of the fillers impact the behavior of mastic.

This study compares the fatigue life of asphalt mastic resulting from different fatigue tests. The mode of loading, specimen geometries, and failure definitions vary. The clear objective of this study is to investigate the comparability of fatigue tests. On the one hand, the different modes of loading will be compared, and on the other hand, the different failure definitions will be compared. Due to the system limitations of DSR tests at higher material stiffness levels, comparability between cylindrical and hyperbolic specimens is also considered. The hyperbolic specimen shape allows the measurement of stiffer mastic samples. These results will then be used to screen out those test methods that will serve as the basis for a large-scale series of tests that will produce an accurate prediction model for the fatigue behavior of asphalt mixtures based on DSR fatigue testing of asphalt mastic. Since all tests are performed on two specimen shapes (cylindrical and hyperbolic), this study also attempts to derive a calculation apparatus that allows conversion of the measurement results between the two shapes. This study did not investigate the direct influences of different fillers (physio-chemical or geometric characteristics) on fatigue behavior.

2 Materials

For this study, we used four different fillers (predominantly grain size <0.063 mm). Two fillers are from Europe, and two fillers are from India. The two European fillers are limestone and quartz. While limestone is a standard filler for asphalt mixes, quartz is an industrial product that is not used in road construction usually. Stone dust is also a standard filler for asphalt mixes, and glass powder is a by-product of the respective industries. Both fillers (quartz and glass powder) are mostly unexplored materials for asphalt mixes. However, based on the studies carried out so far, both materials show high potential for road construction. Due to the wide range of different materials, we expect a large spectrum of test results.

Asphalt mastic is a mixture of asphalt binder and mineral filler. For this study, a filler binder ratio of 1.5 by weight was selected. We used an asphalt binder with a penetration grading of 70/100 to mix the four different mastics. For the asphalt binder, the needle penetration depth (PEN) according to EN 1426 [43], the softening point (ring and ball) according to EN 1427 [44], and the performance grade (PG) according to AASHTO M 320 [9] was determined. The results are listed in Table 1.

For the preparation of the mastic samples, the two components, filler and asphalt binder, are weighed according to the filler-binder ratio. Next, the dry filler is heated to 180 °C in an oven for at least 1 h. Afterward, the asphalt binder is heated to 180 °C. Then the two materials are mixed manually for about 5 min, without heating, until the mixture starts to stiffen. The result is a homogeneous mastic, without fine particles can settle down to the bottom during cool down. Table 2 lists the mastic mixes produced with their source materials. The gravimetric filler binder ratio is the same for all mixes. However, due to the different specific gravities, the filler volume ratio is not the same for all mixes, as shown in Table 2.

Table 1 Properties of the asphalt binder used in this study

Properties	Values
Needle penetration depth (PEN) [1/10 mm]	85
Softening point (ring and ball) [°C]	45.4
Performance grade (PG)	64–28

For the four mastic mixes and the plain asphalt binder, the softening point and the viscosity were determined. The viscosity was determined with a rotational viscometer for the temperature range from 120 to 180 °C. The results are summarized in Table 3. It can be seen that the addition of filler increases the viscosity and the softening point. While mastic 1 to 3 shows similar values, the mastic 4 with glass powder clearly exhibits the highest values. A correlation between filler-volume-ratio, softening point, and viscosity is discernible but not significant due to the small number of samples.

3 Test methods

The dynamic shear rheometer (DSR) is one of the essential instruments in a road engineering laboratory. Unlike other test equipment, it can be used for a variety of different test routines. Moreover, a large number of different parameters and properties can be derived from the rheological data. Therefore, it is evident that the fatigue behavior of asphalt should also be derived from simple tests at the mastic level. For this purpose, two test methods have asserted themselves in recent years. One is the time sweep (TS) test, and the other is the LAS test.

3.1 Fatigue tests with DSR

The LAS test is defined by AASHTO TP 101-14 [30]. This test method describes the determination of the fatigue resistance of asphalt binders against damage due to cyclic loading with linearly increasing load amplitudes. In this study, the test method is used for mastic samples. The LAS tests in this study are performed at a temperature of $+10$°C. Three replicates per mastic were performed for the LAS test.

The time sweep (TS) test is a well-proven and simple fatigue test. Similar to the loading situation in a road construction, a test specimen is subjected to cyclic loading until it fails. The load amplitude and frequency remain constant over time. However, no normative standardization is available for this test method. Accordingly, there are a large number of different test parameters mentioned in the literature. The temperature, the mode of loading, and the test

Table 2 Mixed mastic

Mixture	Binder	Filler	Filler-Binder Ratio [–]	Filler-volume Ratio [%]
Mastic 1 (M1)	70/100	Lime stone	1.5	24.2
Mastic 2 (M2)	70/100	Quartz	1.5	25.7
Mastic 3 (M3)	70/100	Stone dust	1.5	25.2
Mastic 4 (M4)	70/100	Glass powder	1.5	28.7

Table 3 Properties of the mixed mastics used in this study

	Asphalt Binder	Mastic 1	Mastic 2	Mastic 3	Mastic 4
Softening point [°C]	45.4	61.1	59.3	61.6	72.3
Viscosity at 120°C [mPas]	823	8038	9075	10394	41883
Viscosity at 135°C [mPas]	371	3625	3938	4429	16667
Viscosity at 150°C [mPas]	190	1908	1954	2267	7608
Viscosity at 165°C [mPas]	108	1108	1071	1288	3742
Viscosity at 180°C [mPas]	68	733	633	783	2008

frequency vary in particular. In this study, we perform all tests stress-controlled (CS) and strain-controlled (CD). All TS tests in this study are performed at a frequency of 30Hz. This frequency keeps the test duration as short as possible. A test temperature of +10°C was chosen to avoid a too soft consistency due to a high-test temperature or a too-high stiffness due to too low-test temperature. For each TS test, nine individual tests are carried out at three different shear stresses or strains. For the stress-controlled tests, 300 kPa, 400 kPa, and 500 kPa for hyperbolic specimens and 700 kPa, 1000 kPa, and 1200 kPa for cylindrical specimens were selected stress levels. These stress levels were chosen to achieve similar load cycles to fatigue for both specimen shapes. However, due to the necking for hyperbolic specimens, this is a nominal stress for hyperbolic specimens, since the DSR calculates the stress for a cylindrical specimen and not the actual stress in the necking. For the strain-controlled tests, 0.5%, 0.75%, and 1.00% were chosen as the strain for both specimen geometries. A fatigue curve can be derived from the load cycles until fatigue and the selected loads. A variation of the frequency or temperature was not foreseen in this study due to the very high testing effort but will be further investigated within the research project.

3.2 Fatigue criterion of TS tests

The fatigue criterion is also not clearly defined for TS tests, so different fatigue criteria are considered in this study.

- **Reduction of stiffness (RS)** Reaching a stiffness modulus of 50% of the initial stiffness is a traditional fatigue criterion. It is widely used and is defined in the standard EN 12697-24 [4] for asphalt mix level.
- **Phase angle peak (PA)** The maximum phase angle is also used as a fatigue criterion. However, there is a slight difference between CS and CD tests. While in CS tests, an apparent rise with a definite maximum can be identified towards the end of the test, there is often a flat rise in CD tests, and there are often several high points.

The following approaches are based on dissipated energy. The energy approach for asphalt and asphalt binder was developed in 1972 by Van Dijk, Moreaud, Quedeville, and Uge. It states a relationship between the fatigue life (N_f) and the cumulative dissipated energy at failure [21, 45]. Energy is dissipated in mechanical work, heat generation, or damage during a load cycle for a viscoelastic material [20, 46].

- **Dissipated energy ratio (DER)** DER is one of the best-known dissipated energy approaches and is accepted among researchers as a fatigue criterion.

The dissipated energy is calculated for each load cycle (W_i) using equation 1.

$$W_i = \pi \cdot \sigma_i \cdot \gamma_i \cdot \sin(\delta_i) \quad (1)$$

W_i is the dissipated energy in cycle i, σ_i, is the stress level in cycle i, γ_i, is the strain level in cycle i, and δ_i is the phase angle in cycle i. The cumulative dissipated energy up to the loading cycle n is calculated by summing the dissipated energy of all loading cycles. Thus, the DER can be described as the ratio of the cumulative dissipated energy up to load cycle n and the dissipated energy in load cycle n, as shown in Eq. 2.

$$\mathrm{DER} = \frac{\sum_{i=0}^{n} W_i}{W_n} \quad (2)$$

The DER increases linearly initially for both loading modes, CS and CD. However, with time, the DER deviates from the linear line. This deviation indicates fatigue. Bonnetti et al. [19] defined a parameter N_{p20} for the load cycles until fatigue. The parameter describes the number of load cycles until the DER deviates from the undamaged linear line by 20% [19]. This definition is used for both CD-TS and CS-TS tests in this study.

- **Ratio of dissipated energy change (RDEC)** The RDEC approach was proposed as a further development of fatigue characterization based on dissipated energy [23, 26]. The new criterion was defined as the change in dissipated energy between cycles n and $n+1$ divided by the total dissipated energy until load cycle n. By dividing the result by the change of load cycles, the RDEC for each load cycle can be calculated. The approach of this new criterion is that a larger portion of the energy dissipates than in the cycle before when a material fails [24]. This behavior cannot be observed in the undamaged sample. The RDEC is defined as equation 3.

$$\mathrm{RDEC} = \frac{W_{(n+1)} - W_n}{W_n \cdot ((n+1) - n)} \quad (3)$$

RDEC is the average ratio of the change in dissipated energy per load cycle in cycle n compared to cycle $n+1$. Thus, W_n is the dissipated energy during load cycle n, and $W_{(n+1)}$ is the dissipated energy during load cycle $n+1$. When evaluating the RDEC, three phases can be observed: an initial phase of decreasing trend, a plateau phase, and a phase of rapid increase. For this study, a fatigue criterion for load cycles was chosen when the RDEC was twice as large as in the plateau phase. The plateau value is the mean value of all RDEC between decreasing and increasing trends.

3.3 Hyperbolic specimen shape

In addition, there are already different specimen shapes besides the cylindrical shape. So we ran all tests in this study with an alternative specimen geometry. A study [29] has shown that CS-TS tests with mastic specimens of high stiffness lead to unstable complex shear modulus changes. These changes affect the test result. The cooling of the DSR drive system could be the reason for this issue. Because of the high system load, a cooling of the drive system is necessary. Therefore, all tests were performed on hyperbolic specimens. The necking in the middle of the specimen reduces the system loading. So, the load on the drive system is much lower, and the cooling system's influence is minimized. Figure 1 shows the cylindrical profile on the left and the hyperbolic profile on the right.

However, this specimen shape has the problem that the recorded measurement data do not correspond to the actual measurement data. Due to the PP08 measurement geometry, the DSR calculates all data related to this diameter. However, the actual diameter in the necking is only 6mm. Therefore, a calculation model is needed to convert the recorded data to the actual diameter. Based on the generally applied formulas of the two-plate model for calculating the maximum shear stress and shear strain of viscous material, the following formulas were determined by comparing the two formulas of the respective specimen geometry with an additional conversion factor. For simplicity, a cylindrical specimen with 8mm diameter and 6mm diameter were compared. This procedure allows determining the magnitude of the conversion factor between the two specimen shapes. According to equations 4 to 8, a relationship could be established between the two measured values.

Fig. 1 Cylindric specimen shape (left) and hyperbolic specimen shape (right)

$$\frac{2 \cdot \text{Torque}_{\text{DSR}}}{\pi \cdot \text{Radius}^3_{\text{DSR,8mm}}} \cdot f_\tau = \frac{2 \cdot \text{Torque}_{\text{DSR}}}{\pi \cdot \text{Radius}^3_{\text{DSR,6mm}}} \tag{4}$$

$$f_\tau = \frac{\text{Radius}^3_{\text{DSR,8mm}}}{\text{Radius}^3_{\text{DSR,6mm}}} = \frac{8^3}{6^3} = 2,37 \tag{5}$$

$$\frac{\alpha_{\text{DSR,8mm}} \cdot \text{Radius}_{\text{DSR,8mm}}}{\text{High}_{\text{DSR,8mm}}} \cdot f_\gamma = \frac{\alpha_{\text{DSR,6mm}} \cdot \text{Radius}_{\text{DSR,6mm}}}{\text{High}_{\text{DSR,6mm}}} \tag{6}$$

$$f_\gamma = \frac{\text{Radius}_{\text{DSR,6mm}}}{\text{Radius}_{\text{DSR,8mm}}} = \frac{6}{8} = 0,75 \tag{7}$$

$$f_{G^*} = \frac{f_\tau}{f_\gamma} = \frac{2,37}{0,75} = 3,16 \tag{8}$$

To be able to validate this relationship, additional tests were carried out using a virtual test geometry. The virtual measurement geometry consists of a PP08 geometry, but the diameter was changed from 8mm to 6mm in the software. Thus, the data is calculated and recorded concerning the actual 6mm diameter. Based on these data, the theoretical approach according to formulas 4 to 8 can be checked. With the calculation factors from the formulas above, the measurement data could be converted in both directions. These measured data are, however, afflicted with several inaccuracies. For example, the hypothesis of a cylindrical specimen with a diameter of 6mm is not given since it is only a necking in the specimen. In addition, the set moment of inertia and the compliance correction are defined for a test geometry with 8mm and not for a 6mm diameter and could influence the calculations.

4 Results and discussion

Four different mastic mixes were tested in this study using two different test methods (LAS and TS) and two different specimen shapes (cylindric and hyperbolic). The TS tests were performed stress-controlled and strain-controlled. This test program results in 144 individual tests for the TS tests. For all 144 individual tests, the fatigue load cycles were evaluated based on the four fatigue criteria mentioned in the Sect. 3.2; Test Methods. A graphical illustration of the tests performed in this study can be found in Fig. 2.

4.1 Correlation of fatigue criterion

Table 4 summarizes the coefficient of determination of the linear regressions between the different fatigue load cycles for the tests with cylindrical specimen shapes. It can be seen that the calculated fatigue load cycles from different criteria correlate perfectly with each other for the TS-CS test. On the other hand, in the TS-CD test, the fatigue load cycles evaluated with the PA criteria do not correlate with the other evaluated load cycles. So, it can be assumed that the PA criterion is not suitable to describe the point of fatigue for mastic. This impracticality can also be observed in the measurement data. In TS-CD tests, the phase angle exhibits a different evolution over the test duration. No recurring trend can be detected in the phase angle curves.

Table 5 summarizes the coefficient of determination of the linear regressions between the fatigue load cycles from different criteria for the tests with hyperbolic specimen shapes. Again, it can be seen that the calculated load cycles for the TS-CS test correlate very well with each other. On the other hand, in the TS-CD test, only the fatigue load cycles evaluated with the RS criterion and the fatigue load

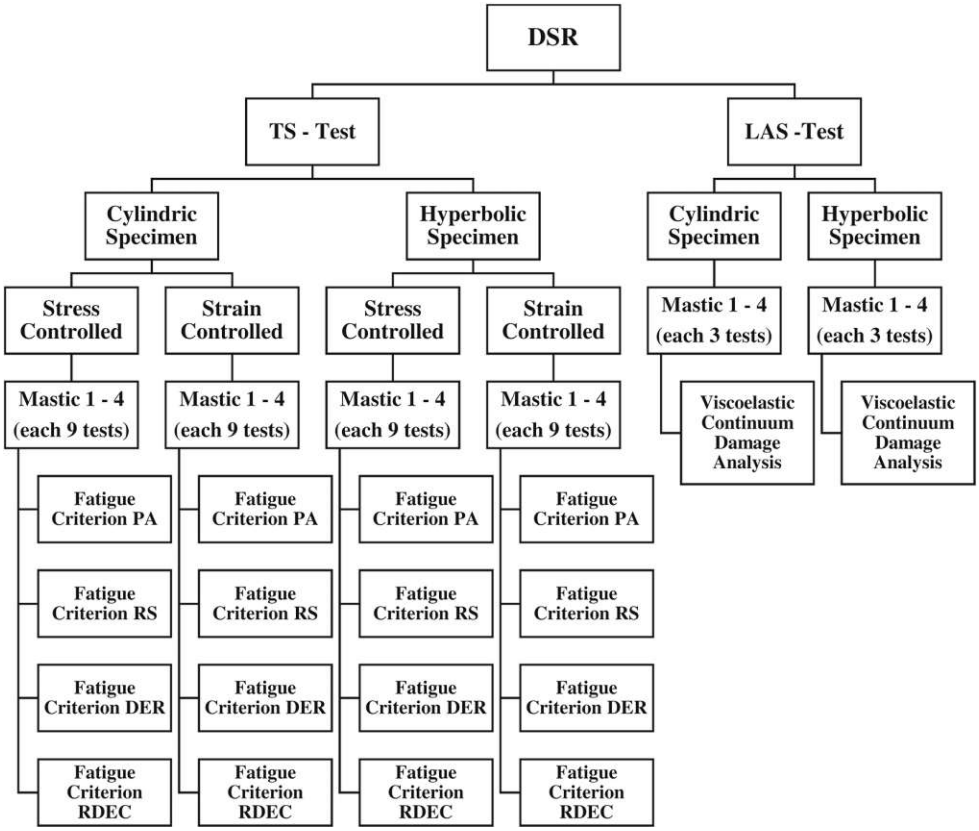

Fig. 2 Overview of the tests performed and the evaluation methods used

Table 4 Coefficient of determination of the linear regressions between the different fatigue load cycles for the tests with cylindrical specimen shape

	Stress controlled				Strain controlled			
	PA	RS	DER	RDEC	PA	RS	DER	RDEC
PA	1.000	1.000	0.999	0.999	1.000	0.450	0.453	0.425
RS		1.000	1.000	0.999		1.000	1.000	0.991
DER			1.000	0.999			1.000	0.992
RDEC				1.000				1.000

Table 5 Coefficient of determination of the linear regressions between the different fatigue load cycles for the tests with hyperbolic specimen shape

	Stress controlled				Strain controlled			
	PA	RS	DER	RDEC	PA	RS	DER	RDEC
PA	1.000	1.000	0.999	0.998	1.000	0.849	0.857	0.472
RS		1.000	0.999	0.998		1.000	0.998	0.507
DER			1.000	0.997			1.000	0.510
RDEC				1.000				1.000

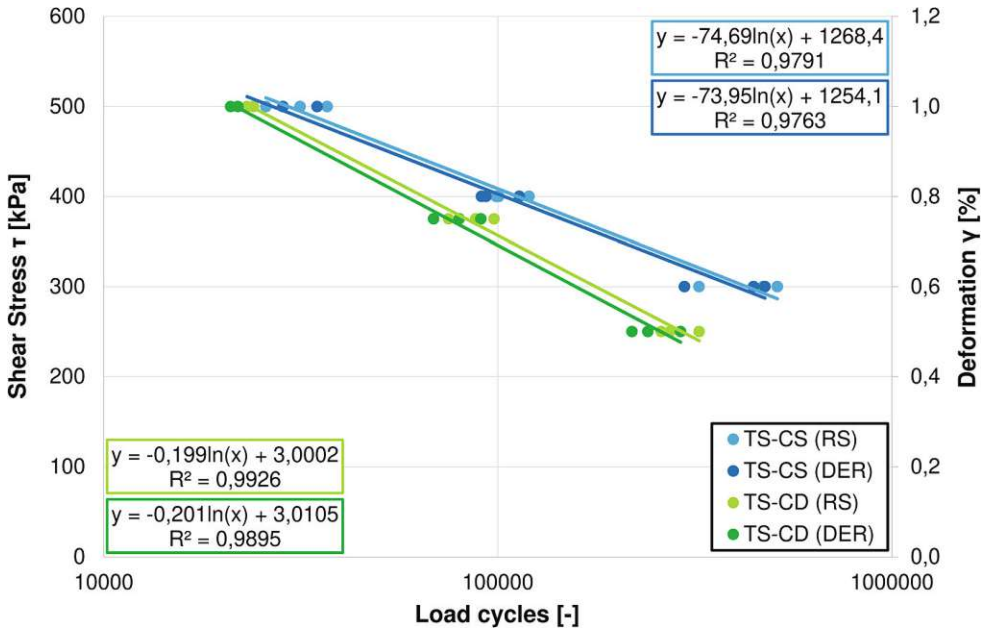

Fig. 3 Fatigue curves for the TS-CS and TS-CD tests on the hyperbolic specimen for mastic 2

cycles evaluated with the DER criterion correlate. Based on both evaluations, it can be concluded that for all four test methods (TS-CS and TS-CD with cylindrical specimen shape; TS-CS and TS-CD with hyperbolic specimen), the RS criterion and the DER criterion are suitable to define the point of fatigue. Both methods are already accepted fatigue criteria and can confirm each other. On average, the load cycles until fatigue using the DER criterion are about 7–10% smaller than using the RS criterion.

Due to the mentioned link between the fatigue criterion above, the RS criterion and the DER criterion will be used for the following evaluations.

4.2 Correlation of fatigue performance

According to the fatigue criteria, fatigue curves can be derived based on the load cycles. Fatigue curves are used to estimate the fatigue performance for different magnitudes of loading. This method is used in many areas of civil engineering. Based on the nine individual tests for each TS test, a fatigue curve can be derived. Figure 3 shows the fatigue curves for the TS-CS and TS-CD tests on the hyperbolic specimen for mastic 2. The two blue curves are the results of the TS-CS test with the different fatigue criteria. Correspondingly, the green curves represent the results of the TS-CD test with the different fatigue criteria.

To compare the results of the different fatigue tests, we calculated the required shear stress to achieve 10^5

Table 6 Required loads to achieve 10^5 load cycles for the different fatigue tests

Shape	Hyperbolic		Cylindric		Hyperbolic			Cylindric		
Test	TS - CS	TS - CS	TS - CS	TS - CS	TS - CD	TS - CD	LAS	TS - CD	TS - CD	LAS
Value	τ_5	τ_5	τ_5	τ_5	γ_5	γ_5	γ_5	γ_5	γ_5	γ_5
Crit.	RS	DER	RS	DER	RS	DER	–	RS	DER	–
Unit	[kPa]	[kPa]	[kPa]	[kPa]	[%]	[%]	[%]	[%]	[%]	[%]
Mastic 1	393.5	387.9	995.7	980.0	0.63	0.61	0.61	0.68	0.66	0.73
Mastic 2	410.1	404.2	1088.5	1075.9	0.72	0.69	0.67	0.76	0.74	0.85
Mastic 3	413.2	407.6	1049.2	1040.9	0.66	0.64	0.88	0.72	0.70	1.06
Mastic 4	468.0	459.9	1231.4	1212.7	0.61	0.59	0.60	0.66	0.64	1.14

load cycles for TS-CS tests. This shear stress is abbreviated as τ_5. For TS-CD tests, we calculated the required strain amplitude to achieve 10^5 load cycles. This strain value is abbreviated as γ_5. The same approach for TS-CD tests was also used for the LAS test. Thus, a γ_5 value can also be calculated for LAS tests.

Table 6 summarizes the loads required to achieve 10^5 load cycles for the different tests. It can be seen that the required loads for the DER criterion are about 1 to 3% smaller than the loads needed for the RS criterion to achieve 10^5 load cycles. Furthermore, it can be observed that the ranking of the mastic tests between hyperbolic specimens and cylindrical specimens is identical. This link cannot be observed in the LAS tests. Accordingly, it can be assumed that the LAS test is not directly applicable to hyperbolic specimen shapes. Furthermore, the ranking between TS-CS tests and TS-CD tests is not identical. For hyperbolic and cylindrical specimen shapes, a different order of the mastic mixture performances is obtained. As an example, we consider mastic 4. The TS-CS test displayed the best fatigue performance. For fatigue failure at 10^5 load cycles, it requires the highest shear stress of all 4 TS-CS tests. In the TS-CD tests, this is exactly the opposite. Here, the mastic 4 displayed the worst fatigue performance. It requires the smallest shear strain of all the TS-CD tests to reach 10^5 load cycles. As a result, it is not possible to directly compare the two different modes of loading. There is also no correlation between the softening point or viscosity of the mastic and the fatigue performance. The main reason for the different rankings is expected to be affected by the modes of loading. In addition, in LAS tests, the high stiffness due to the low temperature and the use of mastic could affect the damage accumulation. The mode of loading is essential for selecting the test method and the interpretation of the results.

4.3 Dissipated energy approach

The fatigue tests performed in this study show that the mode of loading influences the assessment of the fatigue performance of the mastic mixes. However, the mode of loading should not be relevant when assessing fatigue performance. A method of linking TS-CS and TS-CD is via the dissipated energy approach. This approach allows combining the TS test results in one fatigue curve regardless of the mode of loading. One way to combine the two loading methods is the RDEC approach. The plateau value can be used to link the two loading methods. The disadvantage of this option is that the load cycles up to fatigue do not correlate well with the other fatigue methods. The reason for this is most likely the imprecise definition of the fatigue point and the range of the plateau value (start- and endpoint). There is no mathematical definition for this, so the analysis results are always dependent on the user to a certain extent.

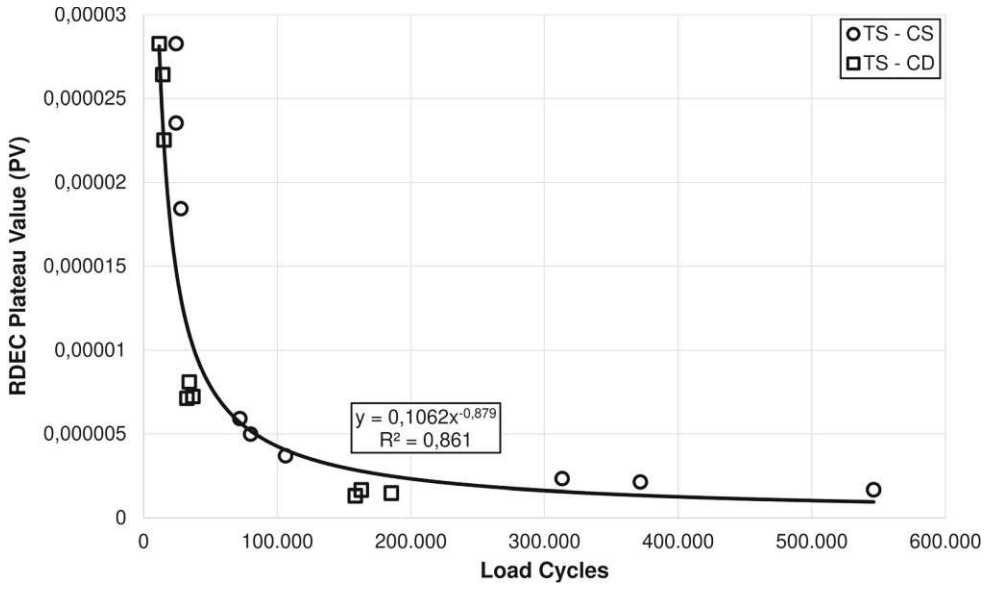

Fig. 4 Fatigue curve according to RDEC for mastic 1

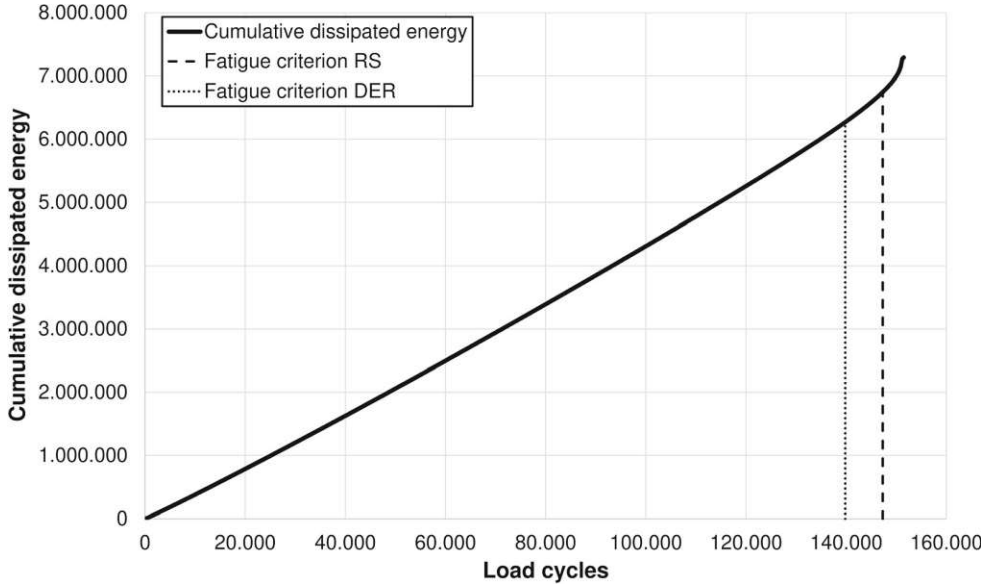

Fig. 5 Cumulative dissipated energy for a TS-CS test

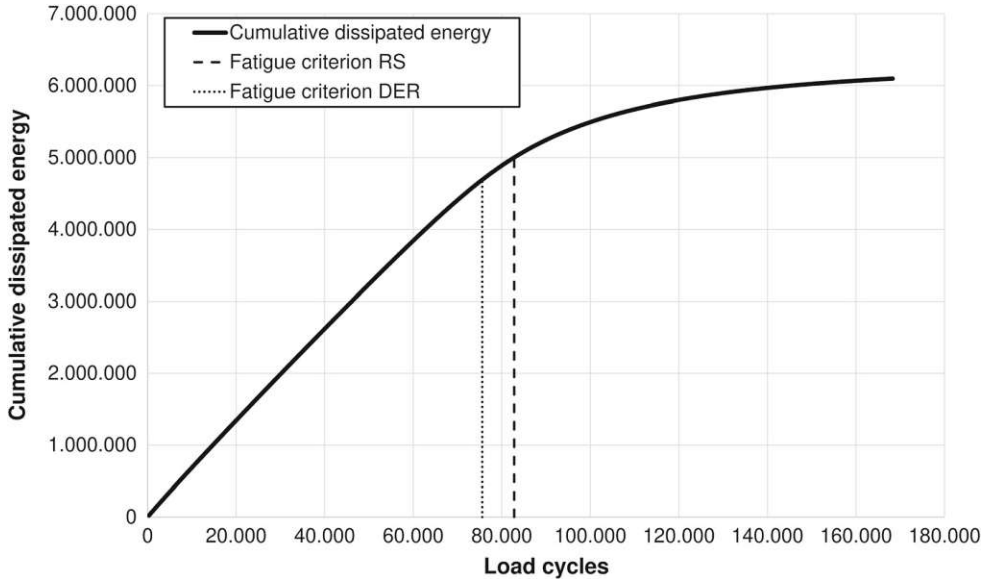

Fig. 6 Cumulative dissipated energy for a TS-CD test

Figure 4 shows the fatigue curve according to RDEC for mastic 1. It shows that both loading methods can be combined. The coefficient of determination of the power-law regression is 0.861.

A new approach was used in this study to find a link between the TS-CS and TS-CD test for the fatigue criterion's RS and DER. Since the two fatigue criteria correlate perfectly, they were used for this approach. In Figs. 5 and 6, the cumulative dissipated energy for a TS-CS and a TS-CD test is depicted.

Figures 5 and 6 show that the curve of the dissipated energy is almost linear up to the two fatigue points. From this, it can be deduced that nearly the same energy is dissipated per load cycle. The initial input measurement parameter (stress or strain) can be brought to a uniform dimension (dissipated energy per load cycle). The dissipated energy per load cycle (DELC) calculation is given in equations 9 and 10.

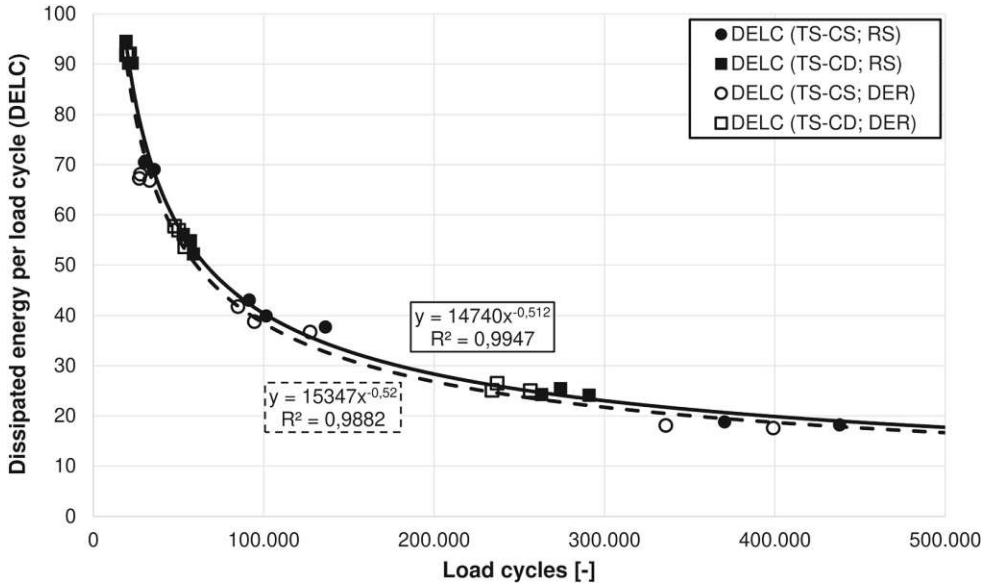

Fig. 7 DELC for the RS criterion and the DER criterion related to the load cycles for mastic 1 with cylindric specimen shape

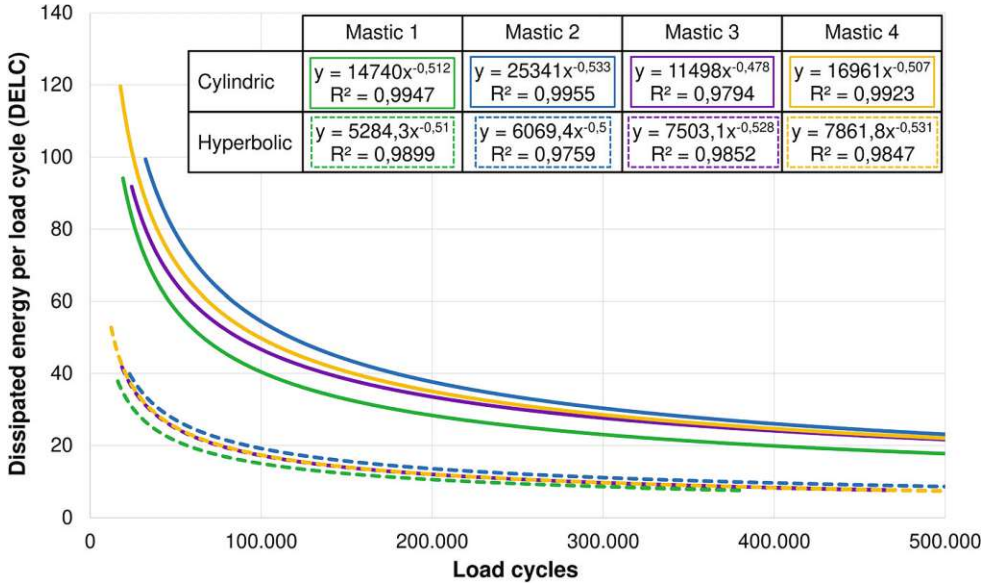

Fig. 8 Potency regression curves for all tests for cylindrical specimen shapes and hyperbolic specimen shapes

$$\mathrm{DELC_{RS}} = \frac{\sum_{i=1}^{N_{RS}} Wi}{N_{RS}} \tag{9}$$

$$\mathrm{DELC_{DER}} = \frac{\sum_{i=1}^{N_{DER}} Wi}{N_{DER}} \tag{10}$$

The results for TS-CS and TS-CD tests can be linked to one fatigue curve by using the above formulas. Figure 7 shows the DELC for the RS criterion and the DER criterion related to the load cycles for mastic 1 with cylindric specimen shape. The solid line is the power-law regression for the test evaluation using the RS criterion. The dashed line is the power-law regression for the test evaluation using the DER criterion. It can be seen that the DELC for the evaluations using the DER criterion is smaller than the DELC for the evaluations using the RS criterion. This difference coincides with all tests performed in this study. It can also be seen that a high fatigue load cycle number is achieved with a low DELC, whereas a

minimal fatigue load cycle number is achieved with a high DELC. With a coefficient of determination of 0.995 and 0.988, the regression is excellent.

Figure 8 shows the power-law regression curves for all tests for cylindrical specimen shapes and hyperbolic specimen shapes. The ranking of the mastic mixes remains the same for both specimen shapes. It can be seen that for cylindrical specimens, the DELC is higher than for hyperbolic specimen shape. Due to the higher load and the larger cross-sectional area of the specimen, more energy is dissipated. From Fig. 8, it can be deduced that the mastic that dissipates more energy per load cycle until failure perform better than the one with a smaller DELC value. This assertion means that mastic 2 has the best fatigue performance and mastic 1 the worst. The challange with this way of assessing the fatigue performance is that it is impossible to distinguish different effects of energy dissipation. Thus, the energy can be dissipated due to internal friction, viscous deformation, or fatigue. These energy dissipations and their proportions are influenced by the physicochemical interaction between asphalt binder and filler and the geometrical properties of the filler. These properties of the mastic are not part of this study, which is why no further analyses were carried out on this. However, due to the different fillers, it could be shown that the filler has a significant contribution to the fatigue performance of the mastic. Which properties of the filler affect the fatigue performance is the subject of current research.

Thus, there are a variety of ways to study the fatigue behavior of mastic. Since the TS test is not standardized, there are many different test methods and evaluation procedures. Comparing the data from Table 6 and Fig. 8,we see that the ranking of the results between hyperbolic and cylindrical specimen shapes does not show any differences. The regression coefficient of the linear correlation between cylindrical and hyperbolic specimen shape is higher than 0.98 for all TS tests. Only the LAS test shows no correlation between the two specimen shapes. On the other hand, the comparison between the different test methods shows partly different rankings of results. None of the tests (TS-CS, TS-CD, and LAS) is comparable with each other. The results also show that there is no correlation between the results ranking of RDEC and DELC. This observation means that the specimen shape does not influence the result in TS tests. Only the scale of the results changes according to the two specimen shapes. On the other hand, LAS tests with hyperbolic specimen shapes are not applicable without further adjustments in the calculation model of LAS. These adaptations are not part of this study.

Table 7 Correlation between the measured results with the PP08 and the VPP06

	PP08	VPP06	f [-]
$\lvert G^* \rvert_{\text{mean initial}}$ [Mpa]	84.63	267.95	3.17
τ_5 - PA [kPa]	396.66	908.77	2.29
τ_5 - RS [kPa]	393.53	900.65	2.29
τ_5 - DER [kPa]	387.91	884.15	2.28

4.4 Validation of calculation model for hyperbolic specimen shape

A theoretical relationship between cylindrical and hyperbolic specimen shape has already been established with equations 4 to 8. TS-CS tests were performed using a virtual 6mm test geometry. Since the virtual geometry causes the DSR to assume that it measures a cylindrical specimen with a diameter of 6mm, these values refer to the necking in the specimen shape. Thus, it can be checked whether the derived equations 4 to 8 can derive the approximate actual stresses and moduli based on the tests. Table 7 shows the measured values of Mastic 1 with an 8mm plate-plate test geometry (PP08) and a virtual 6mm plate-plate test geometry (VPP06).

According to equation 8, a factor between the complex shear modulus of 3.16 was calculated. Table 7 shows the mean value of the initial complex shear modulus of the mastic tests of mastic 1 using PP08 and VPP06. The factor between the measured results is 3.17. According to equations 4 and 5, a factor between the shear stresses of 2.37 was calculated. Table 7 summarizes the required shear stresses for 10^5 load cycles for PP08 and VPP06 for different fatigue criteria. The measured factor is 2.28 to 2.29, which is lower than the theoretical factor.

These slight deviations in the analyzed values are probably due to the simplifying assumption of a cylindrical specimen with a diameter of 6 mm. However, since this is a hyperbolic specimen shape, stress distribution in the necking is not identical to the stress distribution in a cylindrical specimen. In

addition, there are DSR specific correction values (compliance correction, moment of inertia of the test geometry), which have not been changed in the software. Only the diameter has been adjusted in the software from 8mm to 6mm. These settings could also influence the measurement results.

5 Conclusion

This study compares different fatigue test methods for asphalt mastic. There are various fatigue test methods available for asphalt binders performed with the DSR. These test methods were used in this study and examined at the mastic level. Four different mastic mixes were tested. Time sweep (TS) tests (stress and strain controlled) and LAS tests were performed. All tests were carried out on two different specimen shapes (cylindrical and hyperbolic). Different evaluation methods and fatigue criteria were used for the TS tests.

- In TS-CS tests, all fatigue criteria show a perfect correlation. The coefficient of determination of the linear regression of all fatigue load cycles is almost 1. In TS-CD tests, the fatigue criteria RS, DER, and RDEC correlate well with each other for cylindrical specimens. In TS-CD tests, the fatigue criteria RS and DER correlate well for hyperbolic specimens. Accordingly, it is recommended that the fatigue criteria RS or DER is used for TS tests.
- Considering the shear stress or shear strain required to achieve 10^5 load cycles, it can be observed that there is no correlation between the different fatigue tests. The fatigue performance of the mastics is ranked differently in each test method, due to the different modes of loading.
- A good approach to assessing fatigue performance is via dissipated energy. Through DELC or RDEC it is possible to combine stress and strain-controlled tests. Regardless of the loading mode in the test, uniform fatigue curves can be derived from the tests. The disadvantage of this method is that energy is dissipated not only by fatigue, but also by friction or viscous deformation. Therefore, it must still be determined whether the assessment using these values is possible, i.e. that energy dissipation is predominatly driven by fatique. The classification of the mastics by DELC and RDEC show no correlation. One reason could be the user-dependent test evaluation of the RDEC method.
- A conversion of the measurement results between cylindrical and hyperbolic is confirmed. However. these are afflicted with inaccuracies. On the one hand, the derived equations are based on two cylindrical specimen shapes with different diameters. However, the stresses and strains in the necking of the hyperbolic specimen shape will differ slightly. On the other hand, the cylindrical specimen shape is influenced by trimming, which means that the same diameter of 8mm cannot always be guaranteed at all times.

The study shows that the results, due to different fatigue tests, do not all lead to the same classification of results. However, it is possible to combine stress- and strain-controlled tests using the dissipated energy approach. The fatigue criteria, especially the RS criterion and DER show a good applicability for all TS tests. The hyperbolic specimen shape is not applicable for LAS tests without adjustment. The LAS test may not be the ideal fatigue test for mastic with high stiffness due to low temperature or filler content because this affects the damage accumulation. However, TS tests using the dissipated energy approach appear to be the most promising mastic fatigue tests. Therefore, to identify the fatigue tests' classification, the tests at the mastic level should be compared with test series at the asphalt mix level. Influences due to different temperatures, frequencies and filler properties will be investigated in further studies. In addition, the effects on the test results of aged mastic specimens should be investigated since aged mastic samples have even higher stiffnesses.

Acknowledgements The study reported in this paper is part of a scientific and technological Cooperation with India organized by the center for international cooperation and mobility (ICM) of the Austrian Agency for international cooperation in education and research (OeAD-GmbH) and the Indian Department of Science and Technology (DST). The authors acknowledge TU Wien Bibliothek for financial support through its Open Access Funding Programme.

Funding Open access funding provided by TU Wien (TUW). The research project (IN 09/2018) about "Development and assessment of asphalt mastic from typical Indian and Austrian filler materials with a new test method" is funded by the Federal Ministry of Science, Research and Economy (BMWFW).

Declarations

Conflict of interest The authors declare that they have no conflict of interest.

References

1. Di Benedetto H, De La Roche C, Baaj H, Pronk A, Lundstrom R (2004) Fatigue of bituminous mixtures. Mater Struct 37(3):202–216.https://doi.org/10.1007/BF02481620
2. Liao M-C, Chen J-S, Tsou K-W (2012) Fatigue characteristics of bitumen-filler mastics and asphalt mixtures. J Mater Civ Eng 24:916–923.https://doi.org/10.1061/(ASCE)MT.1943-5533.0000450
3. Poulikakos LD, Pittet M, Dumont A-G, Partl MN (2014) Comparison of the two point bending and four point bending test methods for aged asphalt concrete field samples. Mater Struct 48(9):2901–2913. https://doi.org/10.1617/s11527-014-0366-8
4. EN 12697-24 (2018) Bituminous mixtures-test methods—Part 24: resistance to fatigue. European Committee for Standardization (CEN), Brussels
5. Safaei F, Castorena C, Kim YR (2016) Linking asphalt binder fatigue to asphalt mixture fatigue performance using viscoelastic continuum damage modeling. Mech Time Depend Mater. https://doi.org/10.1007/s11043-016-9304-1
6. Johnson C, Bahia H, Coenen A (2009) Comparison of bitumen fatigue testing procedures measured in shear and correlations with four-point bending mixture fatigue. Paper presented at the 2nd conference on four point bending. University of Minho, Portugal
7. Steineder M, Donev V, Hofko B, Eberhardsteiner L (2021) Correlation between stiffness and fatigue behavior at asphalt mastic and asphalt mixture level. J Test Eval. https://doi.org/10.1520/JTE20210204
8. Soenen H, de La Roche C, Redelius P (2011) Fatigue behaviour of bituminous materials: from binders to mixes. Road Mater Pavement Des. https://doi.org/10.1080/14680629.2003.9689938
9. AASHTO M 320-17 (2017) Standard specification for performance-graded asphalt binder. American Association of State and Highway Transportation Officials (AASHTO), Washington, DC
10. Anderson DA, Kennedy TW (1993) Development of SHRP binder specification. Paper presented at the Asphalt Paving Technology Conference, Austin
11. Zhou F, Mogawer W, Li H, Andriescu A, Copeland A (2013) Evaluation of fatigue tests for characterizing asphalt binders. J Mater Civ Eng 25:610–617. https://doi.org/10.1061/(ASCE)MT.1943-5533.0000625
12. Raithby K, Sterling A (1972) Some effects of loading history on the fatigue performance of rolled asphalt. Transport Road Res Lab Rep 496:32
13. Wang C, Zhang H, Castorena C, Zhang J, Richard KY (2016) Identifying fatigue failure in asphalt binder time sweep tests. Construct Build Mater 121:535–546. https://doi.org/10.1016/j.conbuildmat.2016.06.020
14. AASHTO T 321 (2017) Standard Method of Test for Determining the Fatigue Life of Compacted Asphalt Mixtures Subjected to Repeated Flexural Bending. American Association of State and Highway Transportation Officials (AASHTO), Washington, DC
15. University of California, I. o. T. S. (1994) Fatigue response of asphalt-aggregate mixes. SHRP-A-404. Strategic Highway Research Program. National Research Council, Washington, DC
16. Hospodka M, Hofko B, Blab R (2018) Introducing a new specimen shape to assess the fatigue performance of asphalt mastic by dynamic shear rheometer testing. Mater Struct. https://doi.org/10.1617/s11527-018-1171-6
17. Kim Y-R, Little DN, Lytton RL (2003) Fatigue and healing characterization of asphalt mixtures. J Mater Civ Eng 15(1):75–83. https://doi.org/10.1061/(asce)0899-1561(2003)15:1(75)
18. Reese R (1997) Properties of aged asphalt binder related to asphalt concrete fatigue life. Paper presented at the Asphalt Paving Technology Conference, Salt Lake City
19. Bonnetti KS, Nam K, Bahia HU (2002) Measuring and defining fatigue behavior of asphalt binders. Bituminous Binders 2002(1810):33–43
20. Rowe G (1993) Performance of asphalt mixtures in the trapezoidal fatigue test. J Assoc Asphalt Paving Technol 62:344–384
21. Van Dijk W & Visser W (1977) Energy approach to fatigue for pavement design. Paper presented at the Technical Session of the Association of Asphalt Paving Technologists Proc, San Antonio
22. Boudabbous M, Millien A, Petit C, Neji J (2013) Shear test to evaluate the fatigue of asphalt materials. Road Mater Pavement Des 14(sup1):86–104. https://doi.org/10.1080/14680629.2013.774748
23. Carpenter S, Shen S (2006) Dissipated energy approach to study hot-mix asphalt healing in fatigue. Transp Res Rec J Transp Res Board 1970:178–185. https://doi.org/10.1177/0361198106197000119
24. Ghuzlan KA, Carpenter SH (2000) Energy-derived, damage-based failure criterion for fatigue testing. Transp Res Rec J Transp Res Board 1723(1):141–149. https://doi.org/10.3141/1723-18
25. Shen S, Carpenter S (2005) Application of the dissipated energy concept in fatigue endurance limit testing. Transp Res Rec 1929:165–173. https://doi.org/10.3141/1929-20
26. Shen SH, Airey GA, Carpenter SH, Huang H (2006) A dissipated energy approach to fatigue evaluation. Road

Mater Pavement Des 7(1):47–69. https://doi.org/10.3166/Rmpd.7.47-69
27. Rowe G, Bouldin MG (2000) Improved techniques to evaluate the fatigue resistance of asphaltic mixtures (2000). In: Proceedings of the papers submitted for review at 2nd Eurasphalt and Eurobitume Congress, Barcelona, Spain (2000)
28. ASTM D7460-10 (2019) Standard test method for determining fatigue failure of compacted asphalt concrete subjected to repeated flexural bending. ASTM International, West Conshohocken
29. Kim YS, Sigwarth T, Büchner J, Wistuba MP (2021) Accelerated dynamic shear rheometer fatigue test for investigating asphalt mastic. Road Mater Pavement Des 22(sup1):383-S396. https://doi.org/10.1080/14680629.2021.1911832
30. AASHTO TP 101-14 (2012) Standard method of test for estimating fatigue resistance of asphalt binders using the linear amplitude sweep. American Association of State and Highway Transportation Officials (AASHTO), Washington, DC
31. MTO LS-299 (2001) Method of test for the determination of asphalt cement's resistance to ductile failure using double edge notched tension test (DENT). Ministry of Transportation, Ontario
32. Grabowski W, Wilanowicz J (2007) The structure of mineral fillers and their stiffening properties in filler-bitumen mastics. Mater Struct. https://doi.org/10.1617/s11527-007-9283-4
33. Chen J-S, Peng C-H (1998) Analyses of tensile failure properties of asphalt-mineral filler mastics. J Mater Civ Eng. https://doi.org/10.1061/(asce)0899-1561(1998)10:4(256)
34. Recasens RM, Martinez A, Jimenez FP, Bianchetto H (2005) Effect of filler on the aging potential of asphalt mixtures. Transp Res Rec J Transp Res Board. https://doi.org/10.1177/0361198105190100102
35. Chaudhary M, Saboo N, Gupta A, Hofko B, Steineder M (2020) Assessing the effect of fillers on lve properties of asphalt mastics at intermediate temperatures. Mater Struct. https://doi.org/10.1617/s11527-020-01532-6
36. Huang SC, Zeng M (2007) Characterization of aging effect on rheological properties of asphalt-filler systems. Int J Pavement Eng. https://doi.org/10.1080/10298430601135477
37. Anderson D, Goetz W (1973) Mechanical behavior and reinforcement of mineral filler-asphalt mixtures. Joint Highway Research Project, Indiana Department of Transportation and Purdue University, West Lafayette, Indiana. FHWA/IN/JHRP-73/05. https://doi.org/10.5703/1288284313845
38. Pereira L et al (2018) Experimental study of the effect of filler on the ductility of filler-bitumen mastics. Construct Build Mater. https://doi.org/10.1016/j.conbuildmat.2018.09.063
39. Tunnicliff D (1962) A review of mineral filler. In: Proceedings of Association of Asphalt Paving Technologists, vol 31
40. Kallas B, Puzinauskas V, Krieger H (1961) A study of mineral fillers in asphalt paving mixtures. In: Proceedings of Association of Asphalt Paving Technologists, vol 30
41. Antunes V, Freire A, Quaresma L, Micaelo R (2015) Influence of the geometrical and physical properties of filler in the filler–bitumen interaction. Construct Build Mater. https://doi.org/10.1016/j.conbuildmat.2014.12.008
42. Clopotel C, Velasquez R, Bahia H (2012) Measuring physico–chemical interaction in mastics using glass transition. Road Mater Pavement Des. https://doi.org/10.1080/14680629.2012.657095
43. EN 1426 (2015) Bitumen and bituminous binders—determination of needle penetration. European Committee for Standardization (CEN), Brussels
44. EN 1427 (2015) Bitumen and bituminous binders—determination of the softening point—ring and ball method. European Committee for Standardization (CEN), Brussels
45. Van Dijk W, Moreaud H, Quedeville A, Uge P (1972) The fatigue of bitumen and bituminous mixes. In: Paper presented at the third international conference on the structural design of asphalt pavements, Grosvenor House, London
46. Rowe G (1996) Application of the dissipated energy concept to fatigue cracking in asphalt pavements. Thesis submitted to the University of Nottingham for the degree of Doctor of Philosophy

Appendix 2 (Publication 2)

Journal of Testing and Evaluation

doi:10.1520/JTE20210204 / Vol. 50 / No. 2 / 2022 / available online at www.astm.org

Michael Steineder,[1] Valentin Donev,[2] Bernhard Hofko,[2] and Lukas Eberhardsteiner[2]

Correlation between Stiffness and Fatigue Behavior at Asphalt Mastic and Asphalt Mixture Level

Reference

M. Steineder, V. Donev, B. Hofko, and L. Eberhardsteiner, "Correlation between Stiffness and Fatigue Behavior at Asphalt Mastic and Asphalt Mixture Level," *Journal of Testing and Evaluation* 50, no. 2 (March/April 2022): 803–817. https://doi.org/10.1520/JTE20210204

ABSTRACT

Performance-based tests on asphalt mix level to assess performance behavior are already state of the art, including the fatigue test with the 4-point bending beam. However, this test method requires high effort in material, time, and manpower, making it less practical for routine quality control. This study aims to partially substitute the performance-based tests on asphalt mix level with a practical test method on asphalt mastic level. The tests on asphalt mastic level were carried out with a dynamic shear rheometer (DSR) by time sweep tests on hyperbolic specimens. Fourteen different asphalt mixtures and the corresponding asphalt mastic mixtures were tested. We used a wide range of different asphalt binders and types of aggregates to extend the validity range of the developed model. Correlations between the asphalt mastic performance and asphalt mix performance were investigated using simple and multiple linear regression models. The correlations show that the dynamic modulus $|E^*|_{30Hz}$ at asphalt mix level can be linked to the complex shear modulus $|G^*|_{initial}$ at mastic level by a simple linear regression model. On the other hand, no correlation could be found between the phase angles of both mix levels. However, the characteristic fatigue value of the asphalt mix ε_6 can be linked with high accuracy ($R^2 = 0.92$) to the characteristic fatigue value τ_6 and complex shear modulus $|G^*|_{initial}$ of the asphalt mastic using a multiple linear regression model. In summary, a reliable prediction of the fatigue behavior and stiffness of an asphalt mixture through simple fatigue tests with the DSR on asphalt mastic is feasible.

Keywords

fatigue performance, stiffness, asphalt mixture, mastic, correlation

Manuscript received March 26, 2021; accepted for publication June 7, 2021; published online August 11, 2021. Issue published March 1, 2022.

[1] Institute of Transportation, Vienna University of Technology, Gusshausstraße 28/E230/3, Vienna 1040, Austria (Corresponding author), e-mail: michael.steineder@tuwien.ac.at, https://orcid.org/0000-0003-2223-1785

[2] Institute of Transportation, Vienna University of Technology, Gusshausstraße 28/E230/3, Vienna 1040, Austria, https://orcid.org/0000-0002-3933-971X (V.D.), https://orcid.org/0000-0002-8329-8687 (B.H.), https://orcid.org/0000-0003-2153-9315 (L.E.)

Introduction

Recipe-based, empirical test methods for asphalt mixtures have been the standard approach for mix design optimization and quality control for a long time. With the introduction of performance-based test methods, which simulate the effects of field traffic and climate load on the mechanical properties of asphalt mixtures, new options for assessing asphalt mixtures are available. The main distress mechanism for asphalt pavements is failure due to permanent deformation, fatigue, and low-temperature cracking. There are several methods to test the resistance to permanent deformation at high temperatures,[1] fatigue resistance at moderate temperatures,[2–5] and crack resistance at low temperatures[6,7] of asphalt mixtures in the lab. The advantage of performance-based test methods consists in their effectiveness in predicting the mechanical behavior and performance of asphalt mixtures. However, these tests usually require a high amount of materials and time to be completed, as summarized in Table 1. For the asphalt mix fatigue test using the four-point bending beam (4-point bending beam), 12 days and about 150 kg of material are needed for a complete test set with 18 specimens. Thus, it is of interest to find a more efficient way to assess asphalt mixtures' fatigue performance. One option, pursued in this study, is to shift the performance-based fatigue test from the asphalt mix to the asphalt mastic level.

As mentioned, fatigue is one of the major failure mechanisms that occur in asphalt pavements. The asphalt binder plays a crucial role in this process, as microcracks in the asphalt binder initiate the crack formation.[8] Studies have found that the addition of mineral filler to asphalt binder, defined as mastic, has a significant effect on the binder's fatigue life, as the stiffening effect and filler particles limit crack growth in the mastic.[9] Based on this finding, a fatigue test at the asphalt mastic level using a dynamic shear rheometer (DSR) was chosen to evaluate the fatigue performance of asphalt mixture in this study, since this device is standard equipment in most asphalt laboratories nowadays. In the literature, many studies are dedicated to describing the fatigue behavior of asphalt binders and mastic using DSR.

Anderson et al.[10] studied an alternative test method for the original Superpave asphalt binder specification criterion for fatigue, $G^*\sin(\delta)$. They used a time sweep test with a DSR to describe the asphalt binder's fatigue behavior. The setup was a parallel plate with 8-mm diameter, a gap of 2 mm, and 10-Hz sinusoidal controlled strain mode. Subsequently, other research studies have also considered using DSR to determine the fatigue performance of asphalt binder and mastic. Thus, there are many different test setups with different temperatures, frequencies, test geometries, and loading modes (e.g., stress-controlled versus deformation-controlled). The test temperatures vary between +10°C[8,11–13] and +25°C[8,14–17] and test frequencies vary between 10 Hz[8,10,11,14–18] and 40 Hz[13] with a parallel plate test geometry with a diameter of 8 mm and different specimen shapes in various studies for DSR time sweep fatigue tests. Moreover, parallel plate test geometry with a diameter of 4 mm has also been used to study the rheological properties of bitumen and mastic.[19] In addition, a new testing protocol called the advanced fatigue test using an annular shear rheometer was proposed in the literature.[20] Also, test methods that are not carried out with a shear rheometer, such as the double edge notch tension (DENT) test, are suitable

TABLE 1
Effort for performance-based test methods

	Fatigue Test (EN 12697-24[4])	Deformation Test (EN 12697-25[1])	Low-Temperature Crack Test (EN 12697-46[7])
	Time Needed for Performance-Based Tests of One Asphalt Mix		
Specimen preparation	2 days	2 days	2 days
Test preparation	1 day	…	1 day
Testing	9 days	2 days	3 days
Total	12 days	4 days	6 days
Material Required			
Aggregates	140 kg	40 kg	45 kg
Asphalt binder	10 kg	2 kg	3 kg
Total		Approx. 240 kg	

for characterizing the fatigue behavior of the asphalt binder.[21] Johnson and Bahia[22] introduced the linear amplitude sweep test (LAS) to characterize the accelerated fatigue performance of asphalt binders. The method was developed to replace the time sweep test, as the latter is considered unsuitable for the determination of fatigue performance because of the long duration of the test and issues related to the repeatability of the results.[23] The LAS test is a cyclic torsion test with increasing load amplitude to accelerate the damage performed in the DSR. A comparison between the time sweep test and LAS test results by Hintz and Bahia[24] shows that the damage development is different in both tests. The LAS test is quite complex and may rather be called a damage tolerance test instead of a fatigue test.[24] Nowadays, time sweep tests (strain or stress-controlled) and LAS are used for asphalt binder fatigue testing. In general, time sweep tests in controlled-stress mode or controlled-deformation mode show good agreement even with different failure definitions for neat and modified asphalt binders.[25]

The study conducted in 2013 by Zhou et al.[21] compared various asphalt binder fatigue tests (parameter $G^*\sin(\delta)$, elastic recovery, multiple stress creep recovery (MSCR), LAS, and DENT tension-fatigue tests) of six different binders with the results of the push-pull asphalt mix fatigue test of mixes with equal mix design. They proved that neither the MSCR nor the LAS test correlate well with asphalt fatigue and that the parameter $G^*\sin(\delta)$ shows a poor relationship.[21] The results in Sabouri, Mirzaiyan, and Moniri[26] show a strong correlation between LAS test results on asphalt binder and the results of 4-point bending beam tests on asphalt mixture. The Strategic Highway Research Program (SHRP) binder fatigue index $G^*\sin(\delta)$ does not show a strong correlation with either LAS or 4-point bending beam tests.

Similar to the studies mentioned before, this study aims to predict the fatigue behavior of the asphalt mixture with a quick and less material-consuming test than the 4-point bending beam testing. Added filler in the asphalt binder influences the development of microcracks and the stiffness of the resulting asphalt mastic. Therefore, the mastic (not only the binder) should be used for correlation with fatigue performance at the asphalt mix level. Thus, a time sweep test (stress-controlled) with a hyperbolic specimen shape was applied to determine the fatigue performance of asphalt mastic in this study. This setup is promising because of the moderate test duration and high repeatability of the results. The hyperbolic shape ensures high repeatability and avoids interface failure between the DSR plates and mastic specimen.[27] For this test setup, the test temperature is 10°C and test frequency is 30 Hz. The fatigue performance at the asphalt mix level was determined using the 4-point bending beam test according to EN 12697-24.[4]

We established a correlation between the results of both mixes' levels. This correlation should enable a prediction of the fatigue behavior at the asphalt mix level from fatigue tests at the asphalt mastic level. Thus, the testing effort can be reduced significantly, and it can save costs and material. The sample preparation can be simplified considerably by shifting the tests to the asphalt mastic level. In addition, the DSR is a widely available testing device, and tests can be carried out without any significant adaptations of the DSR.

A further development and validation of the derived prediction model with additional tests is a necessary prerequisite for the implementation of the procedure in the technical standards. Thus, performance-based fatigue tests could be largely carried out on the asphalt mastic level, and only in inconclusive cases or for nonstandard mixes the tests may be carried out on the asphalt mix level as well.

Materials and Methods

MATERIALS

For this research, we used aggregates, fillers (predominantly grain size < 0.063 mm), and asphalt binders from different sources in Central and Western Europe for the production of asphalt mastics and asphalt mixtures. Ten asphalt binders have been selected, representing common commercially available unmodified asphalt binders and polymer-modified asphalt binders (PmB) for asphalt pavements. For three different fractions of the aggregates, the particle size distribution was determined according to the European standard EN 933-1, *Tests for Geometrical Properties of Aggregates - Part 1: Determination of Particle Size Distribution - Sieving Method*.[28] For the limestone fillers from all sources, the particle size distribution was determined according to EN ISO 17892-4, *Geotechnical Investigation and Testing - Laboratory Testing of Soil - Part 4: Determination of Particle Size Distribution*.[29] For

each of the ten asphalt binders, the softening point (Ring and Ball), according to EN 1427, *Bitumen and Bituminous Binders - Determination of the Softening Point - Ring and Ball Method*;[30] needle penetration depth (PEN), according to EN 1426, *Bitumen and Bituminous Binders - Determination of Needle Penetration*;[31] and performance grade (PG) according to AASHTO M 320, *Standard Specification for Performance-Graded Asphalt Binder*,[32] were determined. The results for all ten asphalt binders are listed in Table 2.

A mix design for an asphalt concrete AC 11 D S was developed for each of the three different aggregates, according to TL Asphalt-StB.[33] The designation AC 11 D S specifies a mix with a maximum nominal aggregate size of 11 mm, intended for asphalt surface courses (D) and heavy traffic load (S). The target air void content was set to 3.5Vol.-%.

The required quantities of asphalt binder and aggregates are weighed according to the mix design for the preparation of the asphalt test specimens. Both materials are preheated to 160°C in an oven. Afterward, the asphalt binder and aggregates are mixed for 5 minutes in a heated laboratory mixer. Asphalt slabs are produced using a roller sector compactor. The specimens are cut out from the slabs, and according to EN 12697-6, *Bituminous Mixtures - Test Methods - Part 6: Determination of Bulk Density of Bituminous Specimens*,[34] methods B and C, the density of the test specimens is determined.

Because of the slightly different particle size distribution, the asphalt mixes contain varying amounts of added fillers in the form of limestone powder. For the mixes with gabbro, porphyry, and silicate, the proportion of added filler is 1 M.-%, 8 M.-%, and 4 M.-%, respectively. Based on slightly different mix designs of the asphalt mixtures, the filler-asphalt binder ratio (F/B-ratio) and filler-asphalt binder volume ratio varied between the mixes. In Table 3, the asphalt binders and aggregates and the resulting mixes are listed. A typical mixing temperature of 160°C was specified to minimize the influence of asphalt production on test results.

TABLE 2
Properties of asphalt binder brands used for this study

Label	PG - Grade [-]	Penetration Grade [-]	Penetration [1/10 mm]	Ring and Ball, °C
Asphalt binder 1	58-22	70/100	85	47.3
Asphalt binder 2	64-16	50/70	67	47.9
Asphalt binder 3	64-22	50/70	64	51.3
Asphalt binder 4	64-22	50/70	56	49.7
Asphalt binder 5	70-22	50/70	64	48.8
Asphalt binder 6	76-16	PmB 25/55-55	39	60.7
Asphalt binder 7	76-22	PmB 25/55-55	46	58.0
Asphalt binder 8	76-22	PmB 25/55-55	40	58.5
Asphalt binder 9	82-16	PmB 25/55-55	43	79.8
Asphalt binder 10	82-22	PmB 45/80-65	58	87.0

TABLE 3
Mixed mastic/asphalt

Mixture	PG Grade	Aggregates	Asphalt Binder	F/B - Ratio	Filler Volume Ratio, %
Asphalt A/Mastic A	58-22	Silicate	Asphalt binder 1	1.085	41.0
Asphalt B/Mastic B	58-22	Porphyry	Asphalt binder 1	1.216	44.7
Asphalt C/Mastic C	58-22	Gabbro	Asphalt binder 1	1.327	46.8
Asphalt D/Mastic D	64-16	Gabbro	Asphalt binder 2	1.327	46.8
Asphalt E/Mastic E	64-22	Gabbro	Asphalt binder 3	1.327	46.8
Asphalt F/Mastic F	64-22	Gabbro	Asphalt binder 4	1.327	46.8
Asphalt G/Mastic G	70-22	Gabbro	Asphalt binder 5	1.327	46.8
Asphalt H/Mastic H	76-16	Gabbro	Asphalt binder 6	1.327	46.8
Asphalt I/Mastic I	76-22	Gabbro	Asphalt binder 7	1.327	46.8
Asphalt J/Mastic J	76-22	Gabbro	Asphalt binder 8	1.327	46.8

TABLE 3 *Continued*

Mixture	PG Grade	Aggregates	Asphalt Binder	F/B - Ratio	Filler Volume Ratio, %
Asphalt K/Mastic K	82-16	Gabbro	Asphalt binder 9	1.327	46.8
Asphalt L/Mastic L	82-22	Silicate	Asphalt binder 10	1.085	41.0
Asphalt M/Mastic M	82-22	Porphyry	Asphalt binder 10	1.216	44.7
Asphalt N/Mastic N	82-22	Gabbro	Asphalt binder 10	1.327	46.8

Asphalt mastic is a mixture of asphalt binder and filler (predominantly grain size < 0.063 mm). Based on the asphalt mix designs, the mix design for asphalt mastic was specified. The filler consists of its own filler from the fine and coarse aggregate fractions (gabbro, porphyry, or silicate) and added limestone filler. The design of the asphalt mastics can be calculated based on the grading curve and binder content. **Table 3** shows the F/B-ratio and volumetric F/B-ratio for each asphalt mastic. For the preparation of the mastic samples, the two components, filler and asphalt binder, are weighed according to the mix design. The two materials are heated to 180°C in an oven. Afterward, the two materials are mixed manually for approximately 5 minutes until the mixture begins to stiffen.

TEST METHOD—ASPHALT MIX FATIGUE

For this paper, the fatigue resistance is determined according to EN 12697-24, Annex D,[4] similar to ASTM D8237-18, *Standard Test Method for Determining Fatigue Failure of Asphalt-Aggregate Mixtures with the Four-Point Beam Fatigue Device*.[2] With the 4-point bending beam it is possible to determine the temperature and frequency-dependent dynamic modulus $|E^*|$ of a mix according to EN 12697-26[5] and also to determine the fatigue resistance according to EN 12697-24.[4] The nominal dimensions of the specimens are $60 \times 60 \times 500$ mm. The employed failure criterion assumes that fatigue is reached when the complex modulus drops to half its initial value (the value after the first 100 load cycles). The number of load cycles when fatigue is reached is defined as $N_{f\backslash 50}$.[4] Usually, the fatigue test stops after reaching the failure criterion to keep the test duration as short as possible.

In addition to the failure criterion $N_{f/50}$, which is predominantly used in Europe, the dissipated energy approach is also an option to evaluate the fatigue life. A suitable parameter for this is the change in dissipated energy from one loading cycle to the next. In this way, the damage to the material by a load cycle can be described. A material failure is characterized by a noticeable increase in damage per load cycle, independent of the load type.[35] By using the ratio of dissipated energy change (RDEC) approach, a correlation between a plateau value (in the period where a relatively constant energy input is converted into damage) and $N_{f/50}$ could be shown. This correlation is not dependent on the load type or temperature but only on the material composition.[36] However, because of the stop of the fatigue test after reaching 50 % of the initial stiffness, a criterion based on dissipated energy cannot be applied in this study. The plateau value (PV) could be calculated approximately correctly, but the count of load cycles at fatigue failure point characterized because of the rapid increase of RDEC cannot be determined.

For the asphalt mix fatigue tests presented in this study, at least two strain levels were selected, and three specimens were tested at each strain level. If the scattering of results was too large, additional specimens were tested to improve the quality of results. All tests were performed at +20°C and 30 Hz. The selected strain amplitude refers to the maximum horizontal strain on the bottom of the specimen. All results for a given mixture are combined with a fatigue function that links the number of load cycles to fatigue with the applied strain amplitude. The value ε_6 can be derived from the fatigue function to characterize the fatigue performance of a mix. This value describes the strain amplitude for which an asphalt mix lasts one million load cycles until reaching the state of fatigue.

TEST METHOD—ASPHALT MIX STIFFNESS

For stiffness tests at the asphalt mix level, the method, according to EN 12697-26, Annex B,[5] was applied. For this purpose, the prismatic specimen is subjected to a strain-controlled 4-point bending beam test to derive the dynamic modulus $|E^*|$ and phase lag ϕ as a function of test temperature and frequency. The test temperature is set to +20°C, and a frequency sweep from 0.1 Hz to 40.0 Hz is applied.

TEST METHOD—MASTIC FATIGUE

The fatigue tests on asphalt mastic are carried out by using the DSR. For this purpose, hyperbolic test specimens (see fig. 1) are produced directly in the DSR with a silicone mold. This shape is necessary to avoid adhesive failure at the interface between the asphalt mastic and the DSR test plate. The form of the specimen leads to a stress concentration in the center of the sample. The hyperbolic shape ensures that every sample fails at the same point. This improves the repeatability of results. All asphalt mastic specimens are tested at +10°C to avoid creep deformation of the specimen during the test, which would cause a change of the specimen shape and biased results.[27]

Since the test duration plays an essential role in the daily lab routine, a test frequency of 30 Hz was applied. The high test frequency keeps the testing time at acceptable limits and improves the comparability with 4-point bending beam fatigue tests, which are also carried out at 30 Hz. Therefore, it is necessary to use an active temperature chamber within the DSR, because higher frequency produces higher friction heat due to more dissipated energy. This has an impact on fatigue resistance because the produced heat has to be dissipated by the cooling system. If not, the temperature of the sample will increase and affects the measurement negatively. Shear stress close to the linear viscoelastic range was chosen for each test to avoid the influence of nonlinearity. It needs to be noted that these are nominal shear stresses, since the actual shear stress in the predetermined breaking point is higher because of the specimen shape. However, the DSR calculates only the shear stress at the maximum radius for a cylindrical specimen shape.

In a fatigue test, the evolution of the complex shear modulus over time can be divided into three phases (see fig. 2). The first phase, also called the transient phase, is dominated by thixotropy. In rheology, thixotropy describes a time dependence of the flow behavior. The viscosity decreases because of continuous mechanical stress and increases again when the applied load is removed. Therefore, thixotropy is a reversible effect. The transient phase lasts only very shortly and leads to the second phase. In this phase, microcracks occur because of repeated shear stress cycles, leading to a further decrease of the complex shear modulus. In the final phase, microcracks join to form macrocracks. Over time, the macrocracks connect to a fracture line, and the specimen fails. Since no more forces can be transferred, the complex shear modulus $|G^*|$ drops abruptly.[27]

For asphalt mix fatigue tests in the 4-point bending beam, the fatigue criterion is reached when the stiffness drops to 50 % of its initial value. For asphalt mastic fatigue tests in the DSR, the test is usually continued until complete failure. This is the case when the complex shear modulus drops abruptly and the phase angle reaches a maximum. For this reason, the failure criterion for the mastic fatigue tests was defined as when the maximum phase angle has been reached. Statistical analysis has shown that both the RDEC and a peak in phase angle are suitable for defining fatigue failure, as both give equivalent results in fatigue life.[25] The main advantage over the LAS test, which is often mentioned in the literature, is that the test specimen fails and the point of fatigue is not calculated by mathematical modeling. Thus, the influence of errors by modeling parameters can be avoided.

FIG. 1

Hyperbolic shape of asphalt mastic specimen mounted in DSR.

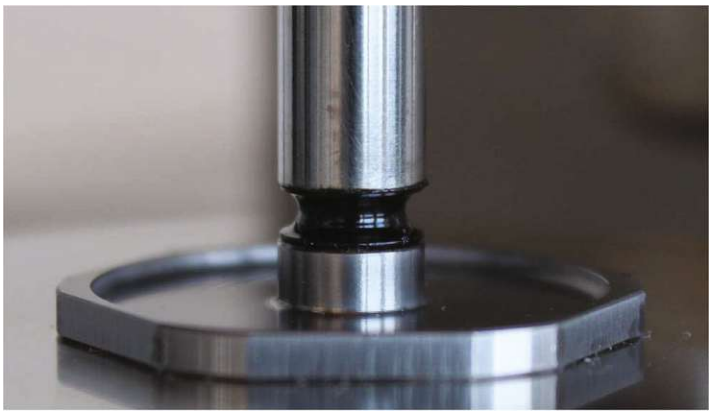

FIG. 2 Three phases of an asphalt mastic fatigue test.

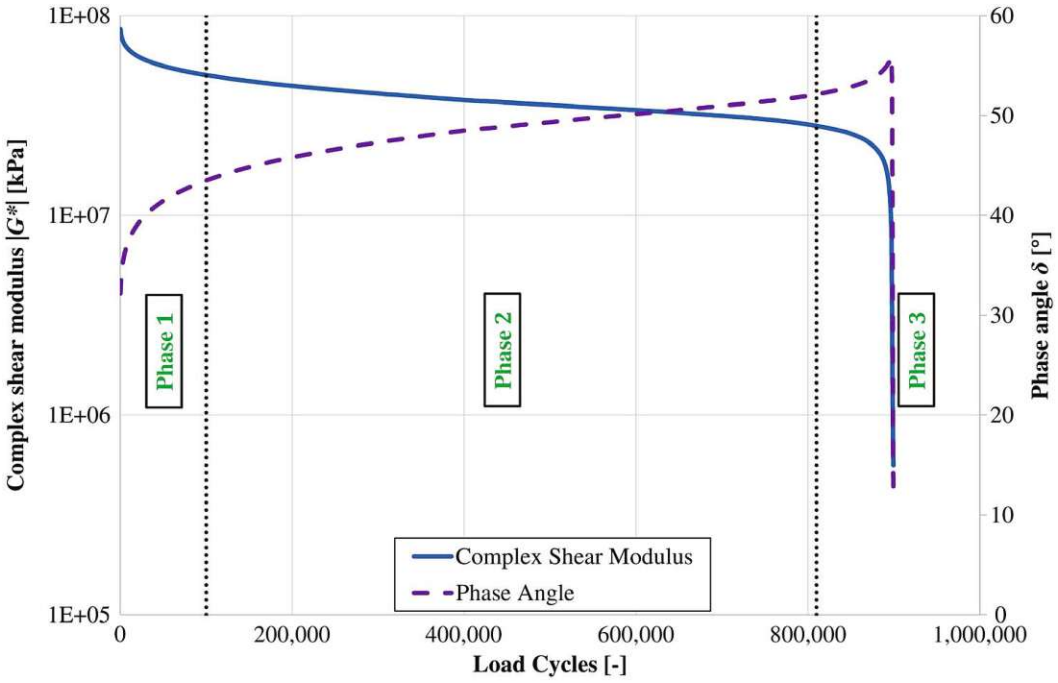

For each asphalt mastic, nine individual tests are necessary: three fatigue tests are carried out at three different shear stress levels. With the obtained data points, a fatigue curve can be derived, linking the number of load cycles to fatigue with the shear stress level. The shear stress level required to achieve one million load cycles, designated by τ_6, can be calculated. The gradient of the fatigue curve can be obtained, which is correlated to the stiffness of the respective asphalt mastic.

Results and Discussion

For this research, 14 different asphalt mixes and the respective asphalt mastic mixes were tested for their fatigue performance. The characteristic fatigue values ε_6 and τ_6 were considered to establish a correlation between the fatigue tests at the two observation levels. Also, the mean values of the dynamic modulus $|E^*|_{30\text{Hz}}$ and phase angle $\phi_{30\text{Hz}}$ at 30 Hz (stiffness test of asphalt mixes) as well as the initial values of the complex shear modulus $|G^*|_{\text{initial}}$ and phase angle δ_{initial} (for the asphalt mastic mixes) were taken into account.

We used simple linear models for the first regression analysis and subsequently moved to multiple linear models. The coefficient of determination R^2 obtained from these models is used to evaluate the correlation between asphalt mix and asphalt mastic level.

In our regression approach, we started by correlating the dynamic modulus $|E^*|_{30\text{Hz}}$ of the asphalt mix at 20°C and 30 Hz with the initial complex shear modulus $|G^*|_{\text{initial}}$ of the asphalt mastic. For this purpose, the mean value of $|E^*|_{30\text{Hz}}$ from all single tests of one asphalt mix is used. On the mastic level, the mean value of the complex shear modulus $|G^*|$ after 300 load cycles from 9 single tests of 1 asphalt mastic mix is used, designated as $|G^*|_{\text{initial}}$.

As shown in figure 3, the $|E^*|_{30\text{Hz}}$ of asphalt mix level (ordinate) can be predicted using the $|G^*|_{\text{initial}}$ of asphalt mastic level (abscissa) with a relatively high coefficient of determination ($R^2 = 0.77$). Figure 3 also contains the 95 % confidence interval. The increase of the stiffness modules has no link to the upper PG nor the lower PG of the used asphalt binders. But as shown in figure 3, asphalt mixes and asphalt mastic mixes with soft asphalt binders have a lower dynamic stiffness modulus $|E^*|_{30\text{Hz}}$ or complex shear modulus

FIG. 3 Correlation between $|E^*|_{30Hz}$ and $|G^*|_{initial}$.

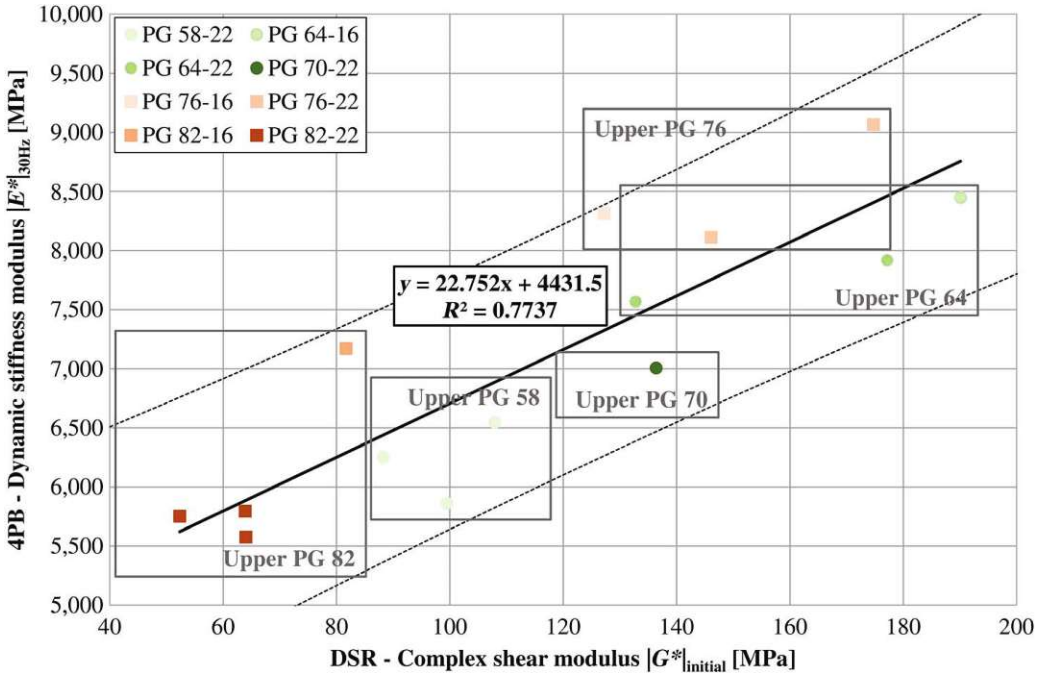

$|G^*|_{initial}$ and vice versa. According to van Heerden et al.,[37] a correlation between complex shear modulus and penetration index on the asphalt binder level is possible. Hard asphalt binders (low penetration index) have higher complex shear moduli, while soft asphalt binders (high penetration index) exhibit lower complex shear moduli.

FIG. 4 Correlation between penetration and fatigue performance on the asphalt mix and mastic level.

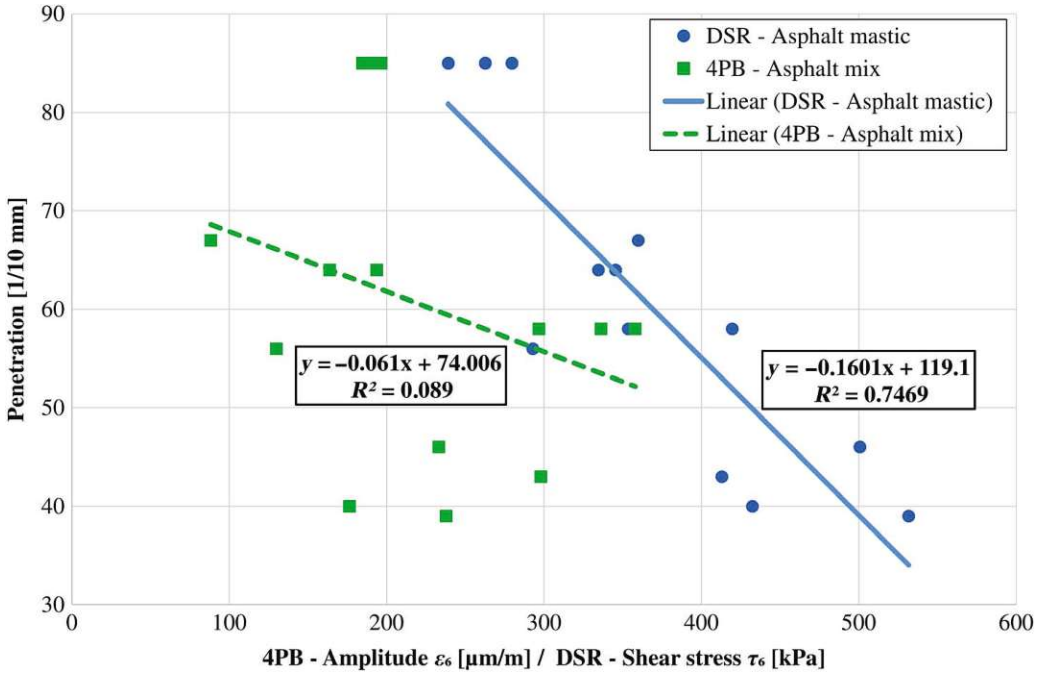

Moreover, a correlation between the penetration depth of each asphalt binder and fatigue performance τ_6 at the asphalt mastic level can be observed. As shown in figure 4, the τ_6 value of the asphalt mastic (ordinate) and penetration depth of the asphalt binder (abscissa) are positively correlated ($R^2 = 0.75$ for the linear model). This implies that a hard asphalt binder in asphalt mastic can be associated with a high fatigue performance of the asphalt mastic. This observation does not confirm that aging has a negative impact on fatigue performance. Aged bitumen leads to a lower penetration index, which would mean higher fatigue performance of the asphalt mastic.

The observations at the aforementioned asphalt mastic level cannot be confirmed at the asphalt mix level because of the higher spreading of results ($R^2 = 0.089$). One possible reason for this can be found in the different loading modes for the tests at asphalt mastic level (stress-controlled) and asphalt mix level (strain-controlled). A high initial complex shear modulus in a stress-controlled test method means a small applied initial strain in the specimen to reach the defined stress. However, small strains suggest that the specimen's damage per load cycle is small, so the number of load cycles until fatigue crack also increases. In a strain-controlled test method, high initial stress would be necessary to reach the defined strain due to the high stiffness, whereby the fatigue criterion will be reached earlier. This fact affects the correlation between both fatigue levels. Besides, the larger variation of the results could be the reason for the higher inaccuracy of fatigue performance tests at the asphalt mix level according to the preparation of asphalt mix specimens. Influencing factors from specimen preparation are slight differences in the grading curve after the weighed portion of aggregates. Also, the compaction method affects the scatter of material test results.[38]

However, there is a correlation between the binder's penetration depth and the phase angle at the asphalt mixture level. Figure 5 shows a good positive relationship with a coefficient of determination for the linear model of 0.79. Thus, softer asphalt binders correspond to higher phase angles.

In a second step, the mean values of the phase angle $\phi_{30\text{Hz}}$ (ordinate) from all single tests of one asphalt mix were predicted based on the respective parameter δ_{initial} (abscissa) at the mastic level. As shown in figure 6, the initial phase angle at the asphalt mix level and asphalt mastic level show a low positive correlation. The coefficient of determination for the model is 0.26.

FIG. 5 Correlation between penetration and phase angle $\phi_{30\text{Hz}}$.

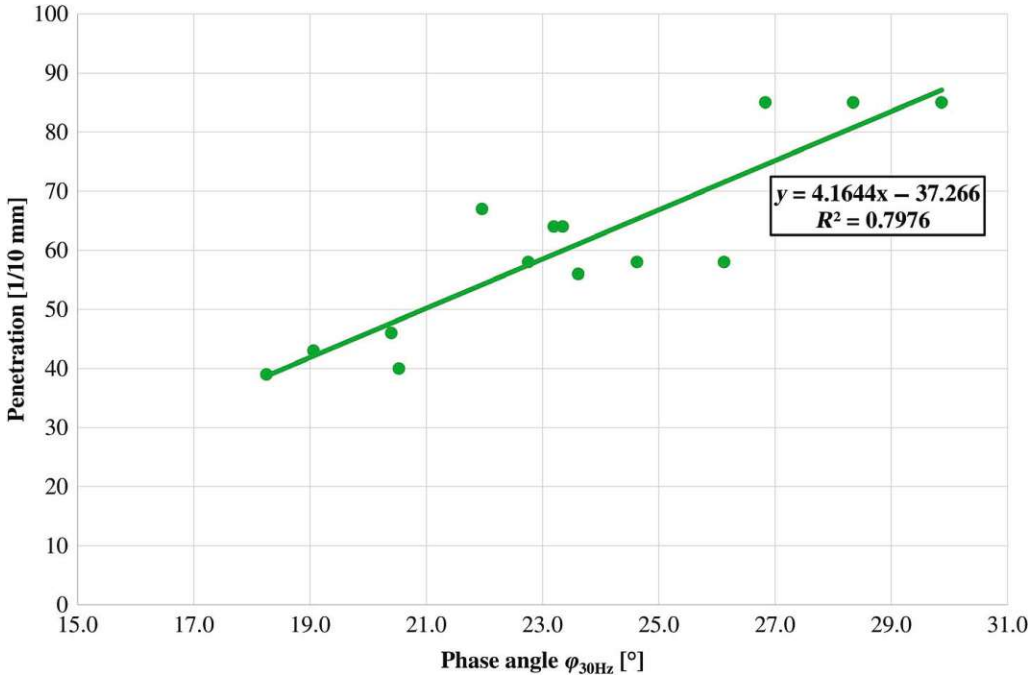

FIG. 6 Correlation between phase lag on the asphalt mix and mastic level.

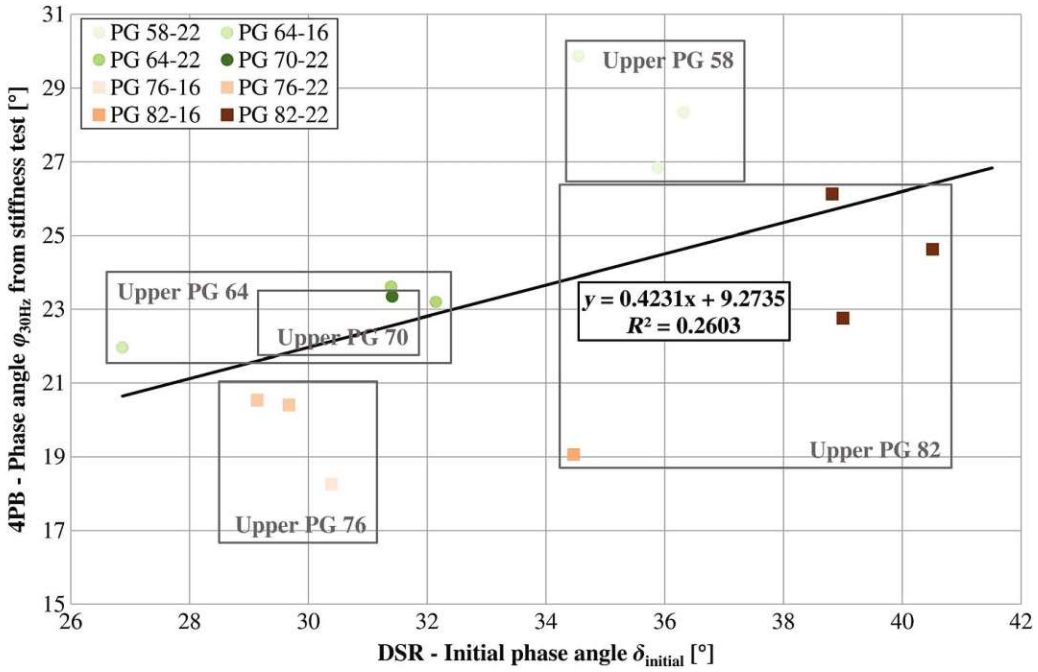

As in figures 3 and 6, we can see that the data points of asphalt binder with the same upper PG are close to each other. But unlike the link between penetration index and $|E^*|_{30Hz}$ or $|G^*|_{initial}$ in figure 3, no connection was observed to a tested asphalt binder parameter in figure 6.

However, there is a good relationship between the phase lag ϕ_{30Hz} and dynamic stiffness modulus $|E^*|_{30Hz}$ of asphalt mixes as well as between the phase lag $\delta_{initial}$ and complex shear modulus $|G^*|_{initial}$ of asphalt mastics.

FIG. 7 Correlation between ϕ_{30Hz} with $|E^*|_{30Hz}$ and $\delta_{initial}$ with $|G^*|_{initial}$.

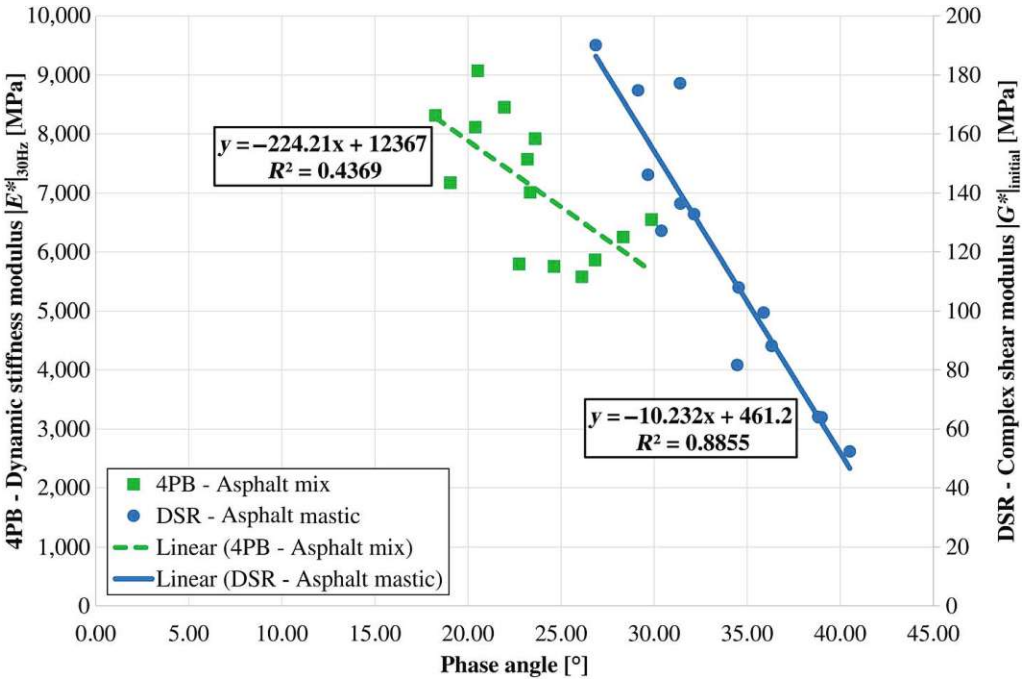

With a larger phase lag, the stiffness modulus decreases, as shown in figure 7. The slightly higher spread of the results at the asphalt mixture level and thus the lower coefficient of determination can be attributed again to the higher inaccuracy of fatigue performance tests on asphalt mix level according to the preparation of asphalt mix specimen.

It can be stated that a prediction of stiffness modulus $|E^*|_{30Hz}$ at the asphalt mix level according to the results at the asphalt mastic level $|G^*|_{initial}$ seems possible. However, the phase angle of asphalt mixtures cannot be derived with a simple linear regression model.

In the third step, the fatigue performances of both levels of observation are correlated with a simple linear regression model. At the asphalt mix and asphalt mastic level, ε_6 and τ_6 were used, respectively. As shown in figure 8, both values exhibit a weak (positive) correlation. The coefficient of determination is 0.51. As already observed in figures 3 and 6, we can see that the data points of asphalt binder with the same upper PG are close to each other in figure 8. The differences in results with the same upper PG may be attributed to the different fillers. During the tests carried out with the same asphalt binder and various fillers, no direct evidence can be found, supporting the current opinions in the literature that a higher F/B-ratio increases fatigue performance. Chemical or physical properties of the filler may have an influence on fatigue resistance besides F/B-ratio. However, this topic will not further be discussed in this paper, as there are too few data sets available at this point. In conclusion, a simple correlation with just the two parameters is not sufficient to link the two levels of observation.

The last step was to derive a multiple linear regression model by introducing an additional parameter $|G^*|_{initial}$ to improve the relationship between the asphalt mix and asphalt mastic. As presented in figure 9, the analysis proves that a multiple linear regression model with $|G^*|_{initial}$ and τ_6 as independent variables achieves a higher accuracy in predicting the corresponding fatigue performance of asphalt mixtures represented by ε_6. The coefficient of determination is 0.92. The multiple regression function stated in figure 9 reveals that an increase in the asphalt mastic fatigue (τ_6) leads to an increase in the asphalt mix fatigue (ε_6). When the mastic stiffness ($|G^*|_{Start}$) decreases, the asphalt mix fatigue increases. The negative influence of the complex shear modulus in the regression model counteracts stiffness effects at stress-controlled tests.

FIG. 8 Simple, linear regression between ε_6 and τ_6.

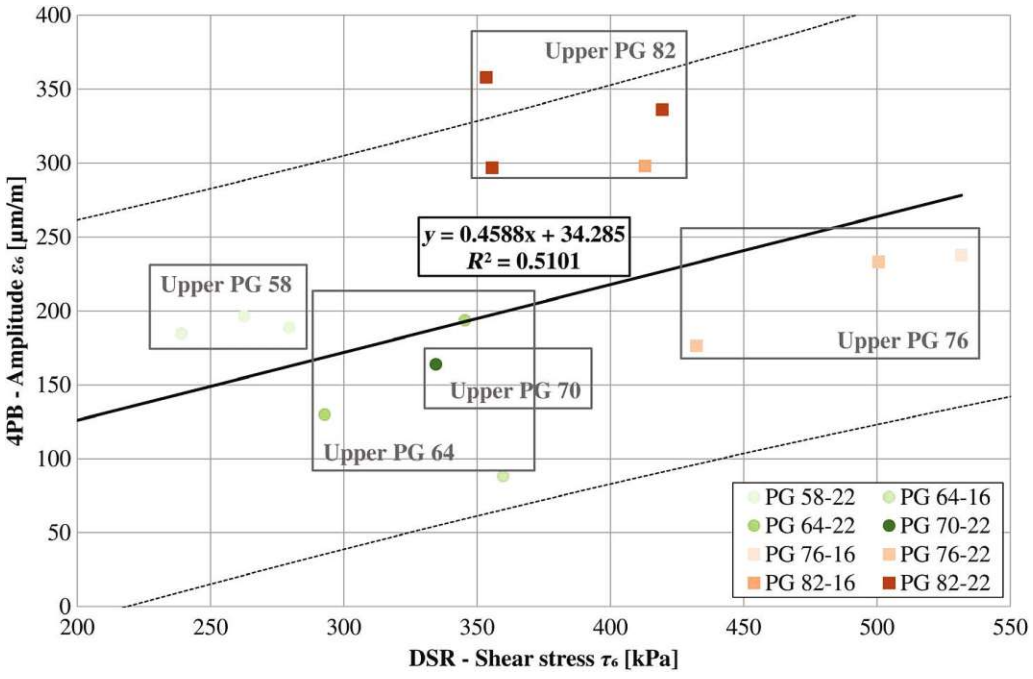

FIG. 9 Prediction model of asphalt mix fatigue from asphalt mastic fatigue and stiffness.

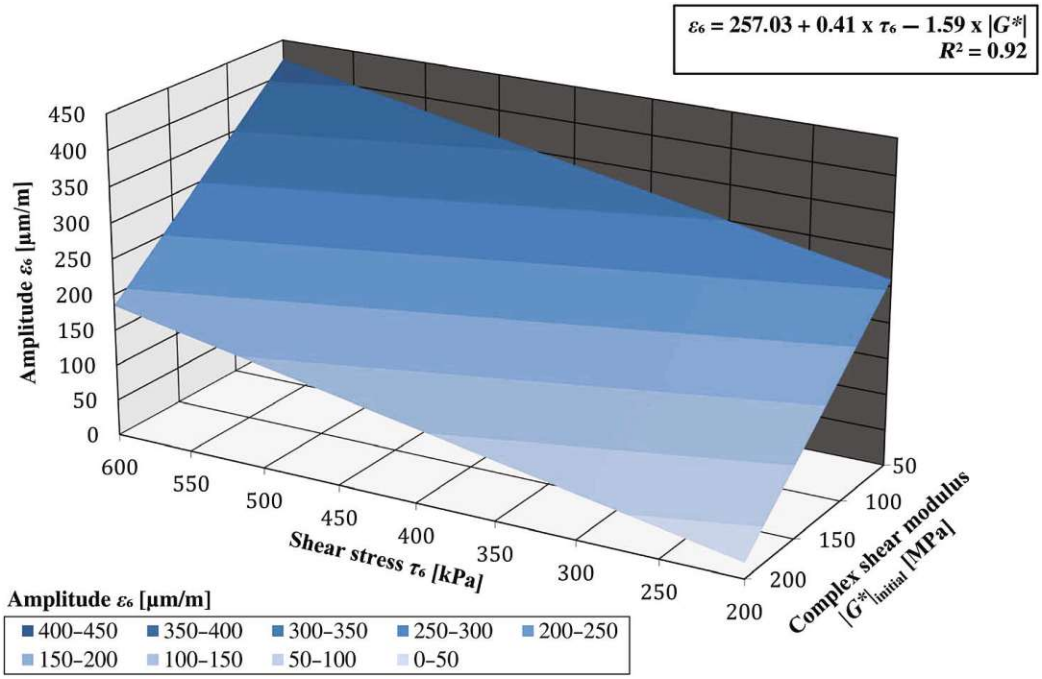

FIG. 10 Predicted versus observed amplitude ε_6 regression plot derived from the multiple linear regression model presented in **figure 9**.

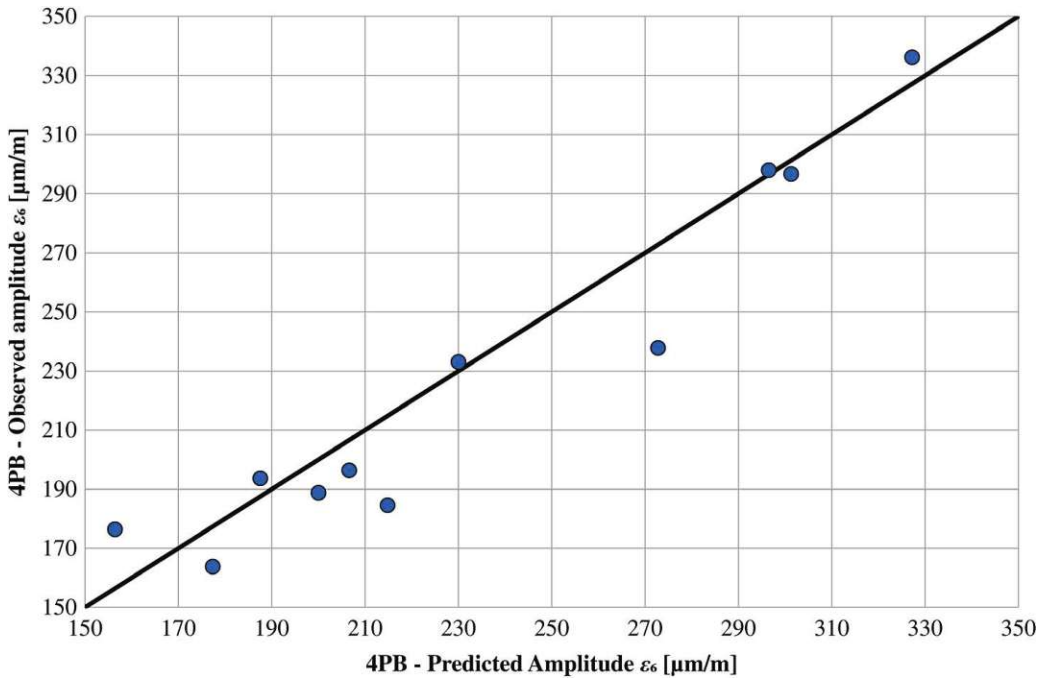

Figure 10 shows the comparison of the predicted fatigue performance ε_6 and observed fatigue performance ε_6 of asphalt mixtures, illustrating the high correlation between asphalt mastic fatigue and asphalt mix fatigue. It can be stated that a prediction of fatigue performance ε_6 of asphalt mixtures with the results of asphalt mastic fatigue test with DSR is possible if stiffness and fatigue of the mastic are taken into account.

Conclusion

To establish a prediction model of fatigue and stiffness properties of asphalt mixture from fatigue tests on asphalt mastic, we tested 14 different asphalt mixes and the respective asphalt mastic mixes. At the asphalt mix level, prismatic specimens were tested for their stiffness and fatigue performance using the 4-point bending beam test method. At the asphalt mastic level, hyperbolic samples were tested in the DSR for their fatigue performance by the use of oscillatory time sweep tests. Based on correlation analysis of the results of both tests, the following conclusions can be drawn:

- The dynamic modulus $|E^*|_{30\text{Hz}}$ of an asphalt mix and complex shear modulus $|G^*|_{\text{initial}}$ of the respective asphalt mastic show a good positive correlation. The coefficient of determination of the corresponding linear regression model is 0.77. The stiffness modulus at both levels cannot be linked to the PG of the asphalt binder.
- The mean values of the phase angle $\phi_{30\text{Hz}}$ from all single tests of one asphalt mix and the respective parameter δ_{initial} at the mastic level show a low positive correlation ($R^2 = 0.26$).
- A good relationship between the phase lag δ_{initial} and complex shear modulus $|G^*|_{\text{initial}}$ of asphalt mastics was observed ($R^2 = 0.89$). Between the phase angle $\phi_{30\text{Hz}}$ and dynamic stiffness modulus $|E^*|_{30\text{Hz}}$ of asphalt mixes, the relationship is moderate with $R^2 = 0.44$.
- Both fatigue performance values ε_6 and τ_6 can be included in a linear regression model, exhibiting a low coefficient of determination ($R^2 = 0.51$).
- Higher fatigue performance of mixtures with PmB can be measured on both levels: asphalt mixture and asphalt mastic mixture.
- A good negative correlation between the depth of penetration of each asphalt binder and the fatigue performance τ_6 on asphalt mastic level can be observed ($R^2 = 0.75$). A lower depth of penetration on asphalt binder level results in higher fatigue performance of asphalt mastic.
- No direct proof could be found suggesting that a higher F/B-ratio increases fatigue performance. Asphalt mastic with different filler and same asphalt binder but different F/B-ratio reveal similar results for stiffness, phase lag, and fatigue performance. Chemical or physical properties of the filler may influence the tested properties besides F/B-ratio.
- A multiple linear regression model with $|G^*|_{\text{initial}}$ and τ_6 as independent variables allow for reliable prediction of the corresponding fatigue performance of asphalt mixtures represented by ε_6. The coefficient of determination is 0.92. It can be stated that a prediction of fatigue performance ε_6 of asphalt mixtures with the results of asphalt mastic fatigue tests performed with DSR is possible.

Because of the missing data from the 4-point bending beam test, a correlation between the fatigue behavior based on the dissipated energy approach is not possible at this point. However, future research should determine if this promising approach leads to a better prediction quality. By expanding the data set presented in this paper in the future, we aim at improving the correlation quality and, thus, the predictability of asphalt mixture fatigue performance and stiffness modulus from the asphalt mastic level.

ACKNOWLEDGMENTS

The study reported in this paper is part of the research project on "Simplified Assessment of Asphalt Mix Performance (Vereinfachung der prüftechnischen Ansprache des Gebrauchsverhaltens von Asphalt)" funded by the Austrian Federal Ministry of Climate Action, Environment, Energy, Mobility, Innovation and Technology and the Federal Ministry for Digital and Economic Affairs.

References

1. *Bituminous Mixtures - Test Methods - Part 25: Cyclic Compression Test*, EN 12697-25:2016 (Brussels, Belgium: European Committee for Standardization, November 1, 2016).
2. *Standard Test Method for Determining Fatigue Failure of Asphalt-Aggregate Mixtures with the Four-Point Beam Fatigue Device*, ASTM D8237-18(2018) (West Conshohocken, PA: ASTM International, approved December 1, 2018). https://doi.org/10.1520/D8237-18

3. *Standard Method of Test for Determining the Fatigue Life of Compacted Asphalt Mixtures Subjected to Repeated Flexural Bending*, AASHTO T 321(2017) (Washington, DC: American Association of State Highway and Transportation Officials, January 2017).
4. *Bituminous Mixtures - Test Methods - Part 24: Resistance to Fatigue*, EN 12697-24:2018 (Brussels, Belgium: European Committee for Standardization, November 2018).
5. *Bituminous Mixtures - Test Methods - Part 26: Stiffness*, EN 12697-26:2018 (Brussels, Belgium: European Committee for Standardization, December 15, 2018).
6. *Standard Test Method for Thermal Stress Restrained Specimen Tensile Strength*, AASHTO TP 10 (Washington, DC: American Association of State Highway and Transportation Officials, January 1, 1993).
7. *Bituminous Mixtures - Test Methods for Hot Mix Asphalt - Part 46: Low Temperature Cracking and Properties by Uniaxial Tension Tests*, EN 12697-46:2012 (Brussels, Belgium: European Committee for Standardization, May 1, 2020).
8. C. Hintz and H. Bahia, "Understanding Mechanisms Leading to Asphalt Binder Fatigue in the Dynamic Shear Rheometer," *Road Materials and Pavement Design* 14, no. sup2 (2013): 231–251, http://doi.org/10.1080/14680629.2013.818818
9. M.-C. Liao, J.-S. Chen, and K.-W. Tsou, "Fatigue Characteristics of Bitumen-Filler Mastics and Asphalt Mixtures," *Journal of Materials in Civil Engineering* 24, no. 7 (July 2012): 916–923, https://doi.org/10.1061/(ASCE)MT.1943-5533.0000450
10. D. A. Anderson, Y. M. Le Hir, M. O. Marasteanu, J.-P. Planche, D. Martin and G. Gauthier, "Evaluation of Fatigue Criteria for Asphalt Binders," *Transportation Research Record* 1766, no. 1 (January 2001): 48–56, https://doi.org/10.3141/1766-07
11. E. Santagata, O. Baglieri, L. Tsantilis, and G. Chiappinelli, "Fatigue Properties of Bituminous Binders Reinforced with Carbon Nanotubes," *International Journal of Pavement Engineering* 16, no. 1 (2015): 80–90, https://doi.org/10.1080/10298436.2014.923099
12. H. Soenen, C. de La Roche, and P. Redelius, "Fatigue Behaviour of Bituminous Materials: From Binders to Mixes," *Road Materials and Pavement Design* 4, no. 1 (2003): 7–27, https://doi.org/10.1080/14680629.2003.9689938
13. B. J. Smith and S. A. M. Hesp, "Crack Pinning in Asphalt Mastic and Concrete: Regular Fatigue Studies," *Transportation Research Record* 1728, no. 1 (January 2000): 75–81, https://doi.org/10.3141/1728-11
14. M. Ameri, M. Seif, M. Abbasi, M. Molayem, and A. KhavandiKhiavi, "Fatigue Performance Evaluation of Modified Asphalt Binder Using of Dissipated Energy Approach," *Construction and Building Materials* 136 (April 2017): 184–191, https://doi.org/10.1016/j.conbuildmat.2017.01.010
15. L. Shan, Y. Tan, S. Underwood, and Y. R. Kim, "Application of Thixotropy to Analyze Fatigue and Healing Characteristics of Asphalt Binder," *Transportation Research Record* 2179, no. 1 (January 2010): 85–92, https://doi.org/10.3141/2179-10
16. Y.-R. Kim, D. N. Little, and I. Song, "Effect of Mineral Fillers on Fatigue Resistance and Fundamental Material Characteristics: Mechanistic Evaluation," *Transportation Research Record* 1832, no. 1 (January 2003): 1–8, https://doi.org/10.3141/1832-01
17. L. Shan, H. Zhang, Y. Tan, and Y. Xu, "Effect of Load Control Mode on the Fatigue Performance of Asphalt Binder," *Materials and Structures* 49 (April 2016): 1391–1402, https://doi.org/10.1617/s11527-015-0584-8
18. M.-C. Liao, G. Airey, and J.-S. Chen, "Mechanical Properties of Filler-Asphalt Mastics," *International Journal of Pavement Research and Technology* 6, no. 5 (September 2013): 576–581, https://doi.org/10.6135/ijprt.org.tw/2013.6(5).576
19. C. V. Phan, H. Di Benedetto, C. Sauzéat, D. Lesueur, and S. Pouget, "Influence of Hydrated Lime on Linear Viscoelastic Properties of Bituminous Mastics," *Mechanics of Time-Dependent Materials* 24 (February 2020): 25–40, https://doi.org/10.1007/s11043-018-09404-x
20. J. Van Rompu, H. Di Benedetto, M. Buannic, T. Gallet, and C. Ruot, "New Fatigue Test on Bituminous Binders: Experimental Results and Modeling," *Construction and Building Materials* 37 (December 2012): 197–208, https://doi.org/10.1016/j.conbuildmat.2012.02.099
21. F. Zhou, W. Mogawer, H. Li, A. Andriescu, and A. Copeland, "Evaluation of Fatigue Tests for Characterizing Asphalt Binders," *Journal of Materials in Civil Engineering* 25, no. 5 (May 2013): 610–617, https://doi.org/10.1061/(ASCE)MT.1943-5533.0000625
22. C. M. Johnson and H. U. Bahia, "Evaluation of an Accelerated Procedure for Fatigue Characterization of Asphalt Binders," *Road Materials and Pavement Design* (2010).
23. C. Hintz, R. Velasquez, C. Johnson, and H. Bahia, "Modification and Validation of Linear Amplitude Sweep Test for Binder Fatigue Specification," *Transportation Research Record* 2207, no. 1 (January 2011): 99–106, https://doi.org/10.3141/2207-13
24. C. Hintz and H. Bahia, "Simplification of Linear Amplitude Sweep Test and Specification Parameter," *Transportation Research Record* 2370, no. 1 (January 2013): 10–16, https://doi.org/10.3141/2370-02
25. C. Wang, H. Zhang, C. Castorena, J. Zhang, and Y. R. Kim, "Identifying Fatigue Failure in Asphalt Binder Time Sweep Tests," *Construction and Building Materials* 121 (September 2016): 535–546, https://doi.org/10.1016/j.conbuildmat.2016.06.020
26. M. Sabouri, D. Mirzaiyan, and A. Moniri, "Effectiveness of Linear Amplitude Sweep (LAS) Asphalt Binder Test in Predicting Asphalt Mixtures Fatigue Performance," *Construction and Building Materials* 171 (May 2018): 281–290, https://doi.org/10.1016/j.conbuildmat.2018.03.146
27. M. Hospodka, B. Hofko, and R. Blab, "Introducing a New Specimen Shape to Assess the Fatigue Performance of Asphalt Mastic by Dynamic Shear Rheometer Testing," *Materials and Structures* 51 (March 2018): 46, https://doi.org/10.1617/s11527-018-1171-6

28. *Tests for Geometrical Properties of Aggregates - Part 1: Determination of Particle Size Distribution - Sieving Method*, EN 933-1:2012 (Brussels, Belgium: European Committee for Standardization, March 1, 2012).
29. *Geotechnical Investigation and Testing - Laboratory Testing of Soil - Part 4: Determination of Particle Size Distribution*, EN ISO 17892-4:2016 (Brussels, Belgium: European Committee for Standardization, November 2016).
30. *Bitumen and Bituminous Binders - Determination of the Softening Point - Ring and Ball Method*, EN 1427:2015 (Brussels, Belgium: European Committee for Standardization, September 15, 2015).
31. *Bitumen and Bituminous Binders - Determination of Needle Penetration*, EN 1426:2015 (Brussels, Belgium: European Committee for Standardization, 2015).
32. *Standard Specification for Performance-Graded Asphalt Binder*, AASHTO M 320-17 (Washington, DC: American Association of State Highway and Transportation Officials, 2017).
33. *Technische Lieferbedingungen für Asphaltmischgut für den Bau von Verkehrsflächenbefestigungen*, TL Asphalt-StB 07/13 (Köln, Deutschland: Forschungsgesellschaft für Straßen- und Verkehrswesen, 2013).
34. *Bituminous Mixtures - Test Methods - Part 6: Determination of Bulk Density of Bituminous Specimens*, EN 12697-6:2020 (Brussels, Belgium: European Committee for Standardization, February 2020).
35. K. A. Ghuzlan and S. H. Carpenter, "Energy-Derived, Damage-Based Failure Criterion for Fatigue Testing," *Transportation Research Record* 1723, no. 1 (January 2000): 141–149, https://doi.org/10.3141/1723-18
36. M. Boudabbous, A. Millien, C. Petit, and J. Neji, "Shear Test to Evaluate the Fatigue of Asphalt Materials," *Road Materials and Pavement Design* 14, no. sup1 (2013): 86–104, https://doi.org/10.1080/14680629.2013.774748
37. J. van Heerden, K. J. Jenkins, G. Harmse, and T. Joubert, "The Use of the Dynamic Shear Rheometer (DSR) to Predict the Penetration of Bitumen" (paper presentation, 10th Conference on Asphalt Pavements for South Africa, KwaZulu Natal, South Africa, September 11–14, 2011).
38. A. A. Tayebali, J. A. Deacon, and C. L. Monismith, "Development and Evaluation of Dynamic Flexural Beam Fatigue Test System," *Transportation Research Record* 1545, no. 1 (January 1996): 89–97, https://doi.org/10.1177/0361198196154500112

Appendix 3 (Publication 3)

ROAD MATERIALS AND PAVEMENT DESIGN
https://doi.org/10.1080/14680629.2023.2172066

Taylor & Francis
Taylor & Francis Group

RESEARCH ARTICLE

OPEN ACCESS Check for updates

Assessing the impact of filler properties, moisture, and aging regarding fatigue resistance of asphalt mastic

Michael Steineder and Bernhard Hofko

Institute of Transportation, Vienna University of Technology, Vienna, Austria

ABSTRACT

Asphalt mastic (bitumen + filler) plays an essential role in the fatigue performance of asphalt pavements. The time sweep test is one of the bestknown test methods for assessing fatigue performance, but fracture initiation in the specimen and the high stiffness of the mastic may bias results. These problems can be avoided with a hyperbolic specimen, but this test geometry is still largely unexplored. Therefore, 20 different asphalt mastic mixes were tested with the dynamic shear rheometer and hyperbolic specimen shape to identify the impact of various fillers and their properties, moisture, and aging on fatigue performance. These results were compared with the findings in the literature to investigate the applicability of this novel test method. Thus, a correlation could be derived between the fractional void and the fatigue performance of asphalt mastic. As also described in the literature, moist filler or water stored mastic reduce fatigue performance.

ARTICLE HISTORY
Received 23 December 2021
Accepted 3 January 2023

KEYWORDS
DSR; asphalt mastic; fatigue performance; material properties

1. Introduction

Rutting, thermal cracking, and fatigue are the main causes of damage on asphalt pavements while cracking is accelerated by asphalt aging. Surface layers' premature failures have increasingly occurred on parts of the national road network, which cannot systematically be attributed to climatic or traffic-related load. Currently, it can be assumed that these damages are caused by a lack of durability of the asphalt mastic (bitumen + filler). In general, it is supposed that cohesive and adhesive microcracks in asphalt mixtures initiate fatigue cracking, and the mastic's essential properties affect this cracking phenomenon (Kim et al., 2003). Mastic is considered the essential bonding component in asphalt and plays a significant role in the overall performance.

In recent years, the assessment of fatigue performance has shifted from the bitumen to the mastic level (Airey et al., 2004). The basis was that the filler properties significantly influence the fatigue behaviour of asphalt mixtures. It has already been shown that adding filler to bitumen increases the stiffness and the resistance to deformation under loading (Hesami et al., 2013). The filler has a significant effect on the fatigue behaviour of asphalt mastic. Also, filler properties such as density, specific surface area, or factional voids RV significantly influence the material behaviour (Mazzoni et al., 2019; Roberto et al., 2018; Rochlani et al., 2019). The choice of filler affects the aging and moisture sensitivity of asphalt mastic (Choudhary et al., 2020; Lesueur et al., 2016). Several test methods have been developed or adapted to characterise the material behaviour of asphalt mastic to study the mentioned effects in recent years. One of the most popular test methods with a dynamic shear rheometer (DSR) is the time sweep (TS) test.

CONTACT Michael Steineder michael.steineder@tuwien.ac.at

The TS test is designed to damage the material structure by repeated loads until a fatigue criterion occurs. Thus, this test setup follows standard experimental methods for evaluating fatigue damage on asphalt mix level. Commonly, cylindrical specimen is used for TS test. However, Anderson et al. (2001), Kim et al. (2021) and Hospodka et al. (2018) showed that TS test with cylindrical specimen is unsuitable. The bitumen or mastic requires the necessary stiffness to create microcracks in the structure, associated with high torque. Not all DSRs available on the market can apply such a large torque or cause a significant measurement error due to motor cooling during long-term tests (Anderson et al., 2001; Kim et al., 2021). For samples with high stiffness, fracture occurs not only in the specimen but also in the transition region to the measurement geometry, which results in an abort of measurement (Hospodka et al., 2018).

The remedy is a hyperbolic specimen shape, introduced by Hospodka et al. (2018). Due to the stress concentration in the necking of the sample, an actual cohesive fracture occurs in the mastic specimen. Furthermore, the load on the DSR is reduced because a smaller torque is required due to the necking. The influences from motor cooling can be limited. It has already been shown that the assessment of the fatigue performance of asphalt mastic determined with DSR on cylindrical and hyperbolic specimens is identical (Steineder et al., 2022).

However, it is of particular interest to see how filler properties, moisture, and aging influence the fatigue performance of asphalt mastic, tested with TS test and hyperbolic specimens and whether the results are comparable to other studies. As part of a large study, intending to derive a reliable prediction model of the fatigue performance of asphalt mixtures by tests on asphalt mastic level, this paper studies the influences of filler properties (grading curve, true density, specific surface area, fractional void, grain shape), aging, and moisture on the fatigue performance of asphalt mastics. Due to the high number of tests necessary to describe one material thoroughly, only one test method could be investigated. The investigation of the different mastic mixes and the bitumen used with other loading modes or test methods could not be examined within the scope of this study. Instead, results are compared with findings in the literature to investigate the applicability of this novel test method. The objective is to examine whether a hyperbolic specimen shape is suitable to correctly describe the influences of filler, aging, and moisture. From this, it will be deduced whether it makes sense to use hyperbolic specimens or to remain with cylindrical specimen shapes to assess the fatigue performance of asphalt mastic.

2. Materials

As part of the extensive study, fatigue tests at the asphalt mix level are planned in the future to compare results on asphalt mix and asphalt mastic levels. Therefore, the required quantities of bitumen and filler for the asphalt mastic are weighed according to a respective asphalt mix design. This mix design will be used to prepare specimens for fatigue tests on the asphalt mix level in the next step of this research. Asphalt concrete (AC) with a binder content of 5.2% and a maximum grain size of 11 mm was selected as an asphalt mix design to study the fatigue performance of asphalt mastic.

Based on the chosen asphalt mix and grading curve of the aggregates and fillers, the mastic mix formulation was derived, and the related materials were selected. Due to national standards and regulations, the weight of asphalt is determined based on its mass. Therefore, the asphalt mastic is mixed in relation to the mass to examine an exact image of the mastic from the reference asphalt mix. All fillers used in this study have a maximum grain size of 0.125 mm. The asphalt mastic comprises bitumen, filler from the coarse aggregates (filler that exists in the coarse aggregates as an undersized particle in the grain groups, designated as own filler in this study), and added filler from various sources. According to EN 13108-1 (2016), the respective proportions were calculated based on the grading curve of the asphalt mixture. The mastic consists of 33.13 M.% (Percent by mass) bitumen and 66.87 M.% filler (own filler + added filler). A wide range of materials was used in this research study to investigate the various influences of added filler and bitumen on fatigue performance. Two different bitumen and six different added fillers were used. Thus, 12 different types of mastic were produced and studied.

A coarse reference aggregate (Granite porphyry) was sieved for the own filler. These sieved coarse aggregates will be used in the future to produce asphalt mix specimens for further studies by adding the different asphalt mastics. The percentage of the own filler with a grain size fraction 0/0.125 mm to the total mass of mastic is 3.79%. Sieving sands extracted the added fillers with the grain size fraction 0/0.125 mm from different mines or industries. The percentage of the added filler to the total mass of mastic is 63.08%. These proportions correspond to a filler bitumen ratio by mass of 2.02 for all mastic mixes. The resulting filler volume ratio by using different fillers in the mastic mix is given in Table 1. The high filler bitumen ratio is due to the selected grain size of 0/0.125 mm for the filler and the derivation of the mix design from the asphalt mixture. As a result, the filler volume ratio is higher than for mastic mixes, with a maximum grain size of 0.063 mm. Table 1 summarises the mixed fillers used in this study and the corresponding abbreviations. Since hydrated lime is not used by itself as an added filler, a mixed filler of lime and hydrated lime is used in this study. For this purpose, both fillers mixed in a ratio of 30:70 in the appropriate steps. 30% hydrated lime corresponds to the common use in road construction (European Lime Association, 2010). The mixed filler will be referred to as hydrated lime in the following sections.

The bitumen grades used in this study can be found in Table 2. The bitumens used in this study are an unmodified bitumen 70/100 and a polymer-modified bitumen PmB 45/80-65.

The needle penetration (Pen) and the softening point with ring and ball (R&B) were determined for the two bitumen grades. The test method for determining needle penetration is regulated in the standard EN 1426 (2015). The determination of the softening point with ring and ball is performed according to the standard EN 1427 (2015). The results of the bitumen tests are also summarised in Table 2.

For the production of the asphalt mastic, the two dry filler components (own and added filler) are weighed according to the quantity of mastic produced. The dry filler is homogenised by stirring for about 5 min. The homogenised mixture is then heated at +180°C for 1 h. The heated filler mixture is then added at +180°C to the pre-heated bitumen and mixed until a homogeneous mastic is produced. The mastic mixture is stirred at room temperature until it solidifies and stored in the refrigerator before use to prevent the fillers from sinking.

3. Test methods

The following section summarises the tests carried out at filler and mastic levels. As specified, the base material for filler for all tests was the mixed filler of own and added filler. Figure 1 shows the experimental plan.

Table 1. Own filler and added fillers used in this study.

Own filler (3.79 M.%)	Added filler (63.08 M.%)	Lab code	Filler volume ratio
Granite porphyry	Granite porphyry	F01	41.75%
Granite porphyry	Granite	F02	42.52%
Granite porphyry	Basalt	F03	40.68%
Granite porphyry	Lime	F04	43.12%
Granite porphyry	Hydrated lime	F05	44.52%
Granite porphyry	Quartz	F06	43.74%

Table 2. Bitumen grades and test results.

Bitumen grade	Lab Code	Pen (1/10 mm)	R&B (°C)
70/100	B01	85	45.4
PmB 45/80-65	B02	51	85.3

3.1. Mastic fatigue test

The fatigue performance tests on the mastic are carried out with DSR and time sweep (TS) tests. The hyperbolic mastic specimens are prepared directly in the DSR using a silicone mold and are conditioned at +10°C. At this test temperature, the asphalt mastic reaches the necessary stiffness to prevent creep of the specimen in the rheometer during the fatigue test; at higher temperatures, the specimen will lose its original shape (Figure 2).

Dynamic tests on the four-point bending beam (4PB) on asphalt mixture level according to EN 12697-24 (2018) are currently one of the most common test methods to describe the fatigue performance of asphalt. A test frequency of 30 Hz is commonly used for these tests and also set by the European Standard EN 13108-1 (2016). Since it is planned to perform the tests at the asphalt mixture level using 4PB, 30 Hz were also chosen as a frequency for mastic tests. Thus, same conditions on the mastic and asphalt mix level are ensured. The hyperbolic specimen shape is used to prevent failure at the interface of the test geometry and mastic specimen due to the high stiffness. The necking in the middle creates a predetermined breaking point due to the stress concentration in this area. Studies by Hospodka et al. (2018) have shown that both dynamic modulus and fatigue life have good repeatability realised with the stresscontrolled TS-Test. In EN 14770 (2012), there is no value for repeatability defined for standard DSR tests. In the study by Hospodka et al. (2018), ten fatigue tests on the hyperbolic specimen at a shear stress level of 400 kPa and a frequency of 30 Hz were performed on the same mastic mix. The fatigue life, expressed as the number of load cycles to failure, and the complex shear modulus after 10 s, corresponding to 300 load cycles, were used to determine repeatability. The complex

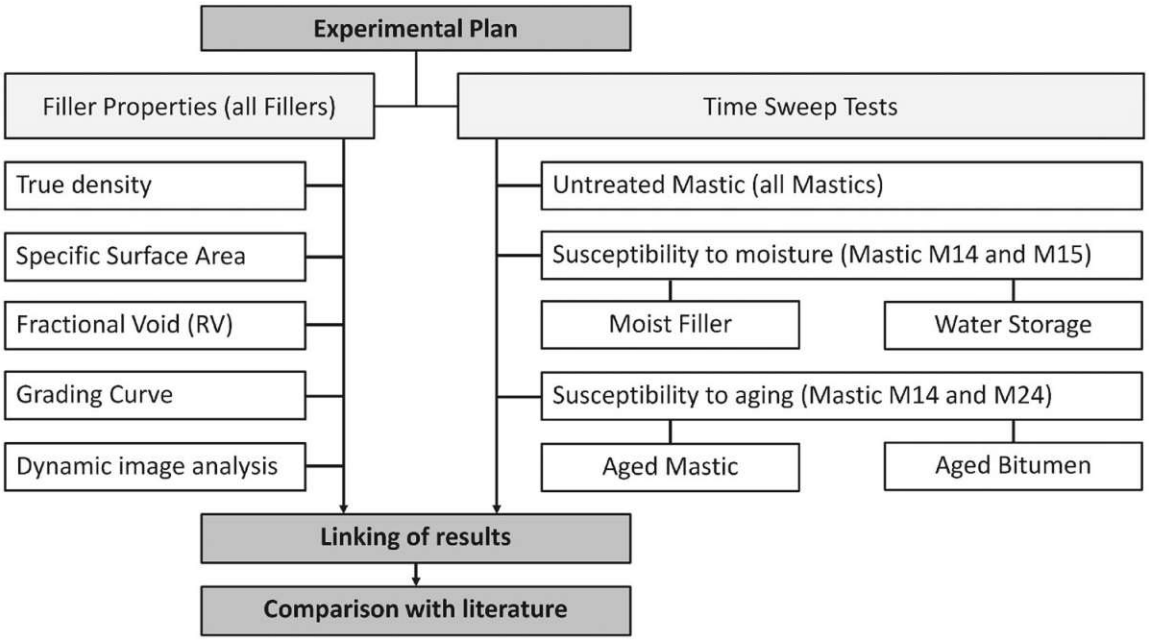

Figure 1. Experimental plan.

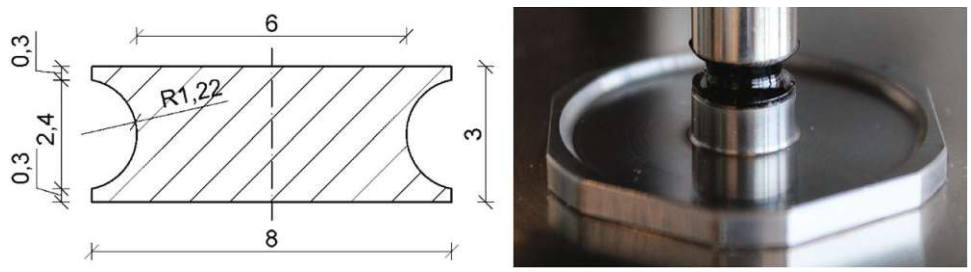

Figure 2. Dimensions of hyperbolic mastic specimens (left) and mounted mastic specimen (right).

shear modulus after 10 s is designated as the initial complex shear modulus in this study. The standard error's median and 95% confidence interval were calculated to investigate the quality of the measured fatigue life. The true fatigue life was between 188,000 and 212,000 load cycles with 95% confidence, corresponding to about ±6% of the mean value and conforming to good repeatability. One reason for the good repeatability is that, due to the silicone mould, the specimen shape is identical for each test, and measurement influences due to trimming are avoided. As in the study by Hospodka et al. (2018), stress-controlled TS tests are used in the present study due to good repeatability. The failure criterion was defined as reaching the maximum phase angle. In stress-controlled TS tests, the independence of the fatigue criteria (reduction of stiffness, phase angle peak, dissipated energy ratio, and ratio of dissipated energy change) on the fatigue evaluation could be shown (Steineder et al., 2022). All measured fatigue load cycles dependent on the selected fatigue criterion correlate with a determination coefficient of approximately 1.0. This means that the fatigue criterion does not influence the correlation analyses for stress-controlled TS tests. For each mastic mix in this study, three stress-controlled TS tests are performed for three different shear stresses, resulting in 9 tests per mastic.

The selected stress levels varied between 300 and 1200 kPa. These stress levels were chosen to obtain similar load cycles. The aim was to achieve around 10,000 load cycles at high and 800,000 load cycles at low-stress levels. It should be noted that these are nominal shear stresses, as the actual shear stress at the predetermined breaking point is higher due to the necked specimen shape. The DSR calculates the shear stress at the maximum radius for a cylindrical specimen shape. Because the complex shear modulus is linked with the shear stress, this study also deals with nominal complex shear modulus. The actual initial complex shear modulus due to necking is larger. The nominal values are used since there is still no method of converting nominal values into actual values resulting from the necking.

3.2. True density

The true density was determined using a helium pycnometer for the fillers, according to DIN 66137-2 (2019). The volume of the sample is precisely determined based on gas displacement. Each test consists of 10 measuring cycles, and from the results obtained, the mean value of the true density of the fillers was calculated.

3.3. Specific surface area

The BET test method can be used to measure the specific inner and outer surface area of disperse or porous solids according to ISO 9277 (2014). The amount of physically adsorbed gas is determined by the method of Grünauer, Emmett, and Teller (BET method) (Brunauer et al., 1938). This method is based on determining the amount of adsorbate or adsorptive gas required to cover the outer and inner accessible sample surface of the solid with a complete adsorbate monolayer. Inaccessible pores cannot be included. The BET method cannot be used for materials that absorb the gas (ISO, 9277, 2014).

3.4. Fractional void (RV)

The fractional void of dry compacted mineral filler, referred to as RV, is determined according to EN 1097-4 (2008). The filler is compacted using a standardised compaction device, and the volume of the compacted filler is determined by measuring the layer height. The RV is calculated using determined height, the mass of compacted filler, the density of filler, and the diameter of the hole in the drop block.

3.5. Grading curve

The grading curve up to 0.002 mm of the fillers was determined using a laser particle sizer. The measurements were performed with a FRITSCH Analysette 22 MicroTec Plus measuring system. The

instrument is used to determine the size distribution of suspensions, emulsions, and powders based on laser diffraction.

3.6. Dynamic image analysis

Dynamic image analysis can investigate the particle shape of the filler. For this purpose, the filler is dispersed in a solution and then fed to the analyzer. The filler particles are imaged using a high-resolution camera and a high-speed flash unit. Individual particle images are recorded directly and captured as high-resolution graphics files for post-processing. The dynamic, turbulent flow path allows random particle orientation and a direct view of moving particles within the capture zone. Various grain shape properties describe the particle shape through the obtained two-dimensional images of the individual particles.

Figure 3 shows basic characteristic values of dynamic image analysis:

- The equivalent circle area diameter ECAD (µm) describes a circle's diameter with the same area as the particle.
- The equivalent circle perimeter diameter ECPD (µm) corresponds to the diameter of a circle with the same perimeter as the particle image silhouette.
- The length L (µm) of a particle is estimated according to the maximum Feret diameter. The maximum Feret diameter corresponds to the largest distance between two parallel lines that do not intersect the particle.
- The width W (µm) corresponds to the minimum Feret diameter. The minimum Feret diameter corresponds to the smallest distance between two parallel lines that do not intersect the particle.
- The ratio of length by width can be calculated from the two values, referred to as the Feret aspect ratio FA.
- The circularity C is the ratio of the particle area to the area of the bounding circle that surrounds but does not intersect a particle. The diameter of the bounding circle is defined as the diameter of the smallest circle that encloses but does not intersect the particle. For circularity, the value is 1 for a perfectly round particle and becomes smaller the larger the deviation from the perfect circle.
- The ellipticity E is calculated similarly to the circularity. Here, the value for ellipticity corresponds to the ratio of the particle area to the area of the bounding ellipse. A value of 1 will conform to a perfect elliptical shape. If the particle shape deviates from the elliptical shape, the value becomes smaller.
- The rectangularity R is the ratio of the particle area to the area of the minimum bounding rectangle. The smallest possible area defines the bounding rectangle encloses but does not intersect the particle. The rectangularity has a value of 1 for an exactly rectangular particle and becomes smaller as it deviates from this shape.

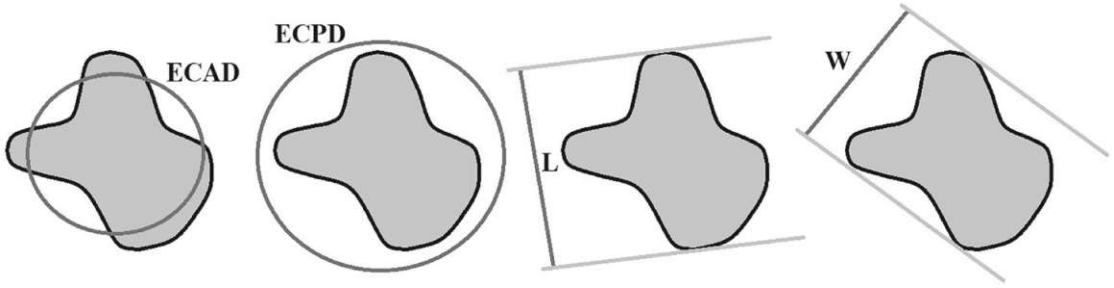

Figure 3. Characteristic values of dynamic image analysis.

3.7. Susceptibility to moisture

Two different manufacturing methods were used for the mastic to examine the impact of moisture on the fatigue performance of asphalt mastic. The first production method results in a mastic mixture with residual moisture in the filler. The filler is mixed with distilled water until complete water saturation is achieved. After a soaking time of 24 h, the filler-water mixture is heated at +180°C in the oven. By regular weighing, the filler is heated until 10% residual moisture is reached in the mix. Immediately after that, the filler is mixed with bitumen heated to +180°C. Water evaporates during the mixing process, so there is residual moisture of around 5% in the cooled mastic. With the second production method, mastic samples are stored in a water bath under the influence of temperature and pressure for 24 h. This preparation method is to test the water sensitivity of the mastic mixes. The increased pressure and temperature should accelerate water penetration into the mastic structure. In addition, water penetration into fine pores and voids benefits from test conditions. The test setup presented in this study is a prototype, as there is no standardised test setup yet.

For this purpose, 2 g of mastic are poured into a silicone mold with a diameter of 25 mm. The resulting thin and round mastic platelets are placed in a glass dish with distilled water. The glass dish with the mastic samples is stored in a pressure vessel for 24 h. The internal pressure is +5bar, and the internal temperature in the vessel is +60°C. Afterward, the mastic samples are stored in the refrigerator. The reason for keeping the mastics under pressure at an elevated temperature is to simulate significantly longer water storage of the mastics under 'normal conditions'. The selected test conditions are based on the performance characteristics of the vessel used. Since no empirical values are available for this type of test setup, an initial trial was performed as part of this study to determine whether possible changes in the fatigue performance of the asphalt mastics can be detected.

The fillers F04 and F05 and the bitumen B01 were used for these two production methods. These are the most commonly used filler materials. The prepared mastics specimens' fatigue performance was then tested in the DSR.

3.8. Susceptibility to aging

Two different manufacturing methods were used for the mastic to investigate the effect of aging on the fatigue performance of asphalt mastic. For the preparation of the aged mastic samples, two different aging methods were used. On the one hand, only the bitumen was aged. The aged bitumen was then used to produce the mastic. On the other hand, the already mixed mastic was aged. Both methods using the RTFOT method according to EN 12607-1 (2015) and PAV method according to EN 14769 (2012) for aging. The aged specimens were then tested for fatigue performance by TS test. The two bitumen grades B01 and B02 with the filler F04 were used for the aging methods.

4. Results and discussion

Regression analyses can be performed based on the numerous tests at filler and mastic levels. Thus, correlations between filler morphology and asphalt mastic can be identified. In addition, the results are compared with findings from the literature to be able to assess the observations. The mastic mixtures are considered separately according to bitumen grades for the analyses since a joint evaluation by means of regression analyses is not possible.

4.1. Mastic fatigue test

Figure 4 summarises the results for the 12 mastic mixes. The designations for the mastic grades are composed of the number of the bitumen and the number of the filler. The first digit represents the bitumen used (M1x and M2x), and the second digit represents the filler used (Mx1; Mx2. Mx3. Mx4. Mx5 and Mx6).

The results in Figure 4 show that the mastic mixes with polymer-modified bitumen achieve a higher τ_6 value (M21–M26). The increase in fatigue performance by using polymer modified bitumen is in accordance with general observations (Micaelo et al., 2017), and the mastic mixes with unmodified bitumen (M11–M16) have a higher stiffness. Also, the mastic mixes with filler F01 and F05 (M11, M15, M21, and M25) show a higher τ_6 value than the corresponding mastic mixes. Furthermore, the results show no direct correlation between fatigue performance and initial complex shear modulus (the complex shear modulus after 10 s). In general, mixtures with hydrated lime show higher stiffness and better durability than normal filler (Kim et al., 2003; Lesueur et al., 2012). This effect can be observed in the results. The positive influence of granodiorites on fatigue performance has also already been observed in another study (Rochlani et al., 2019).

4.2. True density

Table 3 lists the determined true densities of the six investigated fillers using a helium pycnometer. Accordingly, F05 with 2.57 g/m^3 has the lowest true density, while F03 with 3.0 g/m^3 has the highest true density. The other fillers have true densities between 2.7 and 2.9 g/m^3. Considering the coefficient of determination ($R^2 = 0.049$ and $R^2 = 0.017$) of the correlations between the fatigue value τ_6 and the true density, it can be assumed that the true density does not influence the fatigue performance. Studies show that increasing particle density causes a higher mastic stiffness but no clear trend on fatigue performance (Mazzoni et al., 2019). However, no correlation between the true density and the initial complex shear modulus could be found either. Due to the massrelated weighed portion of mastic, all mixtures have a filler bitumen ratio of 2.02 by mass. However, the true density affects the filler volume ratio. Based on the volume, the filler content by volume changes as summarised in Table 1. The stiffness increases as the filler content by volume increases (Liao et al., 2012; Miro et al., 2017). This increase in stiffness cannot be observed in the results. The reason for this is probably the low variation of the filler content by volume in the mastic mixes. If we look at the correlation between filler volume ratio, there is no correlation between filler volume ratio and the fatigue parameter τ_6 ($R^2 = 0.36$ and $R^2 = 0.64$) or the initial complex shear modulus $|G^*|_{initial}$ ($R^2 = 0.065$ and $R^2 = 0.29$). It is undisputed that adding filler to bitumen increases fatigue performance, but excessive filler concentrations lead

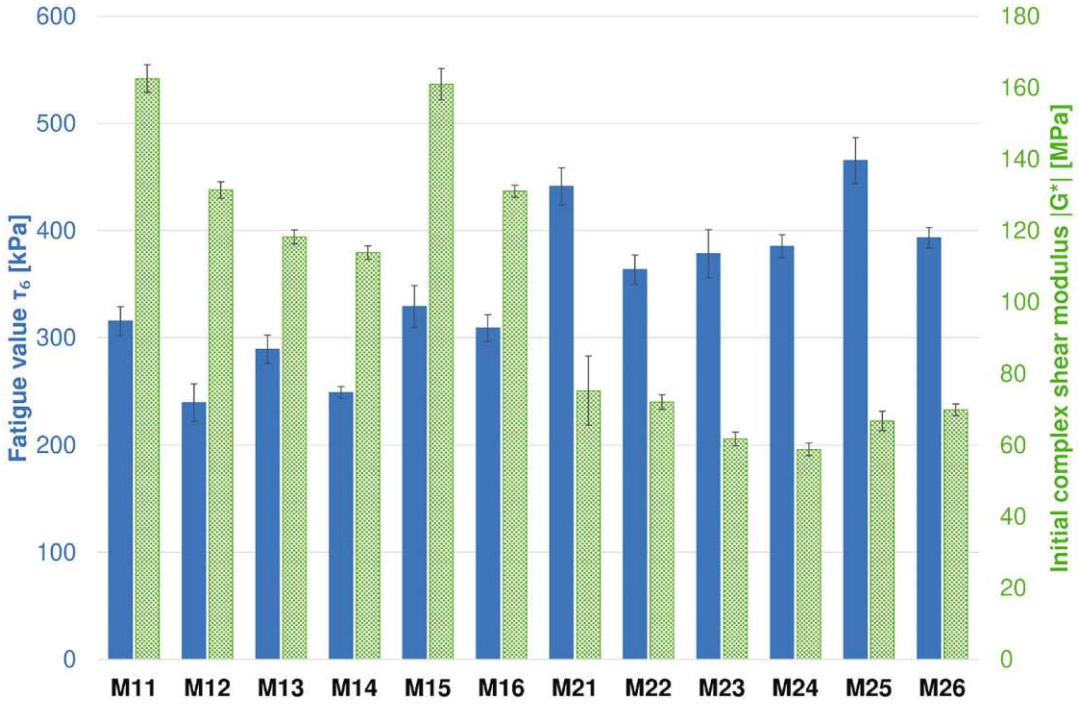

Figure 4. Test results of mastic fatigue performance tests.

Table 3. Results for true density, specific surface and fractional void RV.

Lab code	True density (g/m^3)	Specific surface BET (m^2/g)	RV (m^2/g)
F01	2.87	4.43	39.00
F02	2.78	1.93	33.00
F03	3.00	18.97	36.00
F04	2.72	1.54	31.00
F05	2.57	5.43	43.00
F06	2.65	1.29	35.00

to a decrease in fatigue performance (Wang et al., 2012). However, due to the large scale of tests, the filler-bitumen ratio was not varied in this study.

4.3. Specific surface area (SSA)

Table 3 summarises the specific surface areas (SSA) determined for the six fillers investigated using the BET method. Especially the filler made of basalt stands out due to the large SSA. The reason for the high SSA of F03 is probably a high amount of tiny pores in the fine grain. In literature (Rochlani et al., 2019), the fillers' specific surface area affects the mastics' rheological and mechanical performance. A filler with a higher specific surface area mixed with bitumen shows better stiffness, aging, fatigue, and rutting performance.

Considering the coefficient of determination of the correlations between the fatigue value τ_6 and SSA ($R^2 = 0.0321$ and $R^2 = 0.01$), no correlation would be expected. But due to the high SSA of F03 and the small sample quantity, the regression is excessively influenced by Mx3 samples. Especially brecciated and altered basalt samples can have an SSA value up to 52 m^2/g (Nielsen & Fisk, 2010). Without the M13 mix, the coefficient of determination of the correlation between τ_6 and SSA increases to $R^2 = 0.47$ for mastic mixes with the bitumen B01. The coefficient of determination of the correlation between τ_6 and SSA increases to $R^2 = 0.86$ for mastic mixes with the polymer-modified bitumen B02 without the M23 mix. The reason for the low coefficient of determination for the mastic mixes with the unmodified bitumen B01 is the sample with quartz as filler. Due to its smooth surface, it has a very small SSA of only 1.29 m^2/g. This observation concludes a correlation between the fatigue value τ_6 and SSA if mastic mixes with fillers with high or low SSA are not considered. Excluding these two mastic mixes, the coefficient of determination of the correlations between the τ_6 and SSA is $R^2 = 0.96$ and $R^2 = 0.93$, respectively.

Thus, SSA impact the fatigue performance of asphalt mastic, measured with a stress-controlled TS test and hyperbolic specimen shape. The situation is similar for the initial complex shear modulus and the SSA. Here, the mastic mixes with unmodified bitumen (excluding M13) show a good correlation ($R^2 = 0.84$). However, no correlation with stiffness can be derived for mastic mixes with modified bitumen. It is assumed that due to the larger surface area of the filler, there is a better adhesion between bitumen and filler, which minimises the crack initiation between bitumen and filler. In addition, chemical reactions between bitumen and filler can be enhanced (Rochlani et al., 2019).

4.4. Fractional void (RV)

Correlations between the physical properties of fillers show that RV can be used as a suitable candidate to characterise the physical behaviour of fillers (Chaudhary et al., 2020). The results of the fractional void tests are summarised in Table 3. Especially F01 and F05 have a high RV value. Figure 5 shows the correlation between the fatigue value τ_6 and the RV separately for both bitumen grades. The green line represents the regression line for the mastic mixes with the unmodified bitumen B01. The blue line represents the regression line for the mastic mixes with the polymer-modified bitumen B02. The coefficient of determination of the two correlations is $R^2 = 0.76$ and $R^2 = 0.80$.

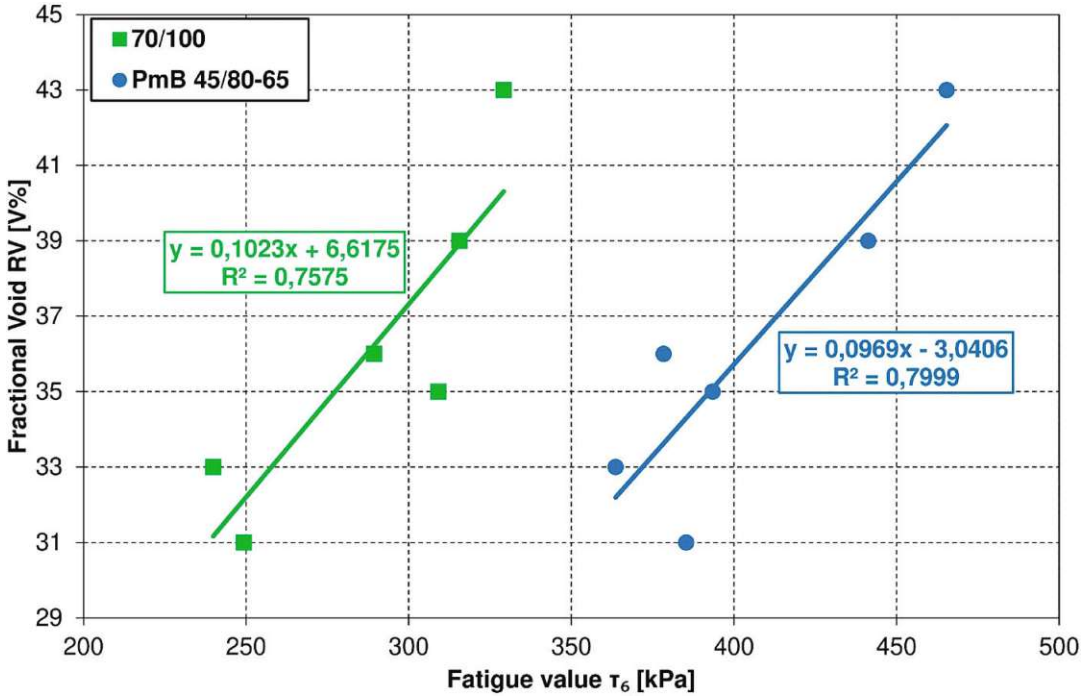

Figure 5. Correlation between the fatigue value τ_6 and the RV.

Table 4. Characteristic values related to the grading curves.

Lab code	S – 2 µm	S – 16 µm	D – 30%	D – 60%	Cc	U
F01	8.34	38.13	11.35	32.09	1.65	13.18
F02	7.06	29.21	12.50	38.49	1.77	16.79
F03	9.24	41.61	10.25	27.36	1.75	12.45
F04	12.74	57.66	5.56	17.23	1.12	10.78
F05	11.96	49.14	7.22	23.23	1.34	13.88
F06	12.80	51.47	6.74	20.20	1.38	12.36

These two correlation analyses allow the conclusion that the RV of the filler influences the fatigue performance of the asphalt mastic. The study by Roberto et al. (2018) show that the filler type and RV affect the fracture limits. Accordingly, the fatigue value τ_6 of the asphalt mastic can also be estimated from the RV of the filler. Thus, this parameter is suitable to characterise the filler quality in terms of fatigue performance of the asphalt mastic. A series of further tests must be carried out to validate this observation. The initial complex shear modulus $|G^*|_{initial}$ and RV show no correlation. This observation does not correspond to the literature observations; with higher RV, the stiffness increases (Chen et al., 2020; Mazzoni et al., 2019).

4.5. Grading curve and dynamic image analysis

Figure 6 shows the grading curves of the different fillers. It is possible to derive characteristic values relevant to the grading curves from the data obtained. The characteristic values describe the different grading curves and are used for subsequent analyses. The most important characteristic values related to the grading curves include the passage rate through a selected sieve (S), the coefficient of curvature Cc, the coefficient of uniformity U and the calculated maximum mesh size in millimetres of a sieve with a defined mass percent of the filler passes through (D).

All characteristic values are summarised in Table 4. From the grading curve and the characteristic values relevant to the grading curve, it can be seen that the fillers F04 to F06 have a high proportion of very fine grain in the filler.

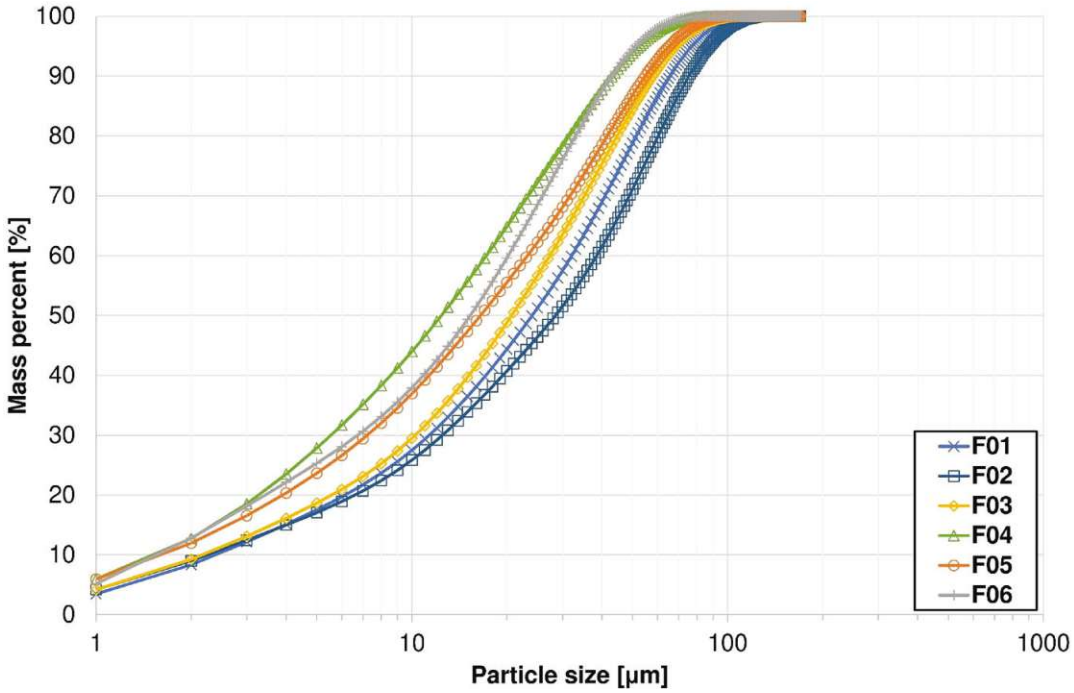

Figure 6. Grading curves of used fillers.

Table 5. Results of the dynamic image analysis represented as mean values.

Lab code	ECAD	ECPD	L	W	FA	C	E	R
F01	6.87	9.66	8.3	7.1	1.711	0.658	0.837	0.627
F02	6.46	8.10	8.2	6.3	1.630	0.726	0.864	0.647
F03	6.86	8.50	8.7	6.6	1.602	0.734	0.866	0.646
F04	5.89	6.93	7.3	5.6	1.551	0.773	0.891	0.660
F05	5.57	6.55	6.9	5.3	1.551	0.780	0.894	0.661
F06	6.50	8.32	8.3	6.3	1.657	0.705	0.85	0.632

Studies show that grain size and roundness influence material behaviour (Antunes et al., 2015; Grabowski & Wilanowicz, 2007). Table 5 summarises the results represented as mean values of the dynamic image analysis. It can be observed that F04 and F05 have small ECAD and ECPD, while F01 has the largest values. F01 also has the largest deviations from the perfect circle and ellipse compared to the other fillers. On the other hand, F05 has the highest circularity and ellipticity values. According to the results for rectangularity, no clear differences can be found among the fillers.

Table 6 summarises the coefficients of determination of the regression analyses between the fatigue value τ_6 and the characteristic values relevant to the grading curve and the grain shape. None of the determined values shows a correlation with τ_6. Consequently, there is no direct correlation between the fatigue performance of asphalt mastic and grading curve or grain shape. The observations from the literature, that grain size and roundness influence material behaviour (Antunes et al., 2015; Grabowski & Wilanowicz, 2007), are not confirmed by the results. A possible reason for the missing impact of the grain shape on τ_6 could be the small scatter in the results of the grain shape of the fillers used in this study. To exclude the effect of grain shape, fillers with a higher variation of grain shape have to be used.

The coefficient of determination for the correlation between FA and $|G^*|_{initial}$ for the mastic mixes with polymer-modified bitumen (M2x) is 0.66. Since this is only valid for the M2x mastic mixes, it can be assumed that there is no direct correlation between the initial complex shear modulus and the characteristic values according to grading curve or grain shape.

Table 6. R^2 of the regression analyses between τ_6 and the characteristic values relevant to the grading curve and the grain shape.

	τ_6 of M1x	τ_6 of M2x	$\lvert G^* \rvert_{initial}$ of M1x	$\lvert G^* \rvert_{initial}$ of M2x
S – 2 µm	0.08	0.05	0.03	0.27
S – 16 µm	0.04	0.04	0.06	0.40
D – 30%	0.03	0.04	0.05	0.36
D – 60%	0.05	0.03	0.08	0.42
Cc	0.00	0.06	0.01	0.25
U	0.04	0.01	0.11	0.38
ECAD	0.00	0.14	0.01	0.16
ECPD	0.02	0.01	0.03	0.37
L	0.01	0.28	0.07	0.10
W	0.01	0.04	0.01	0.30
FA	0.05	0.00	0.13	0.66
C	0.05	0.00	0.11	0.57
E	0.04	0.01	0.05	0.53
R	0.09	0.00	0.07	0.50

4.6. Susceptibility to moisture

The mineralogical composition of fillers influences the moisture resistance of asphalt mixes (Choudhary et al., 2020). The results of the fatigue tests including moisture conditioning are shown in Figure 7. It can be seen that the water storage only affects the mastic with filler F05. The fatigue value τ_6 and the initial complex shear modulus $\lvert G^* \rvert_{initial}$ decrease. These changes are probably due to the water sensitivity of hydrated lime since the mastic with filler F04 remains unaffected by water storage. An evident influence can be seen in the mastic specimens with wet filler. The fatigue value τ_6, as well as the initial complex shear modulus $\lvert G^* \rvert_{initial}$ decreases for both mastic mixes. As a result of the mastic's mounting temperature of over +100°C, the bonded water in the mastic dissolves as vapour. As the water evaporates from the mastic, tiny air bubbles occur in the hot liquid mastic. These air bubbles probably generate voids in the solidified mastic sample and harm the mastic structure. As a result, a smaller transmission area is available in the necking of the specimen, which reduces fatigue resistance. The reduced initial complex shear modulus also indicates that the stiffness decreases due to the smaller transmission area. Thus, the shear deformation to reach the selected shear stress is higher, leading to a faster formation of microcracks.

4.7. Susceptibility to aging

Figure 8 shows that the fatigue parameter τ_6 and the initial complex shear modulus $\lvert G^* \rvert_{initial}$ increase as a result of aging. Studies show that aging increases the complex shear modulus (Xing, Fan, et al., 2020). Also, an increased amount of aged bitumen independent of the filler considered increases mastic stiffness (Mazzoni et al., 2019). These observations are consistent with the results. According to Li et al. (2018), the stiffness increases while the fatigue resistance decreases with the increase of aging time.

However, the increase in fatigue performance is contrary to the expectations and is due to the stress-controlled test method used in this study. In a stress-controlled TS test, a high initial stiffness implies a small applied strain in the specimen to reach the defined stress. However, small strains mean that the fatigue deformation in the specimen is small, which is why the number of load cycles to fatigue also increases. The energy lost due to internal friction and viscous deformation is minimised. It can be seen that the mastic samples with aged bitumen and the aged mastic samples lead to different results. These different results are probably by physio-chemical processes or due to the aging of the mastic by the RTFOT process. As a result of the aging process, a thin bitumen film remains in the glass vessel of the RTFOT system. which changes the bitumen/filler ratio. The increasing filler/bitumen ratio due to the loss of bitumen in the RTFOT glass vessel could also increase mastic stiffness. Other studies were

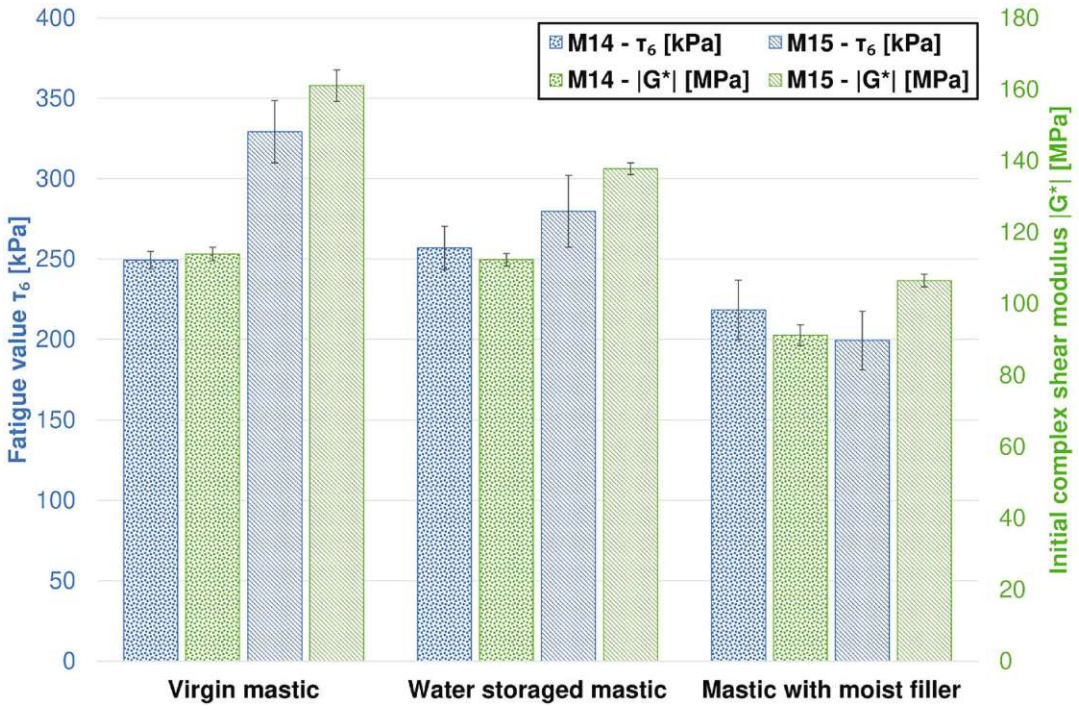

Figure 7. Test results of mastic fatigue performance tests under the influence of moisture.

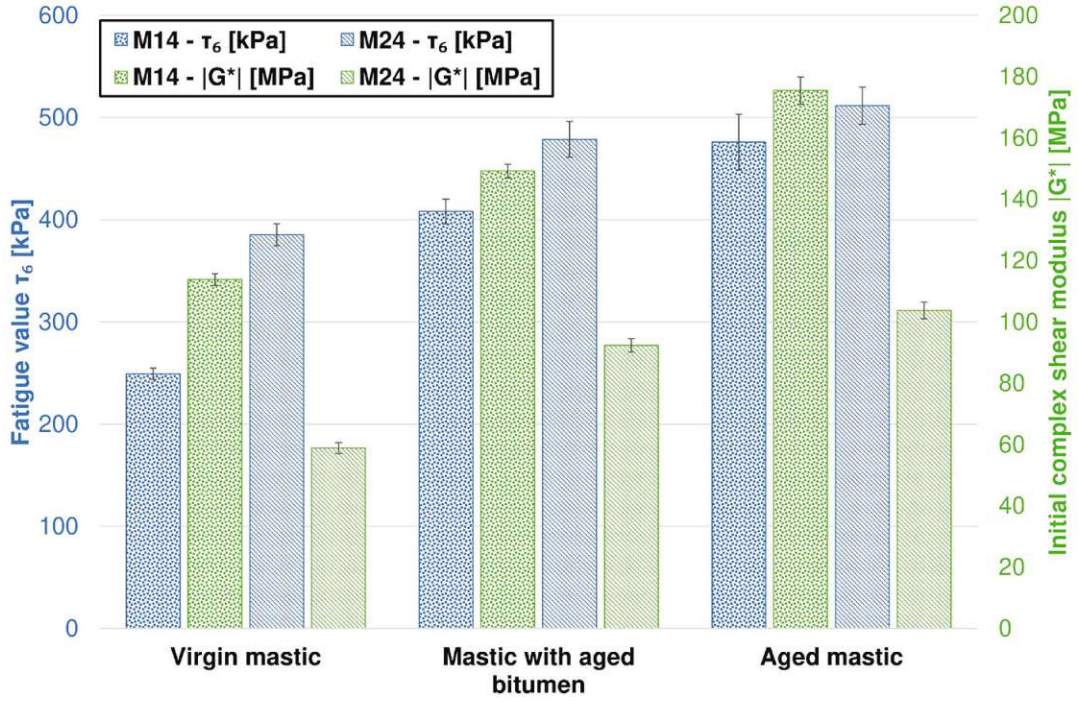

Figure 8. Test results of mastic fatigue performance tests under the influence of aging.

also able to show a change of filler/bitumen ratio of mastics by the traditional PAV aging method (Xing, Liu, et al., 2020).

4.8. Multiple linear regression analyses

Multiple linear regression analyses were performed to investigate the effects of several filler morphological properties on the fatigue performance of asphalt mastic. Due to the small sample quantity

per bitumen grade, a maximum of 2 independent parameters were used for the multiple regression analysis. It was studied whether a rheological parameter of the mastic in combination with a filler parameter produces a better regression model. The multiple regression with the combination of $|G^*|_{initial}$ and RV has a coefficient of determination of 0.58 for M1x and 0.64 for M2x. All other combinations between the rheological parameter of the mastic with a filler parameter have a smaller coefficient of determination. A multiple regression between these parameters does not improve the model. Furthermore, it was studied if two filler parameters produced a better multiple regression model. The multiple regression with RV and BET has a coefficient of determination of 0.57 for M1x and 0.78 for M2x. All other combinations of two filler parameters have smaller coefficients of determination.

Considering the coefficients of determination of the multiple regression analysis, the combination with other parameters does not improve the regression models. However, multiple regressions with RV and any other parameter have significantly better coefficients of determination than with other parameters. This supports the hypothesis that RV is related to the fatigue performance of asphalt mastic.

5. Conclusion

To investigate the effects of filler morphological properties, moisture, or aging on the fatigue performance of asphalt mastic by TS tests and hyperbolic specimen shape, 20 different mastic mixes were analysed in this study. Eight of the twenty mastic mixes were prepared to study the effect of moisture and aging on fatigue resistance, respectively. Based on correlation analysis between results of filler properties and fatigue resistance and initial complex shear modulus of the respective mastic together with a comparison of literature, the following conclusions can be drawn:

- Mastic mixtures with polymer-modified bitumen show better fatigue performance than those with unmodified bitumen and thus follows the general observations in literature.
- Regarding the true density, grading curve's properties, and the grain shape of the filler, no direct impact on the fatigue performance τ_6 of the asphalt mastic could be found.
- As described in other studies, a correlation was found between the fatigue performance τ_6 and the fractional void (RV).
- The specific surface area has only a limited relationship with the fatigue performance τ_6 of asphalt mastic, but corresponds to observations in the literature with a few exceptions. Fillers with a very high or small specific surface area cannot be related to fatigue performance τ_6.
- Moist filler in the mastic leads to tiny steam bubbles during the production of the mastic specimens in the DSR. These bubbles negatively affect the fatigue performance τ_6. Mastic specimens stored in water show deterioration only if the filler is water sensitive, as with hydrated lime.
- Aged mastic specimens increase the initial complex stiffness modulus $|G^*|_{initial}$ and the fatigue value τ_6. An increase in the initial complex shear modulus is consistent with the literature, but the improved fatigue performance contradicts the observations in the literature. The reason for this is probably the choice of the stress-controlled loading mode. In a stress-controlled time sweep test, a high initial stiffness implies a small applied strain in the specimen to reach the defined stress. However, small strains mean that the fatigue deformation in the specimen is small, wherefore the number of load cycles to fatigue also increases. It can be concluded that a stress-controlled TS test with hyperbolic specimen shape is not suitable to investigate the influences of aging on fatigue performance.

In this study, a time sweep test as a fundamental tool combined with a hyperbolic specimen shape was used to assess the fatigue performance of asphalt mastic. The identified influence of RV, SSA and moisture correspond to the observations from the literature. According to the results and the comparison with the literature, it can be confirmed that the hyperbolic specimen shape is a possible

alternative to determine the fatigue performance of asphalt mastic and the effects of filler properties and moisture. The negative experience with cylindrical specimen shape in mastic fatigue tests can be compensated. However, to improve the validity of this study, the mastic mixes should also be tested with other fatigue test methods. Due to the high number of tests necessary to describe one sample thoroughly, this could not be performed in this study. The effects of aging cannot be reproduced with stress-controlled TS tests. Whether this effect could have been avoided by strain-controlled tests was not investigated in this study. By expanding the data set presented in this paper in the future, we aim at improving the correlation quality between asphalt mastic and asphalt mix and establish a new filler criterion in terms of fatigue performance. The implementation of dissipated energy approaches will be considered in subsequent studies.

Acknowledgement(s)

The study reported in this paper is part of the research project on assessment of asphalt mastic quality concerning the durability of asphalt pavements (Beurteilung der Asphaltmastixqualität in Hinblick auf die Dauerhaftigkeit von Asphaltdecken), funded by the Austrian Federal Ministry of Climate Action. Environment. Energy. Mobility. Innovation and Technology and the Federal Ministry for Digital and Economic Affairs.

Disclosure statement

No potential conflict of interest was reported by the author(s).

ORCID

Michael Steineder http://orcid.org/0000-0003-2223-1785
Bernhard Hofko http://orcid.org/0000-0002-8329-8687

References

Airey, G. D., Thom, N. H., Osman, S., Huang, H., & Collop, A. C. (2004). *A comparison of bitumen/mastic fatigue data from different test methods*. Proceedings of the 5th international conference on cracking in pavements, Limoges, France, 5 May 2004.

Anderson, D., Hir, Y., Marasteanu, M., Planche, J.-P., Martin, D., & Gauthier, G. (2001). Evaluation of fatigue criteria for asphalt binders. *Transportation Research Record: Journal of the Transportation Research Board*, *1766*, 48–56. https://doi.org/10.3141/1766-07

Antunes, V., Freire, A. C., Quaresma, L., & Micaelo, R. (2015). Influence of the geometrical and physical properties of filler in the filler–bitumen interaction. *Construction and Building Materials*, *76*, 322–329. https://doi.org/10.1016/j.conbuildmat.2014.12.008

Brunauer, S., Emmett, P. H., & Teller, E. (1938). Adsorption of gases in multimolecular layers. *Journal of the American Chemical Society*, *60*(2), 309–319. https://doi.org/10.1021/ja01269a023

Chaudhary, M., Saboo, N., Gupta, A., Hofko, B., & Steineder, M. (2020). Assessing the effect of fillers on LVE properties of asphalt mastics at intermediate temperatures. *Materials and Structures*, *53*(4), 1–16. https://doi.org/10.1617/s11527-020-01532-6

Chen, Y., Xu, S., Tebaldi, G., & Romeo, E. (2020). Role of mineral filler in asphalt mixture. *Road Materials and Pavement Design*, *23*(2), 247–286. https://doi.org/10.1080/14680629.2020.1826351

Choudhary, J., Kumar, B., & Gupta, A. (2021). Analysing the influence of industrial waste fillers on the ageing susceptibility of asphalt concrete. *International Journal of Pavement Engineering*, *23*(11), 3906–3919. https://doi.org/10.1080/10298436.2021.1927027

DIN 66137-2. (2019). *Determination of solid state density – Part 2: Gaspycnometry*. German Institute for Standardization e.V.

EN 1097-4. (2008). *Tests for mechanical and physical properties of aggregates – Part 4: Determination of the voids of dry compacted filler*. European Committee for Standardization.

EN 12607-1. (2015). *Bitumen and bituminous binders – determination of the resistance to hardening under influence of heat and air – Part 1: RTFOT method*. European Committee for Standardization.

EN 12697-24. (2018). *Bituminous mixtures – test methods – Part 24: Resistance to fatigue*. European Committee for Standardization.

EN 13108-1. (2016). *Bituminous mixtures – material specifications – Part 1: Asphalt concrete*. European Committee for Standardization.

EN 1426. (2015). *Bitumen and bituminous binders – determination of needle penetration*. European Committee for Standardization.

EN 1427. (2015). *Bitumen and bituminous binders – determination of the softening point – Ring and Ball method*. European Committee for Standardization.
EN 14769. (2012). *Bitumen and bituminous binders – accelerated long-term ageing conditioning by a Pressure Ageing Vessel (PAV)*. European Committee for Standardization.
EN 14770. (2012). *Bitumen and bituminous binders – determination of complex shear modulus and phase angle using a Dynamic Shear Rheometer (DSR)*. European Committee for Standardization.
EuLA – European Lime Association. (2010). *Hydrated lime: A proven additive for durable asphalt pavements*. Report to the European Lime Association / Asphalt Task Force.
Grabowski, W., & Wilanowicz, J. (2007). The structure of mineral fillers and their stiffening properties in filler-bitumen mastics. *Materials and Structures*, *41*(4), 793–804. https://doi.org/10.1617/s11527-007-9283-4
Hesami, E., Birgisson, B., & Kringos, N. (2013). Numerical and experimental evaluation of the influence of the filler–bitumen interface in mastics. *Materials and Structures*, *47*(8), 1325–1337. https://doi.org/10.1617/s11527-013-0237-8
Hospodka, M., Hofko, B., & Blab, R. (2018). Introducing a new specimen shape to assess the fatigue performance of asphalt mastic by dynamic shear rheometer testing. *Materials and Structures*, *51*(46), 1–11. https://doi.org/10.1617/s11527-018-1171-6
ISO 9277. (2014). *Determination of the specific surface area of solids by gas adsorption – BET method*. International Organization for Standardization.
Kim, Y.-R., Little, D., & Song, I. (2003). Effect of mineral fillers on fatigue resistance and fundamental material characteristics: Mechanistic evaluation. *Transportation Research Record: Journal of the Transportation Research Board*, *1832*(1), 1–8. https://doi.org/10.3141/1832-01
Kim, Y. S., Sigwarth, T., Büchner, J., & Wistuba, M. P. (2021). Accelerated dynamic shear rheometer fatigue test for investigating asphalt mastic. *Road Materials and Pavement Design*, *22*(sup1), S383–S396. https://doi.org/10.1080/14680629.2021.1911832
Lesueur, D., Petit, J., & Ritter, H. (2012). The mechanisms of hydrated lime modification of asphalt mixtures: A state-of-the-art review. *Road Materials and Pavement Design*, *14*, 1–16. https://doi.org/10.1080/14680629.2012.743669
Lesueur, D., Teixeira, A., Lazaro, M. M., Andaluz, D., & Ruiz, A. (2016). A simple test method in order to assess the effect of mineral fillers on bitumen ageing. *Construction and Building Materials*, *117*, 182–189. https://doi.org/10.1016/j.conbuildmat.2016.05.003
Li, Q., Chen, X., Li, G., & Zhang, S. (2018). Fatigue resistance investigation of warm-mix recycled asphalt binder, mastic, and fine aggregate matrix. *Fatigue & Fracture of Engineering Materials & Structures*, *41*(2), 400–411. https://doi.org/10.1111/ffe.12692
Liao, M.-C., Chen, J.-S., & Tsou, K.-W. (2012). Fatigue characteristics of bitumen-filler mastics and asphalt mixtures. *Journal of Materials in Civil Engineering*, *24*(7), 916–923. https://doi.org/10.1061/(ASCE)MT.1943-5533.0000450
Mazzoni, G., Virgili, A., & Canestrari, F. (2019). Influence of different fillers and SBS modified bituminous blends on fatigue, self-healing and thixotropic performance of mastics. *Road Materials and Pavement Design*, *20*(3), 656–670. https://doi.org/10.1080/14680629.2017.1417150
Micaelo, R., Guerra, A., Quaresma, L., & Cidade, M. (2017). Study of the effect of filler on the fatigue behaviour of bitumen-filler mastics under DSR testing. *Construction and Building Materials*, *155*, 228–238. https://doi.org/10.1016/j.conbuildmat.2017.08.066
Miro, R., Martinez, A. H., Perez-Jimenez, F. E., Botella, R., & Alvarez, A. (2017). Effect of filler nature and content on the bituminous mastic behaviour under cyclic loads. *Construction and Building Materials*, *132*, 33–42. https://doi.org/10.1016/j.conbuildmat.2016.11.114
Nielsen, M. E., & Fisk, M. R. (2010). Surface area measurements of marine basalts: Implications for the subseafloor microbial biomass. *Geophysical Research Letters*, *37*(15), 1–5. https://doi.org/10.1029/2010GL044074
Roberto, A., Romeo, E., Montepara, A., & Roncella, R. (2018). Effect of fillers and their fractional voids on fundamental fracture properties of asphalt mixtures and mastics. *Road Materials and Pavement Design*, *21*(1), 25–41. https://doi.org/10.1080/14680629.2018.1475297
Rochlani, M., Leischner, S., Falla, G. C., Wang, D., Caro, S., & Wellner, F. (2019). Influence of filler properties on the rheological, cryogenic, fatigue and rutting performance of mastics. *Construction and Building Materials*, *227*, 116974. https://doi.org/10.1016/j.conbuildmat.2019.116974
Steineder, M., Peyer, M., Hofko, B., Chaudhary, M., Saboo, N., & Gupta, A. (2022). Comparing different fatigue test methods at asphalt mastic level. *Materials and Structures*, *55*(132), 1–16. https://doi.org/10.1617/s11527-022-01970-4
Wang, D., Wang, L., & Zhou, G. (2012). Fatigue of asphalt binder, mastic and mixture at low temperature. *Frontiers of Structural and Civil Engineering*, *6*(2), 166–175. https://doi.org/10.1007/s11709-012-0157-7
Xing, B., Fan, W., Han, L., Zhuang, C., Qian, C., & Lv, X. (2020). Effects of filler particle size and ageing on the fatigue behaviour of bituminous mastics. *Construction and Building Materials*, *230*, 117052. https://doi.org/10.1016/j.conbuildmat.2019.117052
Xing, C., Liu, L., & Sheng, J. (2020). A new progressed mastic aging method and effect of fillers on SBS modified bitumen aging. *Construction and Building Materials*, *238*, 117732. https://doi.org/10.1016/j.conbuildmat.2019.117732